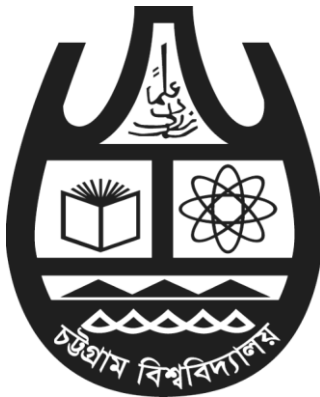


ASSESSMENT OF HALDA RIVER IN CONTEXT OF SURFACE WATER CHANGES AND LAND USE AND LAND COVER IN ITS BASIN BY GOOGLE EARTH ENGINE



COURSE TITLE: PROJECT PAPER

COURSE NO.: ENV 426

THIS DISSERTATION HAS BEEN SUBMITTED AS PARTIAL
FULFILLMENT FOR THE FOUR-YEAR PROFESSIONAL DEGREE OF B. SC.
(HONS.) IN ENVIRONMENTAL SCIENCE

EXAMINATION ROLL NO.: 14208086

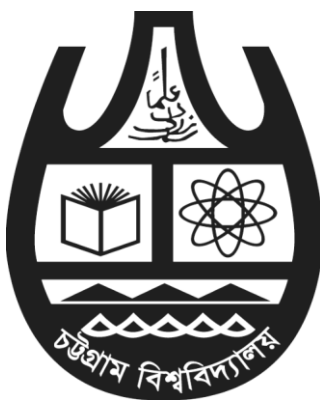
REGISTRATION NO.: 14208086

SESSION: 2013-14

**INSTITUTE OF FORESTRY AND ENVIRONMENTAL SCIENCES
UNIVERSITY OF CHITTAGONG
CHITTAGONG, BANGLADESH**

MARCH, 2019

ASSESSMENT OF HALDA RIVER IN CONTEXT OF SURFACE WATER CHANGES AND LAND USE AND LAND COVER IN ITS BASIN BY GOOGLE EARTH ENGINE



COURSE TITLE: PROJECT PAPER

COURSE NO.: ENV 426

THIS DISSERTATION HAS BEEN SUBMITTED AS PARTIAL
FULFILLMENT FOR THE FOUR-YEAR PROFESSIONAL DEGREE OF B. SC.
(HONS.) IN ENVIRONMENTAL SCIENCE

Submitted to:

Dr. Mohammad Mosharraf Hossain

Professor

Institute of Forestry and Environmental Sciences
University of Chittagong

Submitted by:

Sourav Karmakar

Examination Roll No: 14208086

Registration No: 14208086

Session: 2013-14

Institute of Forestry and Environmental Sciences
University of Chittagong

**INSTITUTE OF FORESTRY AND ENVIRONMENTAL SCIENCES
UNIVERSITY OF CHITTAGONG
CHITTAGONG, BANGLADESH**

MARCH, 2019



DECLARATION

This project paper entitled "**ASSESSMENT OF HALDA RIVER IN CONTEXT OF SURFACE WATER CHANGES AND LAND USE AND LAND COVER IN ITS BASIN BY GOOGLE EARTH ENGINE**" has been prepared by me submitted to Institute of Forestry and Environmental Sciences, University of Chittagong as a requirement for the partial fulfillment of the degree of B. Sc. (Hons.) in Environmental Science. I am confirming with pledge that it has not been submitted in any previous application for a degree. Exclusively the work reported within was executed by me, unless otherwise stated.

.....
Sourav Karmakar

Examination Roll No: 14208086

Registration No: 14208086

Session: 2013-14

Institute of Forestry and Environmental Sciences

University of Chittagong, Chittagong-4331

Bangladesh.



This is to certify that Sourav Karmakar, Examination Roll No. 14208086, Registration No. 14208086, and Session: 2013-14 has prepared this project paper entitled "**ASSESSMENT OF HALDA RIVER IN CONTEXT OF SURFACE WATER CHANGES AND LAND USE AND LAND COVER IN ITS BASIN BY GOOGLE EARTH ENGINE**" under my supervision. This is for the partial fulfillment of B. Sc. (Hons.) in Forestry degree of the Institute of Forestry and Environmental Sciences, University of Chittagong, Bangladesh.

.....

Dr. Mohammad Mosharraf Hossain

Professor

Institute of Forestry and Environmental Sciences
University of Chittagong
Chittagong-4331
Bangladesh.

ACKNOWLEDGEMENT

At first, I express my profound gratitude to the almighty, the most gracious and most benevolent. I would first and foremost like to express my profound sense of gratitude to my respected teacher and project supervisor Professor Dr. Mohammad Mosharraf Hossain, Institute of Forestry and Environmental Sciences, University of Chittagong, for his indispensable and expert guidance, direct concern, constructive criticism, encouragement and inspiration throughout this Project work. I have the pleasure of paying a glowing tribute and indebtedness to my most esteemed and warm hearted teacher and supervisor for his suggestions as well as for spending his valuable time looking through the manuscript and all out co-operation throughout the research work. I would like to express my very great appreciation to all of my Teachers who helped me to increase my knowledge in this field.

I wish to convey my special thanks to my seniors Russel vai, Sahadev vai, Mithun vai for helping me to learn GIS and Remote Sensing related software operations. I owe much to Habiba apu and Mishma apu for their kind co-operation.

I deem to express my deep sense of gratitude to Sourav Dey and Biplob Chakma for their technical support. I am particularly grateful to you guys.

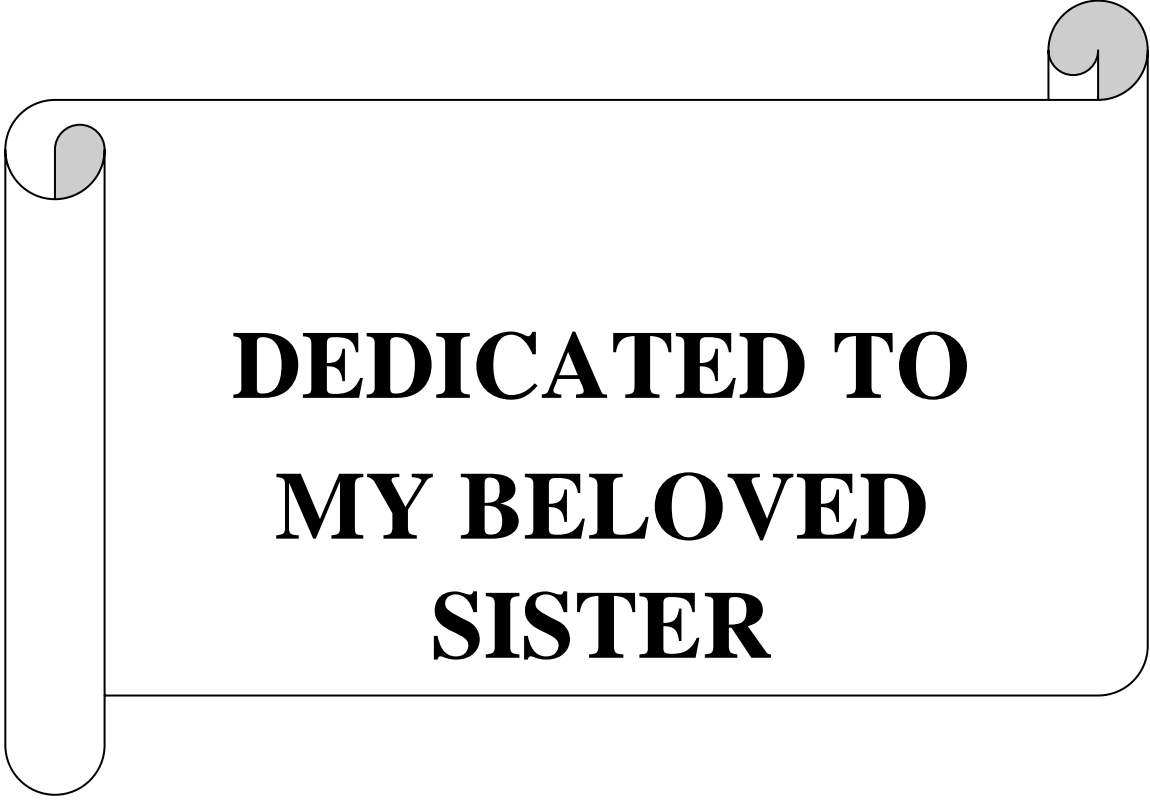
I wish to express my heartfelt gratitude to my roommate Akash, who always inspires me during the project work. I wish to extend my thanks to my friends Rashik, Shuva, Tawsif, Sujan, Faruk and all other mates of 35th batch of IFESCU for being with me through this journey.

I want to express my profound gratitude to officers and other stuffs of IFESCU for their cordial help and collaboration doing accomplishment of this study and also convey my endearment to beloved junior Pritom Barua.

At last I express my hearty gratitude to my beloved parents, brothers, sisters, and all of my relatives for continuous inspiration during entire period of my study.

March, 2019

Author



**DEDICATED TO
MY BELOVED
SISTER**

Table of Contents

CHAPTER 1: INRODUCTION	1
1.1 Preamble	1
1.2 Rationale of The Study.....	2
1.3 Objectives	3
CHAPTER 2: LITERATURE REVIEW	4
2.1 Background	4
2.2 River System of Chittagong Region.....	4
2.3 Halda River	8
2.3.1 Geo-Morphological Characteristics	9
2.3.2 Significance Aspect of Halda	9
2.4 Project Infrastructure in Halda River.....	11
2.4.1 Karnaphuli Irrigation Project (Halda Unit)	11
2.4.2 Halda Extension Sub-irrigation Project	11
2.4.3 Dhurung irrigation project.....	11
2.4.4 Bhujpur rubber dam	12
2.4.5 Halda River Restoration Project	12
2.5 Previous Studies in Halda River System	13
2.6 Oblation of Geospatial Technology	16
2.6.1 Remote sensing	16
2.6.2 Geographic Information System.....	17
2.6.3 Landsat	17
2.7 Land use/Land cover	18
2.8 Land Use Land Cover Change	19
2.9 Land Cover and Land Use Data from Remotely Sensed Data.....	20
2.10 Google Earth	20
2.11 Google Earth Engine	21
2.12 Multidimensional use of Google Earth Engine	27
2.13 Normalized Difference Water Index (NDWI)	30
CHAPTER 3: MATERIALS AND METHODS	31

3.1 Description of The Study Area	31
3.1.1 Location	31
3.1.2 Physical environment.....	32
3.1.3 Biological environment.....	34
3.2 Data Source	34
3.3 Methods	35
3.3.1 Surface water mapping in Google Earth Engine	35
3.3.2 Mapping Occurrence Change Intensity	38
3.3.3 Mapping River Course Change in Google Earth.....	39
3.3.4 Land Use and Land Cover Change.....	40
3.3.5 NDWI Calculation	45
CHAPTER 4: RESULT AND DISCUSSION.....	47
4.1 Land Use and Land Cover of Halda Basin	47
4.1.1 Land use status of the study area from 1990-2015.....	47
4.1.2 Land use scenario of Halda Basin in 1990.....	47
4.1.3 Land use scenario of Halda Basin in 2015.....	48
4.1.4 LULCC assessment of Halda Basin from 1990 to 2015.....	48
4.1.5 Overall accuracy and Kappa (K^*) statistics for 1990 and 2015 supervised classification	51
4.2 NDWI Over the Region	51
4.2.1 NDWI in 1990	52
4.2.2 NDWI in 2015.....	62
4.2.3 NDWI Change Over 1990 to 2015	52
4.3 Water Transition Over Various Region of Halda.....	56
4.4 Measuring erosion and accretion.....	62
4.5 Occurrence Change Intensity	63
4.6 Mapping Changes in the River Course.....	65
4.6.1 Changes in the Length of the river	65
4.6.2 Changes in the Width of the river.....	65
4.6.3 Changes in the number of bends	69

CHAPTER 5: CONCLUSION AND RECOMMENDATIONS	70
5.1 Recommendations	71
5.2 Limitations of the study	71
REFERENCES	73
APPENDICES	83
APPENDIX 1: Error Matrix showing accuracy of 1990 supervised classification of land uses of Halda Basin.....	83
APPENDIX 2: Error Matrix Showing Accuracy Of 2015 Supervised Classification of Land Uses of Halda Basin	83
APPENDIX 3: Screenshot of Transition classes in Halda Basin	84

List of Tables

Table 1: Visualization parameters for Map.addLayer()	25
Table 2: Co-ordinate of location where river width was calculated	40
Table 3: Land Use classes of 1990 and 2015.....	48
Table 4: Land Use Change (2015-1990)	51
Table 5: Overall classification accuracy and Overall kappa statistics of supervised classification of 1990 and 2015 imageries of Halda Basin.....	51
Table 6: Comparison of water cover in NDWI with LULC	52
Table 7: LULC of unions and population density.....	60
Table 8: Water transition class with area and percentage	61
Table 9: River course changing points	65
Table 10: River Width Change in 2001, 2009 and 2018	69

List of Figures

Figure 1: Diagram of components of the Earth Engine Code Editor	23
Figure 2: Map of study area.....	31
Figure 3: Procedure of satellite image classification	41
Figure 4: Procedure of layer stacking	42
Figure 5: Procedure of clipping	42
Figure 6: Procedure of supervised classification	43
Figure 7: Procedure of final map preparation using Arc GIS	43
Figure 8: NDWI calculation process.....	46
Figure 9: Land Use and Land Cover of 1990	49
Figure 10: Land Use and Land Cover of 2015	50
Figure 11: Normalized difference water index in 1990	54
Figure 12: Normalized difference water index in 2015	55
Figure 13: Transition class over various region of Halda River.....	57
Figure 14 (a): LULC of Guman Mardan and Samitirhat	58
Figure 14 (b): LULC of Gahira and Garduara	58
Figure 14 (c): LULC of Gahira and Mekhal	59
Figure 14 (d): LULC of West Guzara and North Madarshah	59
Figure 14 (e): LULC of Ward no. 5 and Noapara	60
Figure 15: Area occupied by each transition class	62
Figure 16: Occurrence change intensity over Halda river.....	64
Figure 17: Halda river with adjacent Unions	66
Figure 18: Shifting of Halda River from 2001 to 2018.....	67
Figure 19: River Width fluctuation on different points	68
Figure 20: Part 1 (Halda Basin)	84
Figure 21: Halda basin (Part 2).....	85
Figure 22: Halda Basin (Part 3)	85

List of Abbreviations

AEZs	Agro-ecological Zones
ALOS	Advanced Land Observing Satellite
API	Application Programming Interface
BBM	Building Block Method
BWDB	Bangladesh water development board
CHT	Chittagong Hill Tracts
CIA	Central Intelligence Agency
CSS	Cascading Style Sheet
CVM	Contingent Valuation Method
DEM	Digital elevation model
ERC	European Research Council
ERDAS	Earth Resource Development Assessment System
ETM	Enhanced Thematic Mapper
GBM	Ganges-Brahmaputra-Meghna
GEE	Google Earth Engine
GIS	Geographic information system
GloVis	Global Visualization Viewer
HTML	Hypertext Markup Language
HYV	High yield variety
IDE	Interactive Development Environment
JRC	Joint Research Centre
LGED	Local Government Engineering Department
LULC	Land Use and Land Cover
MLC	Maximum likelihood classification
MODIS	Moderate Resolution Imaging Spectrometer

NASA	National Aeronautics and Space Administration
NDVI	Normalized Difference Vegetation Index
NDWI	Normalized Difference Water Index
NGO	Non-Governmental Organization
NIR	Near Infrared
NOAA AVHRR	National Oceanographic and Atmospheric Administration Advanced Very High-Resolution Radiometer
NUACI	Normalized Urban Areas Composite Index
OLI	Operational Land Imager
OLI	Operational Land Imager
Roi	region of interest
RPI	River Pollution Index
SDG	Sustainable Development Goals
SLC	Scan line corrector
SNR	Signal-to-noise
SPOT	Satellite for Observation of Earth
SRTM	Shuttle Radar Topography Mission
TIRS	Thermal Infrared Sensor
TM	Thematic Mapper
UCSF	UC San Francisco
USGS	United States Geological Survey
WTP	Water Treatment Plant

ABSTRACT

Bangladesh is considered the largest delta formed by sediments carried by its very active river system consisting of hundreds of rivers. Erosion and accretion are severe due to the dynamic nature of river system. Measuring erosion and accretion by site inspection or satellite imagery is cumbersome and time consuming. It can be measured through global surface water database which is reliable and produce less trouble. We took Halda, as a case to identify erosion and accretion site and quantify how much changes has occurred between 1984 to 2015 from Global Surface Water database developed by European Joint River Commission. Halda is a very important river due to its role as the spawning ground for major Indian carps. Anthropogenic activities accelerate river course change which can hinders significant aspect of Halda river. An effective combination of Google Earth Engine, Google Earth, Land use and NDWI water classes give us the clear idea how Halda river as well as its basin changes over time and helps to identify the most vulnerable sites. Google earth engine generates the surface water map layer considering changes over Halda river in 32 years of study period and divides it into many transition classes. From those classes new permanent and new seasonal water body denotes the total land undergone to river within this period which is 118 ha. While lost permanent and lost seasonal water helps to measure the accreted land area which is 163.02 ha. Water change intensity map shows the region where 100% water gained and lost over the periods by which river course change was observed. To measure the recent trend of river course change, I considered three parameters: length, width, bends by drawing a middle line of river for 2001, 2009 and 2018 in google earth. These two results have shown that, the river course is continuously changing due to erosion and accretion at river bank. Land use and Land cover class along with NDWI for starting and ending periods of database was calculated to capture the amount of water body at Halda basin, both observed a decreasing trend of water body, 0.3% and 0.11% lost respectively. There is scope to improve this study by improving database and analytical algorithm as well as by using higher resolution images. This research will contribute to take protective measures by the authority at specific vulnerable sites identified. The research indicated increasing sedimentation of Halda which could be linked to the loss of vegetation in the Halda basin and immediate measures should be taken to afforest the entire basin quickly. Anyone can apply this approach to other big rivers in Bangladesh to estimate erosion and accretion.

CHAPTER 1: INTRODUCTION

1.1 Preamble

Water resources are critical in promoting sustainable development, as they support human communities, maintain the functions of ecosystems, and ensure economic growth (Connor, 2015) for which a goal of SDG, Goal 6 has been dedicated to clean water and sanitation (Hoekstra et al., 2017). Surface water is the major source of water on which the entire biosphere is dependent. As a land cover type, it plays an important role in climate regulation, biogeochemical cycling, and surface energy balance, among many others (Carroll et al., 2016). In recent decades, many countries, especially developing countries, have experienced rapid urbanization (Goldblatt et al., 2016). Changes in surface water caused by human activities strongly affect surface temperature, erosion, accretion, soil moisture, biological diversity, ecosystem functioning, and even human wellbeing (Koning, 2005; Pekel et al., 2016). Therefore, monitoring the dynamics of surface water and surface water resources is of great importance for natural environmental health and sustainable economic development (Li et al., 2018).

Every year erosion and sedimentation in the river system of Bangladesh causes dramatic change in water occurrence and surface water sources, distribution and morphology (Takagi et al., 2007). Due to its geographical location in GBM deltaic area, the river system of Bangladesh experiences dynamic morphological changes throughout the year. About 7% of the land area of Bangladesh is covered by rivers, streams and canals having an aggregated length of with 24,000 km (Mondal and Water, 2001; Pekel et al., 2016) Every year the Ganges and Brahmaputra rivers in Bangladesh transport 316 and 721 million tons of sediment, respectively and these high loads of suspended sediment reflect the very high rate of denudation in their drainage basins (Islam et al., 1999). Although Bangladesh receives a larger volume of sediment than any other comparable coast anywhere in the world, some sections of its shoreline are experiencing very rapid erosion (Sarwar and Woodroffe, 2013). Overall estimated accretion and erosion of the coast was 315.5 km² and 306.8 km², respectively between 1989 and 2009 (Sarwar and Woodroffe, 2013). The morphology of the coastal zone of Bangladesh coastal is quite unstable with simultaneous erosion and accretion due to variation of river flow, sediment load (Shibly and Takewaka, 2012) and wave action is a common phenomenon here (Hassan et al., 2017). The long-term history of the water-surface of the

planet shows that total global surface water has increased over the past three decades, with over 1,80,000 km² of new permanent water bodies forming in some parts of the planet and almost 90,000 km² of permanent surface water disappearing from other areas (Pekel et al., 2016).

Based on over three million satellite scenes collected between 1984 and 2015, the Global Surface Water Explorer (Global Surface Water Explorer, 2019) database was produced by using google earth engine platform by European Research Council (ERC) which enable users to scroll back in time to measure the changes in the location and persistence of surface water globally, by region, or for a specific area (Pekel et al., 2016). This database facilitates in identifying permanent, new permanent, lost permanent, seasonal, new seasonal, lost seasonal, seasonal to permanent, permanent to seasonal, ephemeral permanent and ephemeral seasonal waterbody over a specific region. Here new permanent water surfaces refer conversion of land into permanent water which is erosion and lost permanent water surfaces means conversion of permanent water into land which is accretion.

The conventional technique for identifying and quantifying erosion and accretion area of river bank is using remotely sensed satellite imagery to predict and estimate river morphology. For longer time period, this process requires a wide range of high-resolution satellite imagery which is time consuming and cumbersome. The European Commission's Joint Research Centre (JRC) developed a new water dataset which maps the location and temporal distribution of water surface at the global scale over the past 32 years and provides statistics on the extent and change of those water surface. Classification performance, measured using over 40,000 reference points confirmed that the classifier produces less than 1% of false water detections, and misses less than 5% of water (Pekel et al., 2016). This dataset can be used to identify the accreted and eroded land based on water occurrence and change intensity.

1.2 Rationale of The Study

Halda river is a unique river located in Chittagong and it has gained extensive media attention and hence the attention of general mass and policy makers altogether due to its significance as the only tidal river in the world that serves as the natural spawning ground the genetically pure major Indian carps (Kabir et al., 2015a). However, the river is under severe anthropogenic pressure and pressure from the water extraction and dwindling water flow due to land use changes in the upper watershed of the river (Akter and Ali, 2012a; Islam et al., 2017) There had been serial publication of scientific

literature on Halda river in recent time. However, no effort has been discerned regarding the analysis of the changes in its direction of flow in relation to the changes in water surface area associated with this unique river. Global Surface Water database would be useful to assess the erosion and accretion over 1984 to 2015 in Halda River, so that we can save our time as well as ensure the maximum accuracy.

In the absence of any effort aiming to measure erosion and accretion from JRC dataset, this research undertakes the task of estimating eroded and accreted river bank area from surface water occurrence over 1984 to 2015 time periods for Halda river. Besides, the land use classification of the river watershed was done in order to relate the changes in water course to land use changes. In addition, the NDWI of the basin area was calculated to see the overall condition of the surface water in the area. The outcome of the research is crucial since an up-to-date knowledge of erosion and sedimentation would help in ensuring remedial measures are taken well in advance so that the reservoir operation schedules can be performed for optimum utilization. Again, to ensure better management of eroded and accreted land, this research considered pre-developed geo-spatial dataset so that we can save our time and can provide better efficiency.

1.3 Objectives

Accordingly, the major objectives of the current research included:

- 1 Estimation of river bank erosion and accretion by quantifying river surface water transition between 1984 and 2015.
- 2 Mapping river course changes of Halda river over 2001 – 2018 to capture the recent trend of river.
- 3 Land use and land cover classification along with NDWI based surface water classification to count the water covered area of starting and ending year and contextualize it to the river course changes.

CHAPTER 2: LITERATURE REVIEW

2.1 Background

Bangladesh is bestowed with its one of the largest river networks in the world with about 700 rivers including their tributaries. The large rivers are the Padma, the Meghna, the Jamuna, the Teesta, the Meghna, the Brahmaputra and the Surma. Including their thousands of tributaries the total length of rivers is about 24,140 km (Alam, 2001). Being a deltaic country, those rivers following through various sections of the country consists of tiny hilly streams, seasonal creeks, muddy canals, some magnificent rivers and their tributaries and distributaries (River and Drainage System - Banglapedia, 2014).

The watercourses of the country are obviously not evenly distributed. They increase in numbers and size from the northwest to northern region to the southeast to southern region. Bangladesh has predominantly four major river systems – (1) the Brahmaputra-Jamuna, (2) the Ganges-Padma, (3) the Surma-Meghna and (4) the Chittagong region river system. Among those, Brahmaputra is the 22nd longest (2,850 km) and the Ganges is the 30th longest (2,510 km) river in the world (River - Banglapedia, 2015).

River valleys are important centers of civilization, provides travel routes and alluvial soils for good agricultural lands. Navigable rivers are of economic importance and influence location of cities (Chatterjee and Prasad, 2011). In Bangladesh, almost all the major cities/towns and commercial centers are located on the bank of rivers, eg, Dhaka beside Buriganga, Narayanganj beside Shitalakshya, Chittagong beside Halda-Karnaphuli and Mymensingh by the side of Brahmaputra.

2.2 River System of Chittagong Region

The Chittagong region consists of the 5 hilly districts of Chittagong division - Chittagong, Cox's Bazar, Bandarban, Rangamati and Khagrachhari. It is bounded by the Bay of Bengal on the south and west, the Naf river with Myanmar on the southeast, and India on the east. The region is characterized by three distinct ecological zones: inter-tidal zone, coastal plains and extensive hill areas (Chittagong Region River System - Banglapedia, 2014) The northern and eastern parts of the region constitute the hilly areas and are commonly known as the Chittagong Hill Tracts (CHT). The coastline consists of a 100 km long sandy sea beach on the Bay of Bengal. The remainder of the region consists of plains. The total area is approximately 19,956 sq. km with a hilly area of

1,300 sq km (Chittagong Region River System - Banglapedia, 2014) . The major rivers of this region are: Karnaphuli and its tributaries (eg Rainkhiang, Kasalong, Halda, Ichamati etc); Bakkhali, Sangu, Matamuhuri, Naf, and Feni. Kutubdia and Maheshkhali channels are the coastal channels of the region.

Karnaphuli is the principal river of the region. It originates in the Lushai Hills of Mizoram (India), flows through Rangamati and the port city of Chittagong and discharges into the Bay of Bengal near Patenga. A number of streams flow upstream of Rangamati. The streams are: one originating near Thekamukh in Mizoram-Bangladesh border flowing through Harina, barkal and Sublong; one originating at Marishwa through Myanmukh and Langadu till reaching Subhalong; one flowing through Dangumura to Myanmukh; and one flowing through Mahalchhari to Rangamati. The streams meet near Rangamati and their combined flow is known as Karnaphuli. The river is flashy and its length is about 131 km. Rainkhiang, Sublong, Thega, Kasalong, Ichamati and Halda are its main tributaries. Its major distributaries are Saylok and Boalkhali (Chittagong Region River System - Banglapedia, 2014).

The only hydropower station of the country was built by constructing a dam on this river at Kaptai. The Karnaphuli is navigable at Barkal and Kaptai but above Barkal it is shallow. With the construction of the Kaptai dam, this river has been blocked, and a large artificial lake has been created, and the bed of the river has also been much widened. This man-made lake provides a network of all-weather navigable routes in the area. Downstream of the dam the Karnaphuli receives very little water in the dry season. The opening of the sluice gates of the dam creates water movement from the lake downstream. The river finally discharges into the Bay of Bengal. The port city of Chittagong is situated at the mouth of the river. Bangladesh water development board (BWDB) collects water level data through its 3 hydrometric stations located at Kodala, Chittagong and Patenga (Banglapedia, 2015).

Rainkhiang

A number of small streams originating from the eastern hills of Mizoram (India) meet together at the uppermost part of the Rainkhiang reserves (Rangamati) are known as Rainkhiang. The river makes a torturous journey through the deep reserve forests and falls into Kaptai Lake near Belaichhari (Rangamati) about 30 km above Rainkhiangmukh, its original place of confluence with the Karnaphuli. The river is flashy and is 77 km long. During the wet season it is navigable

up to Gobachharimukh but further above it is used only for floating timber tree and bamboo (Banglapedia, 2015).

Thega

One of the main tributaries of the Karnaphuli. It meets the Karnaphuli above Barkal and Subhalong and finally drains into Kaptai Lake (Banglapedia, 2015).

Kasalong

A number of small streams originating in the eastern hills of Mizoram (India) meet at Baghaichhari (Rangamati) to form Kasalong river. It falls into Karnaphuli (Kaptai Lake) at Kedarmara. It is a flashy river and has a length of 65 km (Banglapedia, 2015).

Halda

It originates in the Batnatali hills of Khagrachhari. It flows south and meets the Karnaphuli near Madhunaghat (Chittagong). It is a flashy river and is 88 km long. BWDB has 13 hydrometric stations on it, and data are available since 1959 (Banglapedia, 2015).

Ichamati

A number of small streams meeting near Kawkhali (Rangamati) forms the Ichamati. It is a small tributary of the Karnaphuli and has a length of 30 km. It falls into the Karnaphuli near Rangunia (Chittagong). It is also a flashy river. BWDB has 3 hydrometric stations on this river, and data from 1956 are available (Banglapedia, 2015).

Bakkhali

A number of small streams originating in the southeastern hills of Mizoram meets the Naikhongchhari of Bandarban district to form the Bakkhali. It flows through Naikhongchhari and Ramu of Cox's Bazar district and falls into Maheshkhali channel. This is also a flashy river and has a length of about 67 km (Banglapedia, 2015).

Myani

A number of small streams originating in the eastern hills of tripura (India) meet near Dighinala of Khagrachhari district. The combined flow is known as Myani River. The river flows through

Dighinala and Langadu (Rangamati) and falls into Kaptai Lake near Kedamara (Rangamati). It is 91 km long and flashy (Banglapedia, 2015).

Chingri

A number of small streams originating in the eastern hills of Tripura (India) meet at Panchhari (Khagrachhari). The combined flow, known as the Chingri, flows south through Panchhari, Khagrachhari, Mahalchhari (Khagrachhari) and falls into Kaptai lake near Nannerchar (Rangamati). This is also a flashy river and has a length of about 85 km (Banglapedia, 2015).

Sangu

Sangu originates in the Arakan Hills of Myanmar and enters Bangladesh near Remarki (Thanchi upazila of Bandarban district). It flows north through Thanchi, Rowangchhari and Bandarban upazilas of Bandarban district. Then it flows west through Satkania and Banskhali upazilas of Chittagong district to meet the Bay of Bengal near Khankhanabad (Chittagong). The length of the river is 295 km. The major tributaries of the river are Chandkhali Nadi and Dolu khal. There are 7 BWDB hydrometric stations on this river and data are available from 1965 (Banglapedia, 2015).

Matamuhuri

This is a flashy river that originates in the Moyvar hills of Alikadam (Bandarban). It flows northwest through Alikadam and Lama upazilas of Bandarban and Chakaria of Cox's Bazar. The river discharges into Maheshkhali channel near Saflapur (Chakaria, Cox's Bazar). The length of the river is 148 km. Yanchha khal and Bamu khal are its important tributaries. BWDB has 2 hydrometric stations on this river and data are available from the year 1956 (Banglapedia, 2015).

Naf

It flows along the southernmost border line of the country. It originates in the northern hills of Myanmar and enters Bangladesh near Palong Khali of Ukhia upazila of Cox's Bazar district. The river flows through Ukhia and Teknaf and discharges into the Bay of Bengal near Sabrang (Teknaf upazila, Cox's Bazar). Most of the downstream reach of the river demarcates the Myanmar-Bangladesh border. The river is 62 km long. BWDB has one hydrometric station on the river at Teknaf and data from 1968 are available (Banglapedia, 2015)

Feni

Originates in the eastern hills of Tripura and enters Bangladesh at Belchhari of Matiranga upazila of Khagrachhari district. It flows through Ramgarh (Khagrachhari), Fatikchhari (Chittagong) and then flows along the border of Chittagong (Mirsharai upazila) and Feni (Chhagalnaiya, Feni, Sonagazi upazilas) districts and discharges into the Bay of Bengal near Sonagazi. The length of the river is 108 km. BWDB has 6 hydrometric stations on the river and data are available from 1958 (Banglapedia, 2015).

2.3 Halda River

Halda River is one of the major rivers in the South-East region of Bangladesh and the third main river of Chittagong after Karnaphuli and the Sangu ($22^{\circ}28'56.09''$ North & $91^{\circ}54'07.62''$ East), is a resourceful River of Bangladesh which provides as a source of drinking water supply, income source of adjacent fishermen, natural spawning ground for major Indian carp, a hotspot for biological diversity, place for tourism and so on (Akter and Ali, 2012a).

Originating from Halda chora at the area of 2 no. Patachora union in Ramgarh Upazila under Khagrachari District (Former Chittagong Hill Tracts), Bangladesh, it flows through Fatikchhari, Hathazari and Raozan Upazilas and Chandgaon Thana, and falls into the Karnaphuli River near Kalurghat area (Halda River, 2012). This river is famous as a breeding ground for pure Indian carp fish populations (Ronald WR Patra and Azadi, 1985a). As tidal River, this is the only river in the world where fishermen can collect fertilized eggs directly (Azadi, 2004). Halda river also provides navigation, drinking water supply, and generates a unparallel number of employment opportunities for the local communities (Kabir et al., 2015b).

The Halda is a potential contender for world natural heritage, as it is the only freshwater tidal river in the world that serves as the pure natural gene bank of major Indian carps (Azadi, 2004). It has a very turbulent tributary, the Dhurung River, which rises in the Pakshmimura ranges in the Hill Tracts, traverses the whole of Fatikchari Upazilla, runs almost parallel to the Halda in the east, and joins at Purba Dhalai about 48.25 km downstream. In this way, it plays a vital role in economic and commercial activities. The major environmental issue are salinity intrusion, sand mining in River mouth that might result in changes in river morphology and hydrodynamics and industrial untreated solid and liquid wastes into this river (Akter and Ali, 2012a).

2.3.1 Geo-Morphological Characteristics

Width and depth of Halda river have reduced in many places due to siltation. Width of the river is 50m and 300m in different places and in the rainy season (May-October) water depth ranges from 2m to 10m. Erosion, siltation, submerged sand bars and decreased depth have destroyed the grazing, spawning and nursery habitats of major carps. Moreover, migration routes of fishes were blocked by constructing sluice gates on 12 main feeder canals. The feeder canals are Sarta, Boalia, Chankhalee, Sonai, Kagtia, Parakhalee, Mogdair, Amtua, Madari, Boijjakhalee, Maduna and Krishnakhalee.

2.3.2 Significance Aspect of Halda

The Halda River as a breeding ground

The tidal river, Halda, is the renowned breeding ground in the world from where naturally fertilized eggs of major Indian carps i.e., Catla (*Catla catla*), Mrigal (*Cirrhinus mrigala*), Rui (*Labeo rohita*) and Kali Baush (*Labeo calbasu*) are culled and hatched by the local egg collectors and fishermen during April to June every year with their traditional and instinctive intelligence developed from generation to generation (Alam et al., 2013; Zaman, 2014). The river is also one of the major sources of freshwater shrimp (*Macrobrachium rosenbergii*). The collected eggs are hatched in artificial mud-made scoop on the riverbank to produce carp fries (Azadi and Arshad-ul-Alam, 2011). Oxbow cutting, 12 sluice gates, constructed on the 12 tributaries of the Halda River, and embankment made by the Bangladesh Water Development Board for irrigation and flood control purposes (Zaman, 2014) causes hampered local movement and migration of fish which tremendously reflected in the reduction of egg collection and fry production in the subsequent years. Over fishing and indiscriminate killing of brood fish reduce the fry production in recent times (Halda River - Banglapedia, 2015).

Economic value from Halda

Unlike other rivers, Halda has a great contribution to our national economy. It is one of the effectors of economic development of Chittagong region as well as whole country by becoming the means of productions and services such as fresh water supply, fish production, transportation, waste assimilation, recreation and tourism options etc. This River also facilitates navigation,

drinking water supply and generates an enormous employment opportunity for the local communities. In this way, it plays pivotal role in the local and the national income generation which makes this River a natural resource of immense economic value. Total 988 households in the vicinity of the Halda are directly or indirectly involved for their livelihood (Kabir et al., 2011). In one study, it was found that total value of tangible resources is 20.5 million US\$. Segmented contributions of fishing, fish fry, irrigation, drinking water, water transportation and sand extraction respectively were 0.07, 0.005, 15.78, 1.33, 0.12, 2.51 (US\$) (Kabir et al., 2013). Hatched fry is sold at BDT 40,000-60,000 kg⁻¹ by egg collectors (Saimon et al., 2016). In another study total indirect use value was found Tk. 29.50 million per year. The total non- use value was Tk. 31.46 million which comprised of bequest value of Tk. 14.85 million and option value of Tk. 16.61 million (Kibria et al., 2015). Again, it has a huge contribution to national economy by prawn catching, prawn post larvae catching, irrigation & industrial uses. The total economic worth of benefits derived from provisioning services of the Halda is approximately BDT (Bangladesh Taka) 1753 million. It is also found that total the value of this river is about 2971.85 US\$ (Kabir et al., 2011). A strong chain of economic activities revolves around this river round the year. The eggs collected by the local egg collectors of Halda, hatching them by their indigenous techniques, selling the fry, the broods produced and the fish grown from these broods contribute to our national economy about Tk. 800 crore (Rony et al., 2016; Saimon et al., 2016; Zaman, 2014).

Source of water

The Halda River is one of the major sources of fresh water for the port city of Chittagong. This River also plays important roles in domestic water supply, agriculture, industry and navigation. The Halda River supplies about 50% (90×106 L/d) treated water to the Chittagong City Corporation area. About 30% of the river basin inhabitants are directly involved in agriculture; the river water is supplied for irrigation by single lifting, using the low-lift pump for high yield variety (HYV) rice cultivation during the dry season (Akter and Ali, 2012b).

Industrial use

Main industrial use of the Halda is considered as a Water Industry for Drinking water of 6 million people of Chittagong City. Furthermore, this river is acted as way of water transportation for collection of soil for brickfields. At the same times, these brickfields use the water of this river as a raw material of brick processing. Near about 22 brickfields are found on two banks of the river.

Most of them are solely dependent on Halda for raw material transportation and source of raw material (Kabir et al., 2016).

2.4 Project Infrastructure in Halda River

Bangladesh Water Development Board has taken several projects to enhance agricultural production in this area since 1960s. In addition to these massive irrigation projects, several other smaller schemes have also been implemented in this area. The brief descriptions of important projects are provided below:

2.4.1 Karnaphuli Irrigation Project (Halda Unit)

BWDB undertook Karnaphuli Irrigation project for providing irrigation, flood control and drainage facilities to the farmers. The project period was 1975-76 to 1985-86. The net agricultural land under Halda unit is 15380 ha (Kibria et al., 2015). The area under Halda unit is situated on the wide, flat plains of the lower Halda and includes parts of Raozan and Hathazari upazilla of the Chittagong district. Water control structures were built at the outfalls of streams. During high tide, when the water level in the river is higher than in the streams, the water flows through the gates from the river to the streams which are used for irrigation (BWDB, 2017).

2.4.2 Halda Extension Sub-irrigation Project

This is an important project of BWDB in the study area which is located near Sattarghat, Chittagong with an irrigable area of 1,820 ha (Kibria et al., 2015). Part of Mekhol, Hathazari and Dhalai Unions and Charia and Mirzapur Unions of Hathazari Upazila are within the project area. The objective of the project was to increase agricultural production by reducing crop losses due to flash flood and by increasing land area under high yielding crops (Kibria et al., 2015). The concept of the project was to supply water in the Boalia khal by pumping from the river Halda. A regulator was built at the outfall of Boalia. During dry season, pump was used to supply water into the khal from river (BWDB, 2017). Moreover, Halda Parallel Khal Project was taken to construct the incomplete components of the Halda Irrigation Extension Sub-project in 2004 (Zaman, 2014).

2.4.3 Dhurung irrigation project

This project was taken to provide irrigation facilities in 1953-54 and the work was completed in 1962-63. The area is situated at a distance 45 km from the North of Chittagong city in Fatikchari Upazila. The area covered by this project is 1956 hectares in Sundarpur, Doulatpur, Rosangiri,

Shomitir Hat and Dhurang Unions of Fatikchari Upazila. Embankments were built on the two sides of the khal, which protect the adjacent area from flood and also improve the connectivity of the village area (BWDB, 2017).

2.4.4 Bhujpur rubber dam

A 65.00 m long rubber dam was constructed on the Halda by LGED (Kibria et al., 2015) at Bhujpur of Fatikchari at the upstream of the Fatikchari Khal to provide irrigation. The construction of the dam was completed in 2011 and is in operation since that year. During dry season, a large part of upper Halda becomes dry due to very low flow of water and rainfall. The natural flow of water has been hampering due to blockage of water by rubber dam (Kabir et al., 2011).

2.4.5 Halda River Restoration Project

Halda River Restoration Project within Raozan and Hathazari Upazilla is under the Department of Fisheries. The implementation time was from 2006 to 2011 which was extended up to June 2014. The objective of the project was to protect and develop the natural carp breeding ground of Halda, to develop an institutional framework with the participation of local people for protecting natural carp breeding ground of Halda and to create alternative employment opportunity for related people during fishing prohibited season (Ghose, 2014). The target of the project was to increase carp fry production up to 5000 kg per season. The activities included declaring and establishing fish sanctuary, dredging the river to increase navigability, restoring bends of the river, construction of overhead tank and installation of pumps for cistern (constructed for hatching collected eggs), hiring ponds adjacent to Halda to produce fish fry there which will later be released to the river to increase fish population in the river (Kibria et al., 2009). However, at the end of the project the major activities completed, as reported in Halda river restoration project summary published by Department of Fisheries (Ghose, 2014), were : (1) training, awareness raising workshop, meeting, seminar; (2) tree plantation; (3) construction of hatching unit; (4) placement of bill board and signboard; (5) digging pond; (6) construction of boundary wall; (7) providing loan for alternative employment to fishermen and beneficiaries; and (8) baseline survey of beneficiaries.

2.5 Previous Studies in Halda River System

A number of studies have been accomplished on the river Halda, on its limnology and spawning biology of carps (Azadi, 1979; Ronald WR Patra and Azadi, 1985; Tsai et al., 1981); hydrological factors influencing spawning of carps (Ronald WR Patra and Azadi, 1985b); ecology of plankton (Patra and Azadi, 1987); fish resources including fish diversity and Ichthyofauna (Alam et al., 2013; Azadi and Alam, 2013; Azadi and Arshad-ul-Alam, 2011); fishing intensity (Arshad-Ul-Alam, 2013); fishing gears efficiency (Arshad-Ul-Alam and Azadi, 2015). Moreover, hydro-morphological characteristics, environmental flow requirements and water quality including heavy metals in water and sediment (Akter and Ali, 2012a; Bhuyan and Bakar, 2017; Fubara-Manuel and Jumbo, 2014) and subsequent economic valuation(Kabir et al., 2011, 2013; Kibria et al., 2015); marketing channels Indian carp fry and livelihood of the fry traders (Saimon et al., 2016); ecosystem services from the river (Kibria et al., 2015) also conducted on the river.

Unit hydrographs at Narayanhata, South Sunderpur and Panchpukuria stations in the Halda river and a formula for peak flood discharged at South Sunderpur was developed (Badiuzzaman, 1978) that sometimes shows that peak floods of Halda is in the upstream at Narayanhata and that at South Sundarpur are not closely related because of the difference in drainage area characteristics.

Flood tides influence the spawning of major carps in the Halda River and most of the spawning occurred in low velocity water, at or near the high tide, and the water level related to the spawning in Sonairchar oxbow-bend ranged from 1.5–4.5 m (Tsai et al., 1981). But the Telpari and Enayethat stations were found not to satisfy a water depth of 1.5–4.5 m in each month throughout the year for fish spawning. Some engineering works and water management schemes i.e. canalization, dikes and other regulation are affecting the spawning habitat also noted in this study.

Some hydrologic observations with physio-chemical parameters i.e., heavy rainfall, high water level, high water current (14-65 cm/sec), and high turbidity (400- 2150 ppm), comparatively low water temperature (25-28°C), low conductivity (35.9-168.98 μ -mhos), low DO content (6-9 ppm) and pH (6.2- 6.8) manipulating on the spawning ecology of the major carps in the Halda River during the spawning season from late April to June 1978 recorded (Ronald WR Patra and Azadi, 1985). The spawning was supported not be any single factor, but a combination of environmental conditions enkindling the biological process concluded in this study.

The physical and chemical conditions of the Halda River with respect to their annual variation and the degree of correlation among them were investigated (Ronald WR Patra and Azadi, 1985b). Samples were collected from 4 points i.e. Satterghat, Sonai Khal, Mogdal Khal and Madari Khal from October 1977 to September 1978. Physical conditions of water were comparatively turbulent in summer and monsoon months due to the high current velocity, turbidity and water temperature. Most of the values with respect to chemical measurements were high in winter months. Significant direct or indirect correlations were found among most of the factors.

Ecological studies on the planktonic organisms of the Halda River recorded (Patra and Azadi, 1987) . While working on Halda River, they investigated phytoplankton and zooplankton and also found that the growth cycle on zooplankton was lesser than phytoplankton abundance. A study recorded 92 species (83 fin-fishes and 9 prawns) of the Halda River from January 2007 to December 2008 (Azadi and Arshad-ul-Alam, 2011). Some marine fishes entered the estuary occasionally. Suggestions are provided for protection, conservation, and sustainable yield of the fish population of this river. A research work was conducted for the assessment of fish distribution and biodiversity status in the upper 50 km of the Halda River from Nazirhat bridge to Garduara in which 63 species under 24 families were filed and 5 out of 63 species are immigrant species from the sea in the upper Halda (Alam *et al.*, 2013). But no previous number of migrated marine species to the freshwater was recorded in this study. Another study documented 83 species of fish under 35 families and 10 species of shellfish belonging to 3 families with a sum of 93 species of finfish and shellfish from the Halda River (Azadi and Alam, 2013). However, no published account was found about the finfish and shellfish of the river before major establishment of different govt. irrigation project like 1 rubber dam, 12 sluice gates etc. to compare the diversity of the river.

The fishing gear and intensity of different fishing gears of the Halda River for two years' period was investigated (Arshad-Ul-Alam, 2013) . No research work on the illegal use of fishing gears and craft is found during the banned period declared by the govt. The catch efficiency of fishing gears and estimated the Catch per unit effort (CPUE) for each gear type investigated in the river Halda (Arshad-Ul-Alam and Azadi, 2015) which is important before implementation of fish sanctuary declaration and also divided fishermen into four classes. They are- professional, subsistence, recreational and neo-professional.

There is a study on environmental flow requirements in the Halda River using statistical estimation technique [Building Block Method (BBM) and the Log-Pearson Type III (LPIII) distribution] (Akter and Ali, 2012b). The daily water level data only at Panchpukuria, Telpari, Enayethat and Narayanhat stations and the monthly flow data at Panchpukuria station, and the water quality data only at Mohra Water Treatment Plant (WTP) intake point and Madunaghat Bridge site were collected and used for this study. This study suggested that 1.5 m as minimum water level can be set to ensure satisfactory fish spawning in this river. The results of flow and quality analyses show that both physical degradation and chemical pollution occur in the river, indicating that environmental flow requirements cannot be achieved throughout the year. Moreover, present situation of fresh water flow along with environmental consequences during dry season need to be analyzed, a rubber dam in the upper stream of this river was built (Kibria et al., 2015).

The total economic value of tangible resources i.e. fish, fish fry, irrigation water, drinking water source, water transportation and sand extraction, of Halda is 20.5 million US\$. Policy makers should take into consideration the economic value of tangible resources of this river for its sustainable management was suggested by the study was calculated (Kabir et al., 2013). In another study, total indirect use value was found Tk. 29.50 million per year and total non- use value was Tk. 31.46 million which comprised of bequest value of Tk. 14.85 million and option value of Tk. 16.61 million (Kibria et al., 2015). Again, it has a huge contribution to national economy by catching of prawn, prawn post larvae catching, irrigation & industrial uses. It is also found that total the value of this river is about 2971.85 US\$ (Kabir et al., 2011). A study identified and listed different categories of ecosystem services biodiversity of the Halda River through the direct market price method and the (Contingent Valuation Method) CVM. About BDT 1.75 billion has been provided by this river as an economic value from its provisioning services (Kibria et al., 2015).

The engineering structure on this river has assessed (Kabir et al., 2013). The study tells that rubber dam is hampering the natural flow of water of Halda River due to blockage. As a result, siltation is occurring which consequently reducing the water holding capacity of the river and the river cannot catch all the water received from different tributaries of this river during rainy season due to lower depth. A study was conducted in Bangladesh about performance evaluation of rubber dam projects in irrigation development focusing on financial viability of the rubber dam projects. This study was used socio-economic indicator as a tool for analysis (Bhuyan and Bakar, 2017)

Water quality assessment from the two sampling sites of Kalurghat and Modhunaghat along this river was done to build a River Pollution Index (RPI). It stated that the water of the river is being polluted gradually due to anthropogenic activities of the inhabitants of the catchment (Bhuyan and Bakar, 2017). The contamination levels of heavy metals (Pb, Cd, Cr, Cu, Hg, Al, Ni, Co, Zn, Mn) in surface water and sediment of the Halda River of which were found above the permissible limit that are originated from industrial effluents, municipal wastes and agricultural activities have assessed (M. Bhuyan and Bakar, 2017). The mobility of metals was influenced by seasonal water flows/water discharge, which can cause significance effects on fisheries.

A significant change in land use and land cover of this catchment and also reported that agricultural land use has increased in its riverbank and catchment (Chowdhury et al., 2018). However, historical remote sensed that with lower resolution cannot discrete small land use changes that are relatively a new phenomenon in this region. As a result, a total change in the catchment did not covered to spell out the effect on river sediment load and siltation. (Akter and Ali, 2012b) estimated that about 30% of the river basin inhabitants are directly involved in agriculture. Another study recorded 34 watersheds of the Halda River from which major seven watershed areas namely: Manikchari Khal, Dhurang Khal, Sattar Khal, Fatikchari Khal, Harualchari Khal, Baromasi Khal, Mondakini Khal with different lengths, widths and depths which are directly fall in the river that should be conserved for sustainable ecosystem health management (Podder et al., 2017).

2.6 Oblation of Geospatial Technology

2.6.1 Remote sensing

Remote Sensing can be defined as any process whereby information is gathered about an object, area or phenomenon without being contact with it. Given this rather general definition, the term has come to be associated more specifically with the gauging of interactions between earth surface materials and electromagnetic energy (Eastman, 1999). A remote sensing device records response which is based on many characteristics of the land surface, including natural and artificial cover. An interpreter uses the element of tone, texture, pattern, shape, size, shadow, site and association to derive information about land cover (Eastman, 1999).

The generation of remotely sensed data by various types of sensor flown aboard different platforms at varying heights above the terrain and at different times of the day and the year does not lead to a simple classification system. It is often believed that no single classification could be used with

all types of imagery and all scales. To date, the most successful attempt in developing a general purpose classification scheme compatible with remote sensing data has been by (Anderson, 1976) which is also referred to as USGS classification scheme. Other classification schemes available for use with remotely sensed data are basically modification of the above classification scheme.

2.6.2 Geographic Information System

A computer assisted system for the acquisition, storage, analysis and display of geographic data (Eastman, 1999). GIS is defined as a computerized system capable of capturing, storing, analyzing and displaying geographically referenced information, that is, data identified according to location (Longley et al., 2010). The first GIS, Canada Geographic Information System, was developed in 1963 to analyze the data collected by the Canada Land Inventory and to produce statistics to be used in developing land management plans for large areas of rural Canada.

After four decades, the function of GIS has been greatly improved and it has been widely applied in resource management, marketing, geosciences, real estate, crime prevention, planning of health care faculties etc. The geographical data, which GIS handle, includes two main classes: geometric data and attribute data. Geometric data refer to location information of geographic features and are often in the form of map. Attribute data are descriptions, measurements and classifications of the geographic features (Longley et al., 2010).

2.6.3 Landsat

The Landsat program is the longest running enterprise for acquisition of satellite imagery of earth. On July 23, 1972 the Earth Resources Technology Satellite was launched. This was eventually renamed to Landsat. The images, archived in the United States and Landsat receiving stations around the world, are a unique resource for global change research and applications in Agriculture, Cartography, Geology, Forestry, Environmental Science, Regional Planning, Surveillance and Education (Herring, 2000).

Landsat 5 is the fifth satellite of the Landsat program. It was launched on March 1, 1984. It has a maximum transmission bandwidth of 85 Mbit/s. It was deployed at an altitude of 705.3 km. It takes some 16 days to scan the entire Earth. The satellite is an identical copy of Landsat 4 and was originally intended as a backup. It therefore carries the same instruments, including the Thematic Mapper and Multi-Spectral Scanner. The Multi-Spectral Scanner was powered down in 1995. Again, it was reactivated in 2012.

Landsat 7, launched on April 15, 1999. Landsat 7 was designed for five years and has the capacity to collect and transmit up to 532 images per day. It is in a polar, sun-synchronous orbit, meaning it scans across the entire earth's surface. With an altitude of 705 kilometers +/- 5 kilometers, it takes 232 orbits, or 16 days, to do so. The satellite weighs 1973 kg, is 4.04 m long and 2.74 m in diameter. Unlike its predecessors, Landsat 7 has a solid-state memory of 378 gigabits (roughly 100 images). The main instrument on board Landsat 7 is the Enhanced Thematic Mapper Plus (ETM+).

The Landsat 8 satellite was launched in February 11, 2013. Landsat 8 satellite images the entire Earth every 16 days in an 8-day offset from Landsat 7. Data collected by the instruments onboard the satellite are available to download at no charge from Earth Explorer, GloVis, or the Landsat look viewer within 24 hours of acquisition. Landsat 8 carries two push-broom instruments: The Operational Land Imager (OLI) and the Thermal Infrared Sensor (TIRS). The spectral bands of the OLI sensor provide enhancement from prior Landsat instruments, with the addition of two additional spectral bands: a deep blue visible channel (band 1) specifically designed for water resources and coastal zone investigation, and a new shortwave infrared channel (band 9) for the detection of cirrus clouds. The TIRS instrument collects two spectral bands for the wavelength covered by a single band on the previous TM and ETM+ sensors. Descriptions of the band designations for all Landsat sensors, and information about the comparisons between Landsat 8 and previous bands are also available. These sensors both provide improved signal-to-noise (SNR) radiometric performance quantized over a 12-bit dynamic range. Improved signal to noise performance enables better characterization of land cover state and condition. Products are delivered as 16-bit images (scaled to 55,000 grey levels). A quality assessment band is also included with each Landsat 8 data product. This band allows users to apply per pixel filters to the Landsat 8 Operational Land Imager (OLI)-only and Landsat 8 OLI/Thermal Infrared Sensor (OLI/TIRS)-combined data products (Landsat Missions Timeline | Landsat Missions, 2019).

2.7 Land use/Land cover

Land use is the purpose to which humans put land (Turner et al., 1994) or it is the human activities that are directly related to land, making use of its resources or having impact on it through interference in ecological process that determine the functioning of land cover. Usually land has been used for many purposes; it provides and creates space for agriculture and industrial production, as well as space for settlement. It is also the focus of conflict between a wide range of

land uses including agriculture, mining, forestry and nature protection, leisure, human settlement and urban and industrial development. Competition between users grows more under increasing population pressure and in countries with a mixed economy (Verheyen, 1997).

Land cover denotes the quantity and type of surface vegetation, water, and earth materials. Land cover can be conceptualized as the layer of soils and biomass, in particular vegetation, that covers the land surface. About 90% of the land surface of the earth is covered by vegetation of some sort. Light, temperature, energy, available water, natural or induced soil fertility are the determining factors. It seems necessary to accept or to establish an interrelationship between the different uses of land. It's needed to determine the present and future minimum requirements of land quantity and quality for the growing number of people and for sustainable life. Such investigations are required for global, regional and national levels (Turner et al., 1994).

2.8 Land Use Land Cover Change

Changes in the cover, use and management of the land cover have occurred throughout history in most parts of the world as the population has changed and human civilizations have risen and fallen. Land use affects land cover and changes in land cover affect land use. A change in either however is not necessarily the product of the other. Changes in land cover by land use do not necessarily imply degradation of the land. However, many shifting land use patterns driven by a variety of social causes, result in land cover changes that affects biodiversity, water and radiation budgets, trace gas emissions and other processes that come together to affect climate and biosphere (Riebsame et al., 1994).

Land cover can be altered by forces other than anthropogenic. Natural events such as weather, flooding, fire, climate fluctuations and ecosystem dynamics may also initiate modifications upon land cover. Globally, land cover today is altered principally by direct human use, by agriculture and livestock raising, forest harvesting and management and urban and suburban construction and development. There are also incidental impacts on land cover from other human activities such as forest and lakes damaged by acid rain from fossil fuel combustion and crops near cities damaged by tropospheric ozone resulting from automobile exhaust (Meyer, 1995).

Hence, in order to use land optimally, it is not only necessary to have the information on existing land use land cover but also the capability to monitor the dynamics of land use resulting out both

changing demands of increasing population and forces of nature acting to shape the landscape. Conventional ground methods of land use mapping are labor intensive, time consuming and are done relatively infrequently. These maps soon become outdated with the passage of time, particularly in a rapid changing environment. In fact according to (Olorunfemi, 1983), monitoring changes and time series analysis is quite difficult with traditional method of surveying. In recent years, satellite remote sensing techniques have been developed, which have proved to be of immense value for preparing accurate land use land cover maps and monitoring changes as regular intervals of time. In case of inaccessible region, this technique is perhaps the only method of obtaining the required data on a cost and time effective basis (Burrough, 1986).

2.9 Land Cover and Land Use Data from Remotely Sensed Data

Remote sensed data provides the capability to monitor a wide range of landscape biophysical properties important to management and policy, where information on these variables is needed in the past, present and future. However, remote sensed data are not capable to register the internal structural composition of the landscape, such as species composition of communities, soil chemical characteristics, soil management practices, etc. Remote sensed techniques need to be combined and complemented with in-situ measurements and modeling systems of terrestrial processes and climate (McVicar et al., 2003).

2.10 Google Earth

Google Earth is a virtual globe, map and geographical information program that was originally called Earth Viewer 3D created by Keyhole, Inc, a Central Intelligence Agency (CIA) funded company acquired by Google in 2004. It maps the Earth by the superimposition of images obtained from satellite imagery, aerial photography and Geographic Information System (GIS) onto a 3D globe. Google Earth displays satellite images of varying resolution of the Earth's surface, allowing users to see things like cities and houses looking perpendicularly down or at an oblique angle. Imagery resolution ranges from 15 meters of resolution to 15 centimeters. Most areas in Google Earth are only shown in 2D aerial imagery, but for other parts of the surface, 3D images of terrain and buildings are available. Google Earth uses digital elevation model (DEM) data collected by NASA's Shuttle Radar Topography Mission (SRTM) (Joseph, 2013).

2.11 Google Earth Engine

A variety of passive and active remote sensors with visible and microwave bands have been used to identify earth surface material and helped in acquiring valuable information by providing huge amounts of images that cover the Earth's surface over a period of 40 years (Alonso et al., 2016). However, traditionally, data acquisition and storage, obscure file formats, and multitudes of geospatial data processing frameworks are significant obstacles to take full advantage of these images, especially in large-scale and long-term applications(Gorelick et al., 2017a). Recently, a free cloud computing platform called the Google Earth Engine (GEE) has been used to store and process large volumes of remote sensing images.

Google Earth Engine is a cloud-based platform that made it easy to access high-performance computing resources for processing very large geospatial datasets, without having to suffer the IT pains currently surrounding either. Earth Engine is also designed to help researchers easily disseminate their results to other researchers, policy makers, NGOs, field workers, and even the general public. Once an algorithm has been developed on Earth Engine, users can produce systematic data products or deploy interactive applications backed by Earth Engine's resources, without needing to be an expert in application development, web programming or HTML (Gorelick et al., 2017a).

GEE has two interactive platform, (1) Graphical User Interface (Explorer), which is user friendly way to begin exploring and analyzing data and Application Program Interface (Code Editor), where custom analysis is possible using JavaScript and Python programming language. GEE is accessed and controlled through an Internet-accessible Application Programming Interface (API) and an associated web-based Interactive Development Environment (IDE) that enables rapid prototyping and visualization of results.

Datasets

The data repository is a collection of over 40 years of satellite imagery for the whole world, with many locations having two-week repeat data for the whole period, and a sizeable collection of daily and sub-daily data as well. The data available is from multiple satellites, such as the complete Landsat series; Moderate Resolution Imaging Spectrometer (MODIS); National Oceanographic and Atmospheric Administration Advanced Very High-Resolution Radiometer (NOAA AVHRR);

Sentinel 1,2, and 3; Advanced Land Observing Satellite (ALOS) etc. (Gorelick et al., 2017b). Some public data catalogues are also available in earth engine (Earth Engine Data Catalog, 2019).

Earth Engine uses a simplified and generalized data model based on 2D gridded raster bands in a lightweight “image” container. Pixels in an individual band must be homogeneous in data type, resolution and projection. Each image has associated key/value metadata containing information such as the location, acquisition time, and the conditions under which the image was collected or processed. However, images can contain one or more bands and the bands within an image need not have uniform data types or projections.

Code Editor

An online Integrated Development Environment (IDE) for rapid prototyping and visualization of complex spatial analyses using the JavaScript API. Google Earth Engine allows users to run algorithms on georeferenced imagery and vectors stored on Google's infrastructure. The Google Earth Engine API provides a library of functions which may be applied to imagery for display and analysis. Earth Engine's public data catalog contains a large amount of publicly available imagery. Vector datasets are available through Google Fusion Tables. Developers can access existing vector datasets or create their own.

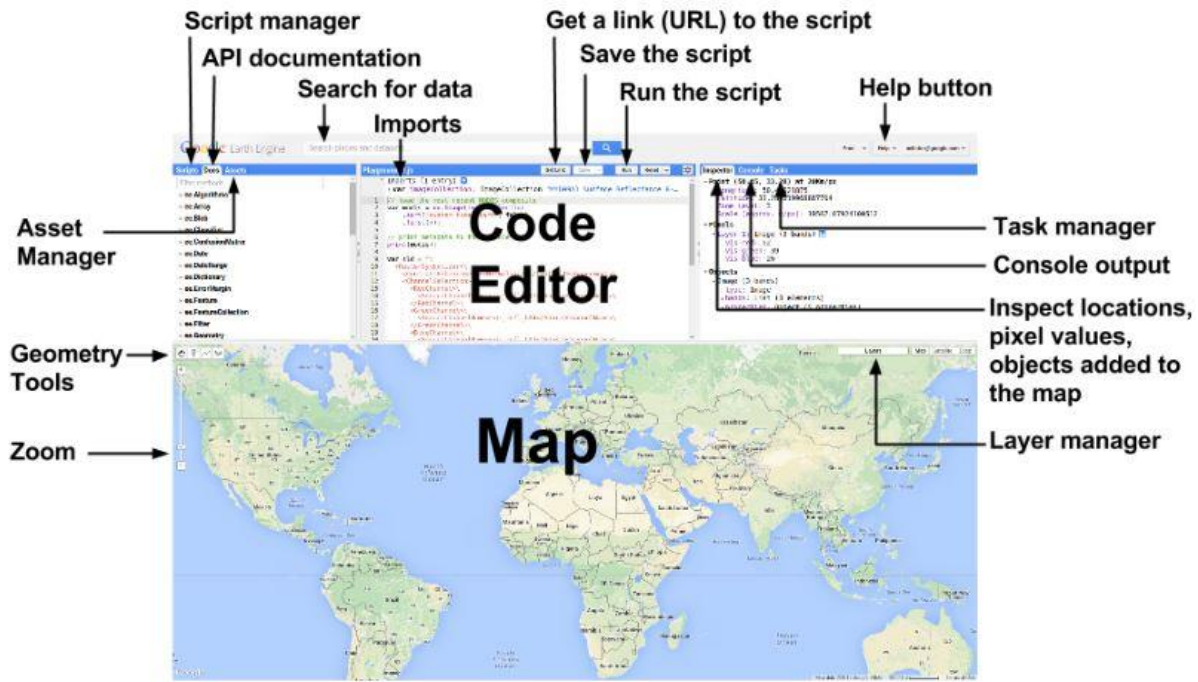


Figure 1: Diagram of components of the Earth Engine Code Editor (Earth Engine Code Editor, 2019)

The Code Editor has a variety of features to take advantage of the Earth Engine API (Figure 1). Scripts tab helps to view example scripts or save users scripts. Through inspector tab, users can query objects on map. Get Link button is for sharing URL with collaborators and friends. Scripts developed in the Code Editor are sent to Google for processing and the generated map tiles and/or messages are sent back for display in the Map and/or Console tab.

On the left side of the Code Editor is the Docs tab, which contains the complete JavaScript API documentation. The documentation can be searched and browsed from the Docs tab. The Scripts manager stores private, shared and example scripts in Git repositories hosted by Google. The Asset Manager is in the Assets tab in the left panel which helps to upload and manage users own image assets in Earth Engine. To find and import datasets one can use search option to select required images or places.

The Map object in the API refers to the map display in the Code Editor. Use the layer manager in the upper right corner of the map to adjust the display of layers added to the map. Specifically, user can toggle the visibility of a layer or adjust its transparency with the slider. When one ‘print()’

something from script, such as text, objects or charts, the result will be displayed in the Console. The console is interactive, so one can expand printed objects to get more details about them. One can also import geometries to script by drawing them on screen. Geometry tool facilitates to draw point, polygon or line over the map. By clicking the Help button user can be able to see links to this Developer's Guide, the help forum, a guided tour of the Code Editor and a list of keyboard shortcuts that help with coding, running code, and displaying data on the Map (Google Earth Engine API, 2019).

Image

Raster data are represented as Image objects in Earth Engine. Images are composed of one or more bands and each band has its own name, data type, scale, mask and projection. Each image has metadata stored as a set of properties. In addition to loading images from the archive by an image ID, one can also create images from constants, lists or other suitable Earth Engine objects.

Image Visualization

If a layer is added to the map without any additional parameters, by default the Code Editor assigns the first three bands to red, green and blue, respectively. To achieve desirable visualization effects, user should provide visualization parameters to `Map.addLayer()`. Specifically, the parameters are given in Table 1.

Color palettes

To display a single band of an image in color, set the palette parameter with a color ramp represented by a list of CSS-style color strings. For example, color palettes for red, green and blue are ('FF0000'), ('00FF00'), ('0000FF'). One can use hex color code or simply writing the color names.

Table 1: Visualization parameters for Map.addLayer()

Parameter	Description	Type
bands	Comma-delimited list of three band names to be mapped to RGB	list
min	Value(s) to map to 0	number or list of three numbers, one for each band
max	Value(s) to map to 255	number or list of three numbers, one for each band
gain	Value(s) by which to multiply each pixel value	number or list of three numbers, one for each band
bias	Value(s) to add to each DN	number or list of three numbers, one for each band
gamma	Gamma correction factor(s)	number or list of three numbers, one for each band
palette	List of CSS-style color strings (single-band images only)	comma-separated list of hex strings
opacity	The opacity of the layer (0.0 is fully transparent and 1.0 is fully opaque)	number
format	Either "jpg" or "png"	string

Source: (Google Earth Engine API, 2019)

Masking

Masking pixels in an image makes those pixels transparent and excludes them from analysis. Each pixel in each band of an image has a mask. Those with a mask value of 0 or below will be transparent. Those with a mask of any value above 0 will be rendered. User can use image.updateMask() to set the opacity of individual pixels based on where pixels in a mask image are non-zero. Pixels equal to zero in the mask are excluded from computations and the opacity could be set to 0 for display.

Clipping

The “image.clip()” method is useful for achieving cartographic effects. Clipping is used to select the region of interest from large database. Clipping can be obtained by using geometry polygon, or pre-uploaded shape file to the asset.

Image Collection

An Image Collection is a stack or time series of images. In addition to loading an Image Collection using an Earth Engine collection ID, Earth Engine has methods to create image collections. The constructor use “ee.ImageCollection()” or the convenience method “ee.ImageCollection.fromImages()” create image collections from lists of images.

One can also create new image collections by merging existing collections. Data set in Earth Engine are available as image or image collection. There are a variety of ways to get information about an Image or Image Collection. The collection can be printed directly to the console, but the console printout is limited to 5000 elements. Collections larger than 5000 images will need to be filtered before printing. Printing a large collection will be correspondingly slower (“Google Earth Engine API,” 2019).

Filtering an Image Collection

An Image Collection contains plethora of information from where we need to filter our requirements. Earth Engine provides a variety of convenience methods for filtering image collections. Specifically, many common use cases are handled by `imageCollection.filterDate()` for specifying date, and `imageCollection.filterBounds()` for specifying location of the desired area.

Reducing an Image Collection

Reducers are the way to aggregate data over time, space, bands, arrays and other data structures in Earth Engine. The “ee.Reducer” class specifies how data is aggregated. To composite images in an Image Collection, use “`imageCollection.reduce()`”. This will composite all the images in the collection to a single image representing, for example, the min, max, mean or standard deviation of the images. “`.median()`” argument is used for compositing median of an Image Collection, to create an Image that’s counts only the median of the Image Collection (“Google Earth Engine API,” 2019).

Compositing and Mosaicking:

In general, compositing refers to the process of combining spatially overlapping images into a single image based on an aggregation function. Mosaicking refers to the process of spatially

assembling image datasets to produce a spatially continuous image. In Earth Engine, these terms are used interchangeably, though both compositing and mosaicking are supported.

To make a composite which maximizes an arbitrary band in the input, use “imageCollection.qualityMosaic()”. The “qualityMosaic()” method sets each pixel in the composite based on which image in the collection has a maximum value for the specified band.

Feature Collection

Groups of related features can be combined into a Feature Collection, to enable additional operations on the entire set such as filtering, sorting and rendering. There are verities of ways to create a Feature Collection. One way is to provide the constructor with a list of features. The features do not need to have the same geometry type or the same properties. Earth Engine hosts a variety of table datasets. To load a table dataset, the table ID to the Feature Collection constructor should be given. Tables stored in Google Fusion Tables can also be uploaded as Feature Collection. To load a Feature Collection from a Fusion Table, supply the constructor with the table ID appended to ‘ft:’.

As with images, geometries and features, feature collections can be added to the map directly with “Map.addLayer()”. The default visualization will display the vectors with solid black lines and semi-opaque black fill. Visualization parameter can be applied to make the feature collection more interactive. Mapping, filtering and reducing over Feature Collection is also possible (“Google Earth Engine API,” 2019).

Charting

Earth Engine uses the Google Visualization API to provide support for charting in the “ui.Chart” class. Charts can be displayed interactively through the Code Editor console, added to user interface components, viewed as separate web pages, or exported as images. Histogram, Pie chart, Image region chart, Time series chart, Array data chart, Day of year chart and many more charts can be displayed by using specifying chart in GEE (“Google Earth Engine API,” 2019).

2.12 Multidimensional use of Google Earth Engine

Google Earth Engine is a new technology platform that enables monitoring and measurement of changes in the earth's environment, at planetary scale, on a large catalog of earth observation data.

Google Earth Engine allows observation of dynamic changes in agriculture, natural resources, and climate using geospatial data from the Landsat satellite program, which passes over the same places on the Earth every sixteen days. It makes Landsat and Sentinel-2 data easily accessible to researchers in collaboration with the Google Cloud Storage.

The Google Earth Engine (GEE) portal provides enhanced opportunities for undertaking earth observation studies. Established towards the end of 2010, it provides access to satellite and other ancillary data, cloud computing, and algorithms for processing large amounts of data with relative ease. Analysis of published literature showed that a total of 300 journal papers were published between 2011 and June 2017 that used GEE in their research (Kumar and Mutanga, 2018). Kumar and Mutanga (2018) also found that, fifty papers out of 300 (17%) covered the whole world as an application region, while there were 28 studies at a continental scale. Sixty-three studies were at the country scale and 139 at the sub-country scale. That result indicates the potentiality of GEE in upcoming future of geospatial science for analyzing large study area.

The multi-temporal global urban land maps based on Landsat images for the 1990–2010 period with a five-year interval developed by (Liu et al., 2018) in GEE platform. They proposed the method of Normalized Urban Areas Composite Index (NUACI) and utilized the Google Earth Engine to facilitate the global urban land classifications from an extensive number of Landsat images. Tracking annual changes of coastal tidal flats was done in China during 1986–2016 through analyses of Landsat images with Google Earth Engine analyzed the total area of coastal tidal flats in China which is considered as a breakthrough in that area (Wang et al., 2018).

A study in Africa automated cropland mapping using Google Earth Engine explained about 90% for crop extent in different agro-ecological zones (AEZs) which overcomes the challenge because of the heterogeneous and fragmental landscape, complex crop cycles, and limited access to local knowledge (Xiong et al., 2017). Another study (Patel et al., 2015) on multitemporal settlement and population mapping from Landsat using Google Earth Engine showed that the automated classification from GEE produced accurate urban extent maps, and that the integration of GEE-derived urban extents also improved the quality of the population mapping outputs. Industrial oil palm plantations on Landsat images with pixel-based classification via supervised learning was detected in Google Earth Engine (Lee et al., 2016). The overall accuracy and Kappa coefficient were the highest using all bands for land cover classification in GEE.

A team led by University of Maryland's Matt Hansen used Earth Engine to survey over a decade of global tree cover extent, loss, and gain. The study, analyzed nearly all global land, excluding only Antarctica and some Arctic islands. This area comprises 128.8 million km², which is the equivalent of 143 billion pixels of Landsat data at a thirty-meter spatial resolution. To conduct such extensive analysis, Earth Engine performed computations in parallel across thousands of machines, as well as automatically managed data format conversion, reprojection and resampling, and image-to-pixel metadata association (Hansen et al., 2013). Global Forest Watch, an initiative of the World Resources Institute, is a dynamic online forest monitoring system designed to enable better management and conservation. Global Forest Watch uses Earth Engine to measure and visualize changes to the world's forests; users can synthesize data from over the past decade or receive alerts about possible new threats in near-real-time (Global Forest Watch, 2019).

A team of University of Minnesota developed a monitoring system to track changes to prevent loss to critical endangered wild tiger habitats. The team assessed the changes to all critical tiger habitats over a 14 years period. The assessment is the first to track all 76 areas prioritized for wild tiger conservation across 13 different countries. Their analysis found that the international goal to double the wild tiger population by 2022 is achievable with effective forest protection and management (Joshi et al., 2016). UC San Francisco (UCSF) is working to create an online platform that health workers around the world can use to predict where malaria is likely to be transmitted using data on Google Earth Engine. The goal is to enable resource poor countries to wage more targeted and effective campaigns against the mosquito-borne disease, which kills 600,000 people a year, most of them children. When their tool is released, local health workers will be able to upload their own information about known cases of malaria, and the platform will combine it with real-time satellite data to predict where new cases are likely to occur (UCSF, 2014).

The European Commission's Joint Research Centre (JRC) has used Earth Engine to develop high-resolution maps of global surface water occurrence, change, seasonality, recurrence, and transitions. The study, analyses Landsat images collected over the past three decades to identify both permanent and seasonal water bodies. Understanding these changes is vital for ensuring the security of our global water supply for agriculture, industry, and human consumption; for assessing water-related disaster reduction and recovery; and for the study of waterborne pollution and the spread of disease (Pekel et al., 2016).

2.13 Normalized Difference Water Index (NDWI)

The Normalized Difference Water Index (NDWI) is a new method that has been developed to delineate open water features and enhance their presence in remotely-sensed digital imagery. The NDWI makes use of reflected near-infrared radiation and visible green light to enhance the presence of such features while eliminating the presence of soil and terrestrial vegetation features. In general, the waterlogged areas exhibit sharp contrast with the adjacent areas on the satellite images and these spectral properties of waterlogged areas can be easily picked by visible and infrared domain of optical sensors(Mahmud et al., 2017). The standing water areas appear as dark blue to black in colour/tone depending upon the depth of water, while the wet areas appear as dark grey to light grey on the imagery (Chowdary et al., 2008). Normalized Difference Vegetation Index (NDVI) quantifies vegetation by measuring the difference between near-infrared (which vegetation strongly reflects) and red light (which vegetation absorbs). NDWI shows the opposite result of NDVI (Normalized Difference Vegetation Index). As per (Sims and Gamon, 2003), the NDWI is an appropriate water absorption index in comparison with NDVI. It also ranges from -1 to +1 (McFeeters, 1996). (Chowdary et al., 2008) mentioned that for water-logged areas NDWI ranges from zero to +1. Here, +1 signifies the presence of extensive deep-water bodies where -1 is for vegetation cover. From the Landsat 8 imagery, following (McFeeters, 1996), NDWI can also be calculated using the formula as follows:

$$NDWI = (Band\ 3 - Band\ 5) / (Band\ 3 + Band\ 5)$$

In Landsat 8 imagery, Band 3 is for visible Green light radiation and Band 5 is for Near infrared radiation.

CHAPTER 3: MATERIALS AND METHODS

3.1 Description of The Study Area

3.1.1 Location

The tidal river, Halda ($22^{\circ}54' N$ and $91^{\circ}48' E$ to $22^{\circ}24' N$ and $91^{\circ}53' E$) is one of the most unique resourceful river located in South-East region of Bangladesh originated and ended in our country (Akter and Ali, 2012b); which is a major tributary of the river, Karnaphuli in Chittagong district originated from the hilly Haldachora fountain at the Patachara hill ranges of Ramgarh in the Khagrachari hill district (Halda River - Banglapedia, 2015).

Study Area Map

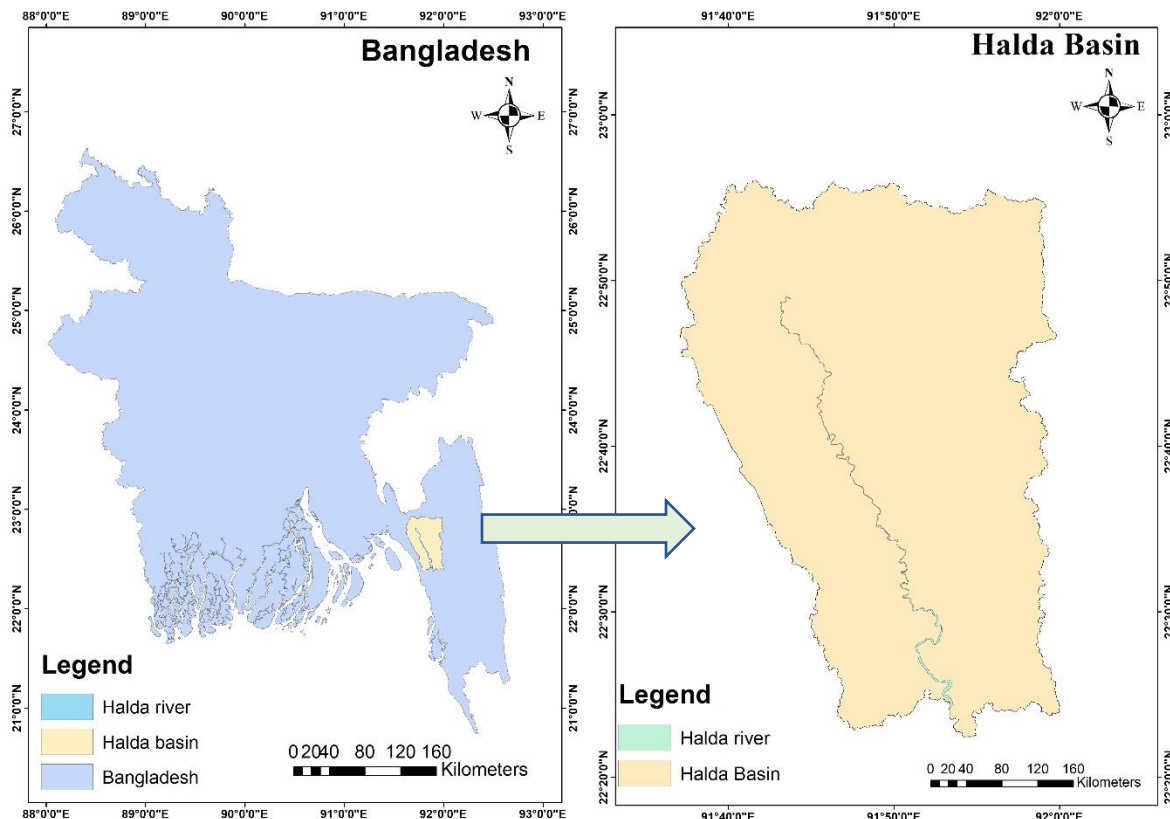


Figure 2: Map of study area

It flows through Manikchari Upazila, Fatickchari Upazila, Hathazari Upazila, Raozan Upazila and Chandgaon Thana of Chittagong metropolitan that finally meets with the Karnaphuli River near

Kalurghat bridge at latitude 22°25'13" N and longitude 91°52'33" E (Kamal et al., 2013). However, the origin of river is known as Haldachori canal which is passed through Jominer Aga and connected with Belchori canal in the village Belchori para of Ramgarh (Halda River - Banglapedia, 2015). At Noapara of Khagrachari district, Haldachori is connected with another canal called Saldachori which is originated from Kampru para. At origin, Haldachori canal is very narrow and named as Halda khal after meeting with Manikchori khal (M. S. Bhuyan and Bakar, 2017).

A number of canals such as Manikchori khal, Harualchori khal, Baromasia khal, Durung khal and Sartar khal are connected with Halda khal and makes Halda khal a river (Akhter, 2015; Kibria et al., 2018). The total length of this river is about 98 km, where a 29 km reaches up to Nazirhat navigable by big boats throughout the year and small country boats sailing 16–24 km further upstream to Narayanhata (K. Islam et al., 2017; Kabir et al., 2011). The river is also famous for breeding pure Indian major carps (Halda River - Banglapedia, 2015). The area of the present study is located at the whole watershed of the river Halda (Figure 2).

3.1.2 Physical environment

Topography

The study consists of mostly hilly areas with some flat terrain. The elevation of the area varies from about 30m to about 2m. The area is surrounded by human settlements, agricultural lands and char land. There are several streams which cross the area in east west direction. These streams carry huge flood flow with sediments in the river every year (Qadery and Muhibullah, 2008; Tsai et al., 1981).

Soil and sediment characteristics

Soil textures of the study area on the both sides of the Halda River ranges from loam to clay, with silty clay loam and silty clay being the most common. Soil permeability is low to moderate and is excellent for rice production. The river, Halda collects sediment from its upper watershed and carries it through the estuary of the Karnaphuli River to the Bay of Bengal. The sediment it carries is the primary source of nutrients for the aquatic life, the source of siltation for agricultural land. The area is seasonally flooded in the rainy season. The total annual sediment load at Panchpukuria station is 288849.9326 ton per year (Bhuyan and Bakar, 2017).

Tidal characteristics

Tides are semi-diurnal. The difference between the maximum daily high tide level and low tide level was 4.2 m. Tidal stations at Enayethat, Telpari and Panchpukuria points are maintained for observation and record of daily tide (Dhar et al., 2015).

Meteorological conditions

The meteorological conditions of the study area are almost similar to the other parts of Chittagong region. Chittagong is situated in the tropical zone, which is subjected to tropical climate. It is characterized by high temperature, and heavy rainfall with often-excessive humidity. The study area has three main seasons: the monsoon from June to October, during which about 80% of total annual rainfall is recorded; the dry season from November to February, which has very little rainfall and the lowest temperatures and humidity, and the pre-monsoon season from March to May (BBS, 2013).

Temperature

The mean annual air temperature is of 25.7°C (Akhtaruzzaman et al., 2015); which varies from maximum 32.5°C to minimum 13.5°C (BBS, 2013). The average maximum temperature is the lowest in December and January which ranges from 28.6°C to 26.2°C and the highest from April to July which ranges from 32°C to 33.3°C. The average minimum temperature is the lowest in December at 16.9°C and January of 14.1°C and the highest from May to September which ranges from 25.4°C to 25.7°C. From November to February, the sky is almost cloudless, but humidity is high owing to the proximity of the sea (BBS, 2013).

Rainfall

The rainfall in the study area is almost similar to the Chittagong city. The average annual rainfall in Chittagong city is 3378 mm (BBS, 2013). The monthly rainfall is high from May to September 250 to 700 mm and July is the highest month of 700 mm. While the monthly rainfall is low from November to March less than 100 mm, and December and January 10 to 20 mm are the lowest months. So, it is clear that monthly average rainfall is very little during cold and dry season. Reversely, remaining seasons of pre-monsoon and monsoon have comparatively abundant rainfall. But recently the phenomenon is being changed (BBS, 2013).

3.1.3 Biological environment

Flora

A variety of fruit species were found in this area like Mango, Jackfruit, Coconut, Guava, Jam and other fruit species. Among the timber species Mehagoni, Raintree, Koroi, Gamar etc. were found. Mandar, Akashmoni, Eucalyptus, Jarul etc. were found as the fuel wood species. But most interesting thing is that along with the above species, the riverbank sides possess some mangrove species like *Sonneratia apatella* (locally called Keora). Grass and other herbs and shrubs were found to grow on nearby char land (Zaman, 2014).

Fauna

The nearby villagers raise cows, buffaloes, goats etc. They live on grasses which grow in nearby char land. A variety of fishes and other aquatic animals are found in the Halda River. It is one of the largest natural spawning grounds of major Indian carps and a rich assemblage of shell fish and fresh water dolphins (shushuk). Most common fishes found in this river are rui, cattla, mrigel, kalibauish etc. A large number of people are involved in fishing activities and they earn their livelihood from these (Zaman, 2014).

3.2 Data Source

Based on over three million satellite scenes collected between 1984 and 2015, the Global Surface Water Explorer database was produced with 30 m resolution which enable users to scroll back in time to measure the changes in the location and persistence of surface water globally, by region, or for a specific area. In this study, the historical records of water surface data were used from Global Surface Water explorer. All of the datasets that comprise the Global Surface Water 1984-2015 are being made freely available at online using their own delivery mechanism. For this study, Map Layer dataset was used in Google Earth Engine platform with an asset ID “JRC/GSW1_0/GlobalSurfaceWater”

The latest high-resolution satellite imagery provided by USGS (United States Geological Survey) for Landsat 8 OLI-TIRS (Operational Land Imager/Thermal Infrared Sensor) and Landsat 5 TM (Thematic Mapper) satellite imagery for the time period of 2015 and 1990 were used for visual image interpretation, land use identification and land use classification. Landsat imagery for the study area was not available for 1984, closest available imagery was found for 1990. The spatial

resolution of Landsat 8 and Landsat 5 is 30 m. While image selection, cloud, and unwanted shade free imagery were set as criteria. Imagery having cloud could substantially reduce the accuracy of the classification work (Islam et al., 2017). For this reason, I took pictures only in winter season. Because, in Bangladesh, November to February is winter season and March is the transitional period of winter to summer.

3.3 Methods

3.3.1 Surface water mapping in Google Earth Engine

JRC Global Surface Water Mapping Layers, v1.0 is available in Google Earth Engine data catalogue. This data has 7 bands named as occurrence, absolute change, normalized change, seasonality, recurrence, transition, maximum extent. From above mentioned bands, I choose transition layer and occurrence data layer for my study. The water transition layer captures changes between three classes of water occurrence (not water, seasonal water, and permanent water) along with two additional classes for ephemeral water (ephemeral permanent and ephemeral seasonal).

Water class transition layer for Halda basin is calculated by the following steps –

Loading data layer in Earth Engine code editor:

First, in GEE code editor a variable named ‘gsw’ was declared which contains earth engine snippet for the data layer by using JavaScript language.

```
var gsw = ee.Image('JRC/GSW1_0/GlobalSurfaceWater');
```

Add a map layer for visualizing water transition classes:

Another variable transition was declared for selecting transition band from the whole data set.

```
var transition = gsw.select('transition');
```

The ‘gsw’ images contain metadata on the transition class numbers and names, and a default palette for styling the transition classes. When the transition layer is added to the map, these visualization parameters will be used automatically.

At the bottom of the Map Layers section of my script, the following statement was added to adds a new map layer that displays the transition classes:

```

Map.setCenter(105.26, 11.2134, 9);
Map.addLayer({
  eeObject: transition,
  name: 'Transition classes (1984-2015)',
});

```

This Map Layer displays the results for global water transition from which region of interest for the study was chosen.

Summarizing Area by Transition Class

In this section, region of interest was declared for displaying transition class only for the study area. This could be done by drawing geometry polygon over the site, but the shape files of study area us used instead to declare it as a region of interest. For this, the shape file was uploaded to GEE Assets as FeatureCollection and after uploading it, an Id was generated which has been used in the code editor. The shapefile was the imported to code editor as a default variable named ‘table’.

In order to calculate the area covered by parts of an image, add an additional band was aded to the transition image object that identifies the size of each pixel in square meters using the ‘ee.Image.pixelArea’ method.

```

var area_image_with_transition_class =
ee.Image.pixelArea().addBands(transition);

```

The resulting image object (area_image_with_transition_class) is a two band image where the first band contains the area information in units of square meters (produced by the ee.Image.pixelArea method), and the second band contains the transition class information.

Then the class transitions were summarized within the region of interest (roi) by using the ee.Image.reduceRegion method and a grouped reducer which acts to sum up the area within each transition class:

```

var reduction_results = area_image_with_transition_class.reduceRegion({
  reducer: ee.Reducer.sum().group({
    groupField: 1,
    groupName: 'transition_class_value',
  }),
  geometry: table,
}

```

```

    scale: 30,
    bestEffort: true,
});
print('reduction_results', reduction_results);

```

The console tab output now displays the ‘reduction_results’. The ‘reduction_results’ object does contain information on the area covered by each transition class, but it is not particularly easy to read. For making summary chart a readable format, I had to follow the next step –

Creating a Summary Chart

A chart to better summarize the results was made by starting with extracting out the list of transition classes with areas as follows:

```
var roi_stats = ee.List(reduction_results.get('groups'));
```

The result of the grouped reducer (reduction_results) is a dictionary containing a list of dictionaries. There is one dictionary in the list for each transition class. These statements use the ee.Dictionary.get method to extract the grouped reducer results from that dictionary and casts the results to an ee.List data type, so that the individual dictionaries could be accessed.

In order to make use of the charting functions of the Code Editor, a FeatureCollection that contains the necessary information was built by first creating two lookup dictionaries and two helper functions. To create a dictionary for looking up names of transition classes:

```

var lookup_names = ee.Dictionary.fromLists(
  ee.List(gsw.get('transition_class_values')).map(ee.String),
  gsw.get('transition_class_names')
);
To create a dictionary for looking up colors of transition classes:
var lookup_palette = ee.Dictionary.fromLists(
  ee.List(gsw.get('transition_class_values')).map(ee.String),
  gsw.get('transition_class_palette')
);

```

The ‘lookup_names’ dictionary associates transition class values with their names, while the ‘lookup_palette’ dictionary associates the transition class values with color definitions.

Now a feature was created with the help of a function for a transition class that includes the area covered.

```

function createFeature(transition_class_stats) {
  transition_class_stats = ee.Dictionary(transition_class_stats);
  var class_number = transition_class_stats.get('transition_class_value');

```

```

var result = {
  transition_class_number: class_number,
  transition_class_name: lookup_names.get(class_number),
  transition_class_palette: lookup_palette.get(class_number),
  area_m2: transition_class_stats.get('sum')
};
return ee.Feature(null, result);
}

```

Now, to get the color palette in transition class, another function was declared-

```

function createBarChartSliceDictionary(fc) {
  return ee.List(fc.aggregate_array("transition_class_palette"))
    .map(function(p) { return {'color': p}; }).getInfo();
}

```

For creating a feature function and printing it,

```

var transition_fc = ee.FeatureCollection(roi_stats.map(createFeature));
print('transition_fc', transition_fc);

```

Now the last step is to make a summary chart with above mentioned features -

```

var transition_summary_chart = ui.Chart.feature.byFeature({
  features: transition_fc,
  xProperty: 'transition_class_name',
  yProperties: ['area_m2', 'transition_class_number']
})
.setChartType('BarChart')
.setOptions({
  title: 'Summary of transition class areas',
  slices: createBarChartSliceDictionary(transition_fc),
  sliceVisibilityThreshold: 0
});
print(transition_summary_chart);

```

This summary chart displays the area by each transition class in m² and the chart can be downloaded as CSV, SVG and PNG format.

3.3.2 Mapping Occurrence Change Intensity

The Occurrence Change Intensity map provides information on where surface water occurrence increased, decreased or remained the same between two epochs 16 March 1984 to 31 December 1999, and 1 January 2000 to 10 October 2015. The occurrence difference between two epochs was computed for each pair and differences between all homologous pairs of months were then averaged to create the surface water occurrence change intensity map. The Occurrence Change Intensity dataset contains the following bands: ‘Change_abs’ which is the absolute difference in

the mean occurrence value between the two epochs for homologous months and ‘Change_norm’ which is the normalized difference in the mean occurrence value between the two epochs for homologous months ($\text{epoch1}-\text{epoch2} / \text{epoch1}+\text{epoch2}$). Here absolute change is calculated for mapping out the area of 100% loss in occurrence and 100% increase in occurrence and also the unchanged water area in Halda river.

After mapping water transition classes, A variable is declared for selecting ‘change_abs’ band from global surface water database. Then I clipped it to my region of interest and add a layer of it.

```
var change = gsw.select("change_abs");
var clp = change.clip(table);
var VIS_CHANGE = {
  min:-50,
  max:50,
  palette: ['red', 'black', 'limegreen']
};
Map.addLayer({
  eeObject: clp,
  visParams: VIS_CHANGE,
  name: 'occurrence change intensity'
});
```

3.3.3 Mapping River Course Change in Google Earth

River course change was calculated by using “Google Earth Pro”. Google Earth displays satellite images of varying resolution of the Earth's surface, allowing users to see things like rivers, cities and houses looking perpendicularly down or at an oblique angle. Here, imagery resolution ranges from 15 meters of resolution to 15 centimeters. So, river and river bends are clearly visible in google earth. It also provides tools for measurement operation. Some parameters for mapping river course changes are length, width and number of bends which are counted for the year of 2001, 2009 and 2018.

Length is measured by “Add path” tool along the midline of river for those years. After finishing a path, length is calculated by ‘measurements’ option in the properties of the path. Number of bends are clearly observed from the middle line. Randomly 40 points are taken across the river side, 20 at each side (Table 2). For generalization, each point was named in alphabetical order. Distance between two parallel points are calculated as river width. River length, width and bends are calculated for each year. The variations of results among the parameters for the year 2001, 2009 and 2018 have shown the change in river course.

Table 2: Co-ordinate of location where river width was calculated

Random location	Point no.
22°24'47.63"N, 91°53'8.68"E-22°24'53.43"N,91°53'19.48"E	A
22°25'43.79"N, 91°52'55.23"E- 22°25'51.40"N, 91°52'53.83"E	B
22°28'8.35"N,91°52'32.55"E- 22°28'3.77"N, 91°52'35.35"E	C
22°30'2.49"N, 91°52'2.38"E- 22°30'5.85"N, 91°51'59.64"E	D
22°31'9.08"N, 91°50'52.90"E- 22°31'8.50"N, 91°50'56.78"E	E
22°32'29.60"N, 91°50'37.58"E- 22°32'24.29"N, 91°50'38.18"E	F
22°34'22.01"N, 91°50'6.64"E- 22°34'22.55"N, 91°50'8.50"E	G
22°35'8.44"N, 91°49'3.51"E- 22°35'8.44"N, 91°49'3.51"E	H
22°35'49.68"N, 91°48'58.52"E- 22°35'49.19"N, 91°49'0.54"E	I
22°37'5.15"N, 91°48'12.35"E- 22°37'6.41"N, 91°48'14.45"E	J
22°38'0.07"N, 91°47'29.84"E- 22°38'1.18"N, 91°47'33.31"E	K
22°39'29.88"N, 91°46'57.37"E- 22°39'28.89"N,91°46'59.80"E	L
22°40'22.19"N, 91°46'3.39"E-22°40'23.80"N, 91°46'3.28"E	M
22°42'45.67"N, 91°45'35.69"E-22°42'46.19"N,91°45'37.52"E	N
22°44'21.81"N, 91°46'10.82"E- 22°44'21.19"N, 91°46'12.82"E	O
22°45'6.85"N, 91°45'29.79"E-22°45'7.51"N, 91°45'31.07"E	P
22°46'48.50"N, 91°43'41.94"E- 22°46'50.03"N,91°43'42.78"E	Q
22°48'39.80"N, 91°43'19.44"E- 22°48'41.09"N, 91°43'20.16"E	R
22°48'53.52"N, 91°44'50.52"E- 22°48'54.63"N, 91°44'50.22"E	S
22°49'2.45"N, 91°45'34.24"E- 22°49'3.33"N, 91°45'33.32"E	T

3.3.4 Land Use and Land Cover Change

The base map of the study area was prepared by using satellite imageries and shape file of Bangladesh administrative area which was obtained from Diva-GIS website. For image interpretation, ERDAS Imagine 2015 and ArcGIS 10.5 software were used to prepare land use category map of the study area. Satellite imagery for 1984 was not available. For that, land use and land cover change were calculated for the year of 1990 and 2015. Ground truthing was done by using google earth for each year to find out latitude and longitude of specific land use category.

From the observation in google earth, here considered mainly 4 land uses for study. The procedure of image classification was given in below (Figure 3).

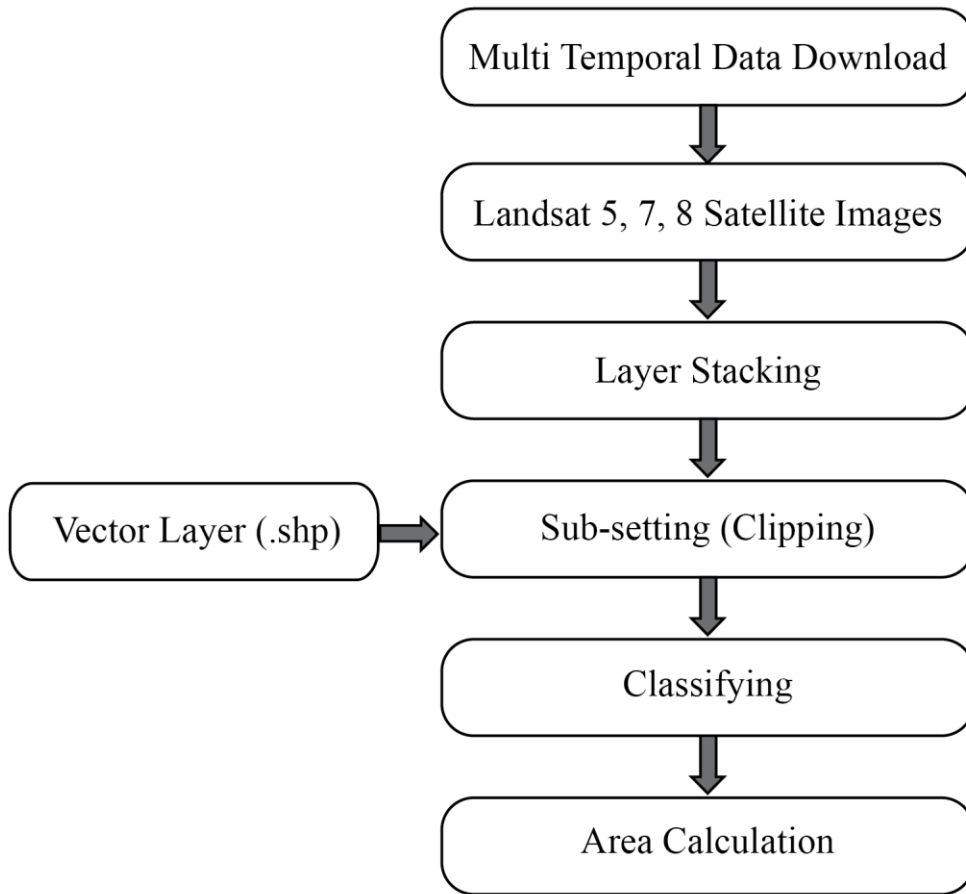


Figure 3: Procedure of satellite image classification

Layer Stacking

Different images representing different bands, so to analyze the remotely sensed images these different bands must be stacked. The flowchart of stacking image procedure is given below:

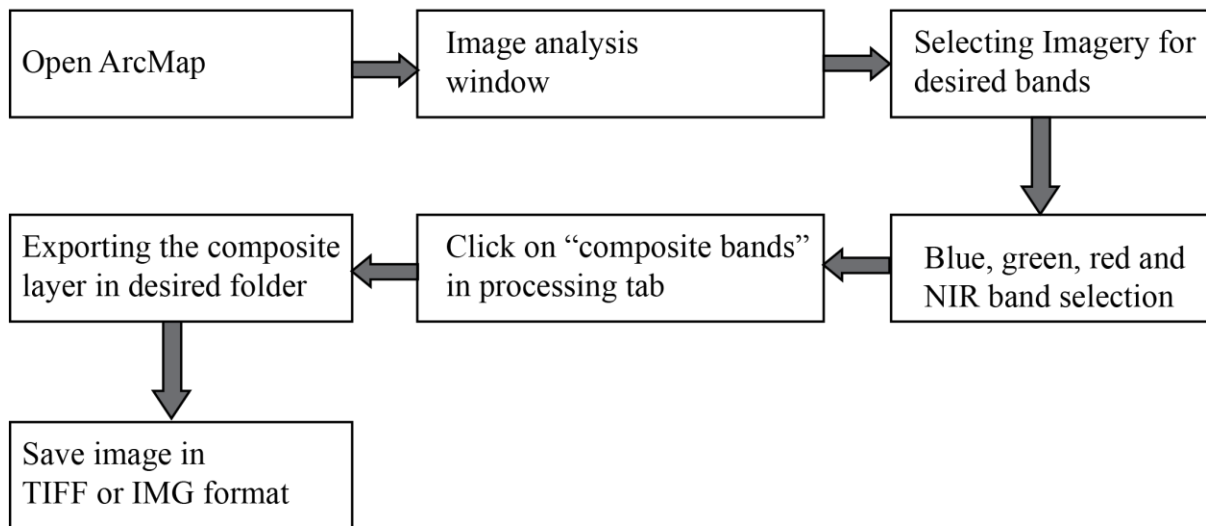


Figure 4: Procedure of layer stacking

Clipping

The next step is to subset the mosaicked image. Area of interest is clipped by using a vector layer (shape) file.

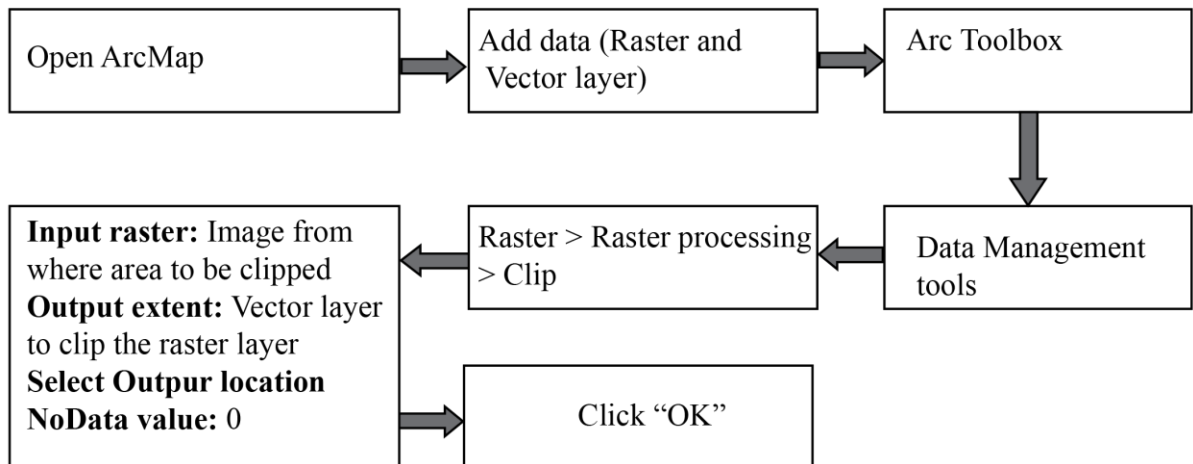


Figure 5: Procedure of clipping

Supervised classification

Supervised classification is the technique most often used for the quantitative analysis of remote sensing image data. At its core is the concept of segmenting the spectral domain into regions that

can be associated with the ground cover classes of interest to a particular application (Richards, 2013).

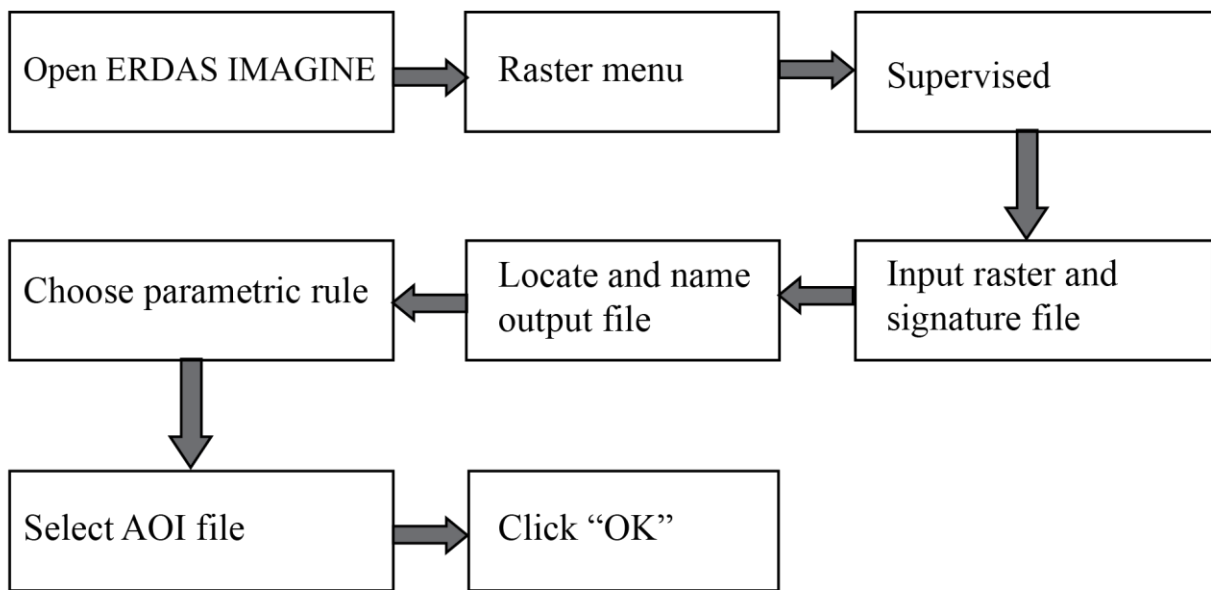


Figure 6: Procedure of supervised classification

Supervised classification was done using Signature Editor. After adding and editing signature for desired number of land use classes, the signature file was saved. During classification, the saved signature file was used.

Final Map Preparation

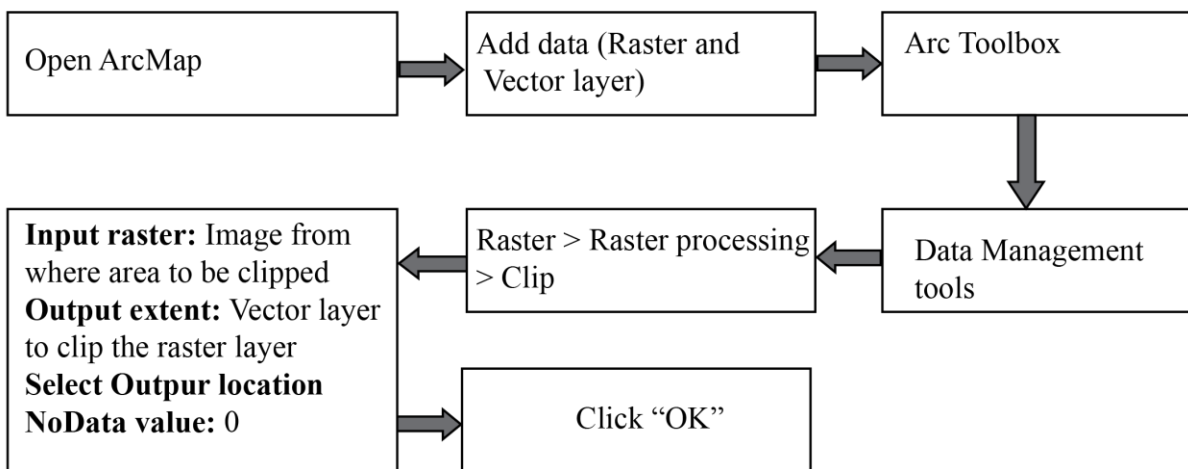


Figure 7: Procedure of final map preparation using Arc GIS

Maximum likelihood classification (MLC) approach is being widely used for land use change assessment (Islam et al., 2018). While reviewing literature it was found that MLC is mostly used and convenient to apply with satisfactory accuracy.

The magnitude change for each land use class was calculated by subtracting the area coverage from the 2nd year and initial year as shown in equation (1)(Islam et al., 2018).

$$\text{Magnitude} = \text{magnitude of the new year} - \text{magnitude of the previous year} \quad (1)$$

Percentage change (trend) for each land use type was then calculated by dividing magnitude change by the base year (the initial year) and multiplied by 100 as shown in equation (2)(Islam et al., 2018).

$$\text{Percentage Change} = \frac{\text{Magnitude of Change} * 100}{\text{Base Year}} \quad (2)$$

To obtain annual rate of change for each land use type, the difference between final year to initial year which represents magnitude of change between corresponding years was divided by the number of study year i.e. 1990-2015 (25 years) as appropriate using equation (3) (Islam et al., 2018).

$$\text{Annual Rate of Change} = \frac{\text{Final year} - \text{Initial Year}}{\text{No. of Years}} \quad (3)$$

Accuracy Assessment

Accuracy assessment for the supervised land use classification was done for 1990 and 2017 image by using ERDAS Imagine 15. From the classifier 40 and 41 points were generated randomly for 1990 and 2015 supervised images, respectively. Each and every point had specific color tone and the pixel value which was recognized by the software itself when the data sets were trained during supervised land use classification. These values were considered as reference values. All the randomly generated points were then identified by the user and assigned in different classes. The correctly identified points were considered as classified values. An Error Matrix and Kappa statistics were also generated from this reference and classified data from the report section of ERDAS Imagine 15 software. In the Error Matrix, the rows denote the categories as derived from the reference values. The diagonal of the matrix shows the agreement of the ‘from-to’ categories which indicate the error (omission and commission errors) that remains between the classified and reference data (Afify, 2011).

Overall accuracy was calculated from the error matrix by dividing the sum of the entries that make major diagonal by the total number of examined pixels. Kappa co-efficient of agreement was also calculated by using following equations (Afify, 2011).

$$K^{\wedge} = \frac{P_o - P_c}{1 - P_c} \quad (4)$$

$$P_o = \sum_{i=1}^r P_{ii} \quad (5)$$

$$P_c = \sum_{i=1}^r (P_{i1} * P_{i2}) \quad (6)$$

Here,

r = The number of rows in the error matrix

P_{ii} = The proportion of pixels in row ‘i’ and column ‘i’

P_{i1} = the proportion of the marginal total of row ‘i’

P_{i2} = The proportion of the marginal total of column ‘i’

3.3.5 NDWI Calculation

Normalized Difference Water Index (NDWI) is an important and most widely used remote sensing indices which involves spectral bands of multi-spectral and multi-temporal satellite datasets to map out earth’s surface landscape in terms of green vegetation cover and surface water cover (Das, 2017). In this study my attempt was to calculate surface water covered area for 1990 and 2015 for comparing result with land use classification. Based on the fact that water has strongest absorption while vegetation has strongest reflectivity at near infra-red, (McFeeters, 1996) proposed the method of NDWI to highlight water body.

$$\text{NDWI} = (\text{Green} - \text{NIR}) / (\text{Green} + \text{NIR})$$

NDWI proved to work well in separating water body and vegetation but has limitations when it comes to soil and built up area (McFeeters, 1996).

Landsat 5 have Band 2 and Band 4 for Green and Near infrared, whereas in case of Landsat 8, Band 3 and Band 5 should be considered.

So, for 1990, NDWI is calculated as, $\text{NDWI} = (\text{Band 2} - \text{Band 4}) / (\text{Band 2} + \text{Band 4})$

And for 2015, $\text{NDWI} = (\text{Band 3} - \text{Band 5}) / (\text{Band 3} + \text{Band 5})$

NDWI is calculated by Raster calculator in ArcMap 10.5. First unsupervised classification was carried out with 9 classes and then the 3 ranges are selected after reclassify.

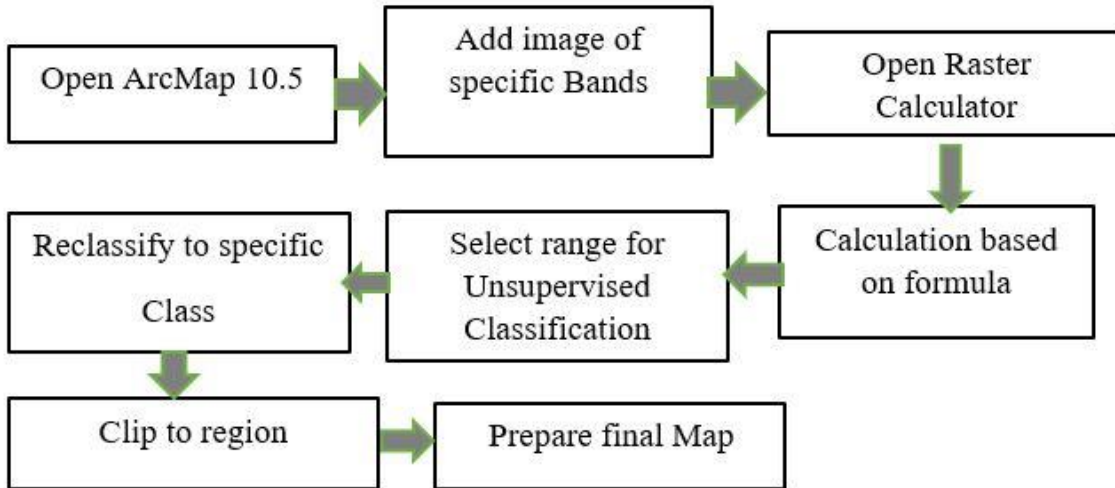


Figure 8: NDWI calculation process

CHAPTER 4: RESULT AND DISCUSSION

4.1 Land Use and Land Cover of Halda Basin

Land use mapping of Halda Basin may provide information on aerial distribution of land use categories and identification and estimation of land use changes over 25 years. The land use maps derived from different Landsat imageries are shown in Figure 9 and Figure 10. The aerial distribution of various land use classes for the year 1990 and 2015 and their change scenarios in between different time frames are shown in Tables 3 and 4.

4.1.1 Land use status of the study area from 1990-2015

During field survey, the study area's land uses were categorized into following 4 groups:

Agriculture: Land devoted to crop production and bare lands were considered under agriculture class. Deforested lands also taken into account under this section.

Vegetation: All kinds of forest including homestead forest were considered as vegetation.

Water body: Rivers, canals, ponds, deghis and other wetlands were taken in this class.

Built area: Settlements, industries, brick fields, roads and other commercial buildings were considered as built area.

After image classification on the basis of above land use categories, relevant map layouts were prepared.

4.1.2 Land use scenario of Halda Basin in 1990

In order to know the past land use pattern of the study area, I tried to focus on Landsat 5 imagery for the year 1990. Different land use categories had been identified and colored for the image 1990. The land use pattern which was identified (4 categories) for the year 1990 are listed in Table 3 and shown in Figure 9. From the identified land use categories, the highest category was Vegetation (85019.43 ha, 49.37% of total land area). The remaining land uses were Agricultural land (83419.11 ha, 48.41%), Water body (1961 ha, 1.14%) and Built area (1859 ha, 1.08%).

Figures 9 show the land use pattern of the study area in 1990. In these figures, green color represents Vegetation which was more prominent in Halda basin and observed at the north-west and north-east part. The red color represents Built area which was at the northern and southern part

in the Halda basin and dominated in the river side area. The blue color pixels indicate Water body which was observed in the southern part of the Halda basin.

Table 3: Land Use classes of 1990 and 2015

Land Use Category	Land Use (A) in 1990		Land Use (B) in 2015	
	Area (ha) 1990	% of land	Area (ha) 2015	% of land
Agriculture	83419.11	48.41	91072.78	52.85
Vegetation	85079.43	49.37	67445.28	39.14
Built area	1859.22	1.08	12358.44	7.17
Water Body	1961.1	1.14	1442.36	0.84
Total	172318.86	100	172318.86	100

4.1.3 Land use scenario of Halda Basin in 2015

In 2015, massive change has been observed in case of vegetation cover and agriculture. Vegetation cover is being destroyed to satisfy the demands of the increasing population. Positive relationship between forest loss and urban population growth has been shown (Foley et al., 2005). In this study, it was found that present vegetation cover of Halda basin is 39.14% (67445.28 ha) which is less than agricultural land that occupy 52.85% (91072.78 ha) of the basin. Again, agricultural schemes put pressure on land use and water system (Meyer and Turner, 1992). On the other hand, water bodies represent mere 0.84% (1442.36 ha) of the total watershed areas whereas settlements occupy about 7.17% (12358.44 ha) of its area.

4.1.4 LULCC assessment of Halda Basin from 1990 to 2015

From 1990 to 2015, significant decline was observed in water class with a rate of 26.45%. Annual average change for water class was 20.75 ha. Besides, vegetation cover was lost by 17634.15 ha (20.72%) with an annual average change of 705.366 ha. Again, significant increment (564.71%) is observed in Built area with an annual rate of 419.96 ha. Over the period, 10499.22 ha area was newly converted to Built area. Annual rate of increase for agricultural land was 306.14 with a rate of 9.17% i.e., 7653.67 ha area has been converted to agricultural land between 1990 and 2015.

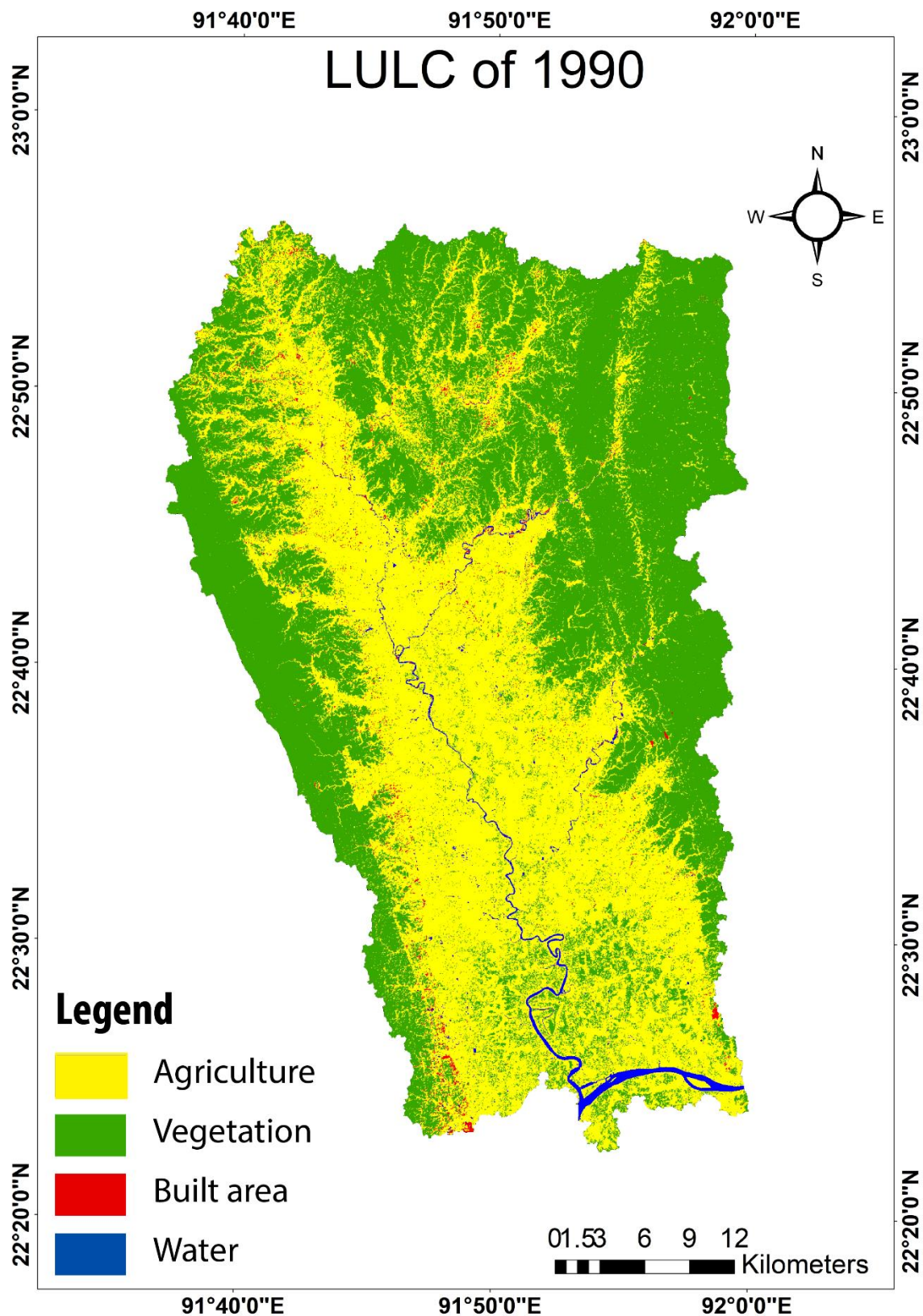


Figure 9: Land Use and Land Cover of 1990

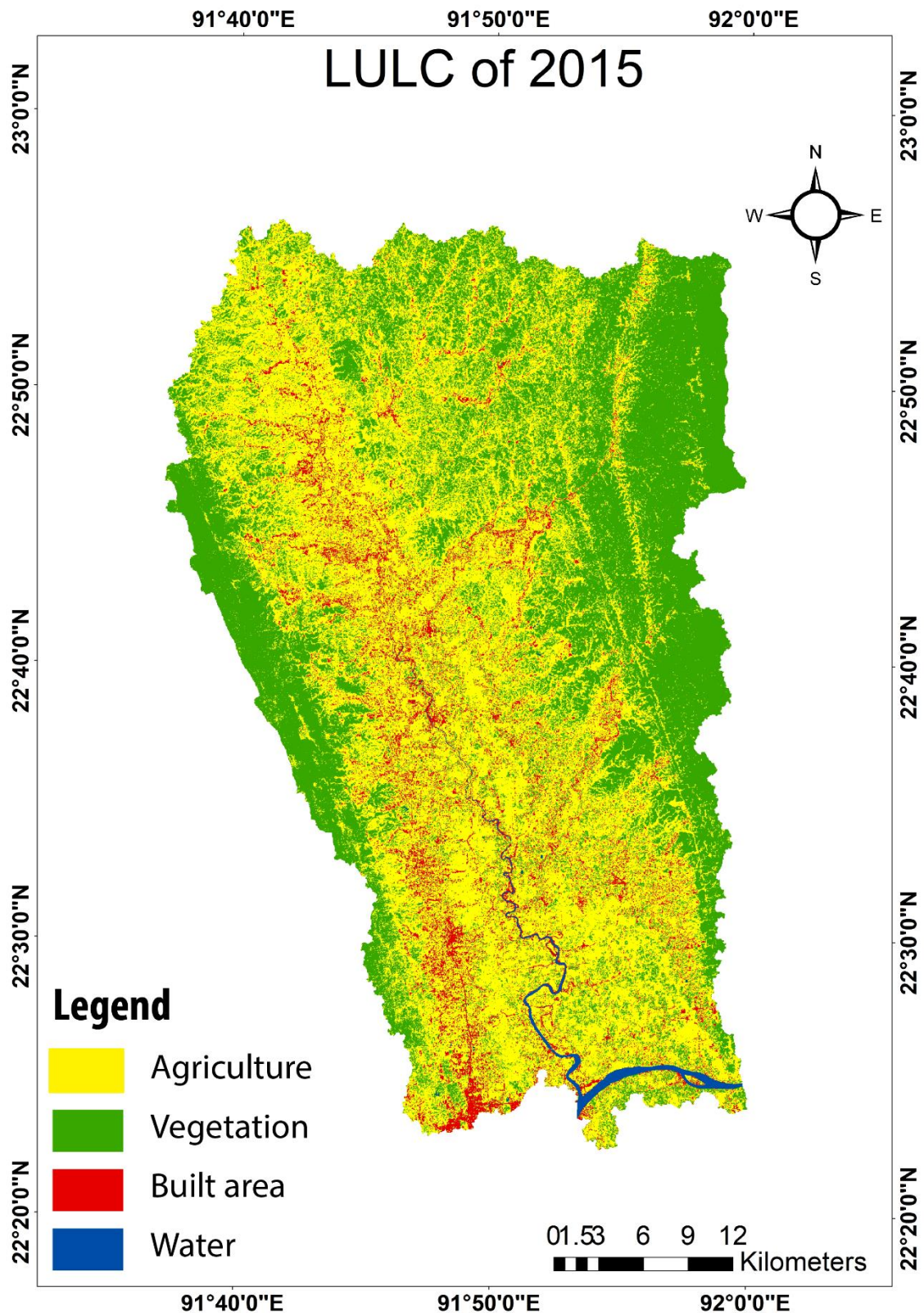


Figure 10: Land Use and Land Cover of 2015

Table 4: Land Use Change (2015-1990)

Land Use Category	Land Use Change (B-A): 2015-1990		
	Changed Area 1977-1997 (Ha)	% Change	Annual rate of change (Ha)
Agriculture	7653.67	9.17	306.15
Vegetation	-17634.15	-20.73	-705.37
Built area	10499.22	564.71	419.97
Water Body	-518.74	-26.45	-20.75

4.1.5 Overall accuracy and Kappa (K^*) statistics for 1990 and 2015 supervised classification

Summary of supervised classification accuracy for the 2 different time frames (1990 and 2015) found from accuracy assessment is shown in Table 5 and Appendix 1 & 2. The highest accuracy was found for 2015 supervised classification (91.23% accuracy) and the lowest for 1990 (88.75% accuracy) (Table 5).

Table 5: Overall classification accuracy and Overall kappa statistics of supervised classification of 1990 and 2015 imageries of Halda Basin

Accuracy Assessment	Overall Classification Accuracy		Overall Statistics	Kappa
	1990	2015	1990	2015
	88.75%	91.23%	0.81	0.87

Kappa statistics is a measurement mechanism between referenced data and user identified classified data. Kappa value is also used to check accuracy in classification and having a kappa value (0.81-1.00) denotes almost perfect/perfect match between the classified and referenced data in the classification system (Landis and Koch, 1977; Vliet et al., 2011; Yang and Lo, 2002). Kappa statistics for 2015 image classification shows a value of 0.87 denoting almost perfect / perfect match between the classified and referenced data in the classification system (Table 5).

4.2 NDWI Over the Region

Normalized Difference Water Index (NDWI) is an important and most widely used remote sensing indices which involves spectral bands of multi-spectral and multi-temporal satellite datasets to

map out earth's surface landscape in terms of green vegetation cover and surface water cover (Das, 2017). In this study my attempt was to calculate surface water covered area for 1990 and 2015.

4.2.1 NDWI in 1990

In 1990, NDWI based unsupervised classification ranges from -0.664 to 0.538. After reclassify, NDWI values from 0.0001 to 0.538 indicates the surface water body. Where the negative values denote the vegetation cover to agricultural or bare lands. Area is calculated for water covered surface and 1814.09 ha area are marked as waterbody. Figure 11 shows different NDWI range and area covered by each class. Here blue color denotes water body.

4.2.2 NDWI in 2015

Values of NDWI has decreased in 2015. Classification ranges was found from -0.565 to 0.253. And after reclassify, NDWI values from 0.0001 to 0.253 range was observed as water surface. Area covered by water surface also decreased in 2015. In that year, 1631.81 ha of land surface was marked as water. Figure 12 shows different NDWI range and area covered by each class. Here blue color represents water body.

4.2.3 NDWI Change Over 1990 to 2015

The values of NDWI range between 0 and ± 1 , and negative values or values close to 0 represent vegetation, whereas positive values or close to 1 represent surface water/deep water bodies (McFeeters, 1996). In the study period, NDWI value range was between -0.664 to 0.538 during 1990, which was changed between -0.565 to 0.253 in 2015. Higher NDWI range indicates greater depth of waterbody. In 1990, larger area was covered by water surface than in 2015. More depth in water body was observed in 1990. A comparison with LULC water body is given in Table 6.

Table 6: Comparison of water cover in NDWI with LULC

	Surface Water in 1990		Surface Water in 2015	
	Area (ha)	% of land	Area (ha)	% of land
Water body as per LULC	1961.1	1.14	1442.36	0.84
NDWI	1814.09	1.05	1631.81	0.94

Both NDWI and LULC indicates that water body has been decreased in Halda basin. The results are not same but has a similar trend of decreasing rate. So, over the period of 1990 to 2015 land surface loss its surface water covering area. NDWI classification took the composite over a long period and LULC analysis was done on a single image which may lead to this variation between the two observations.

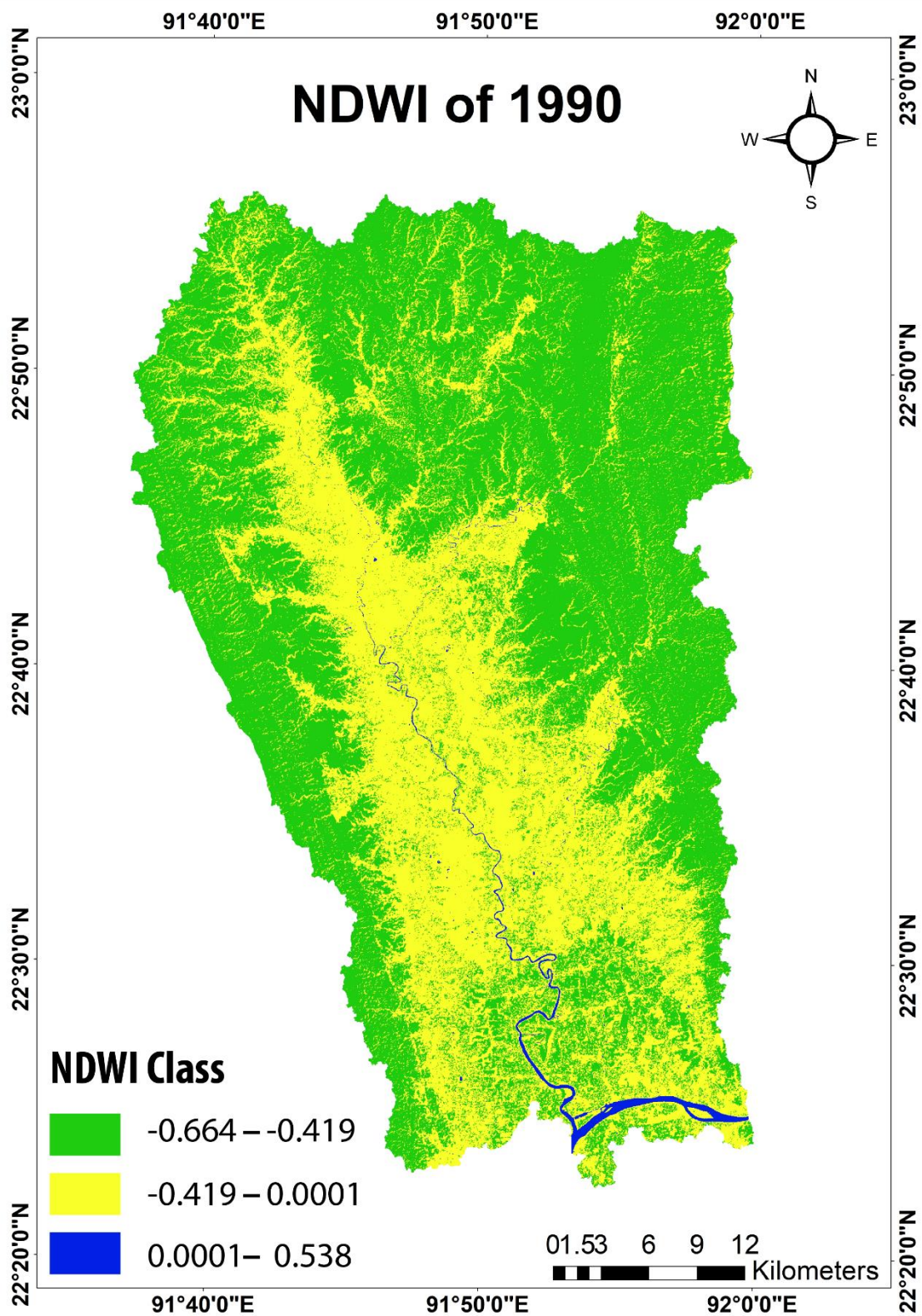


Figure 11: Normalized difference water index in 1990

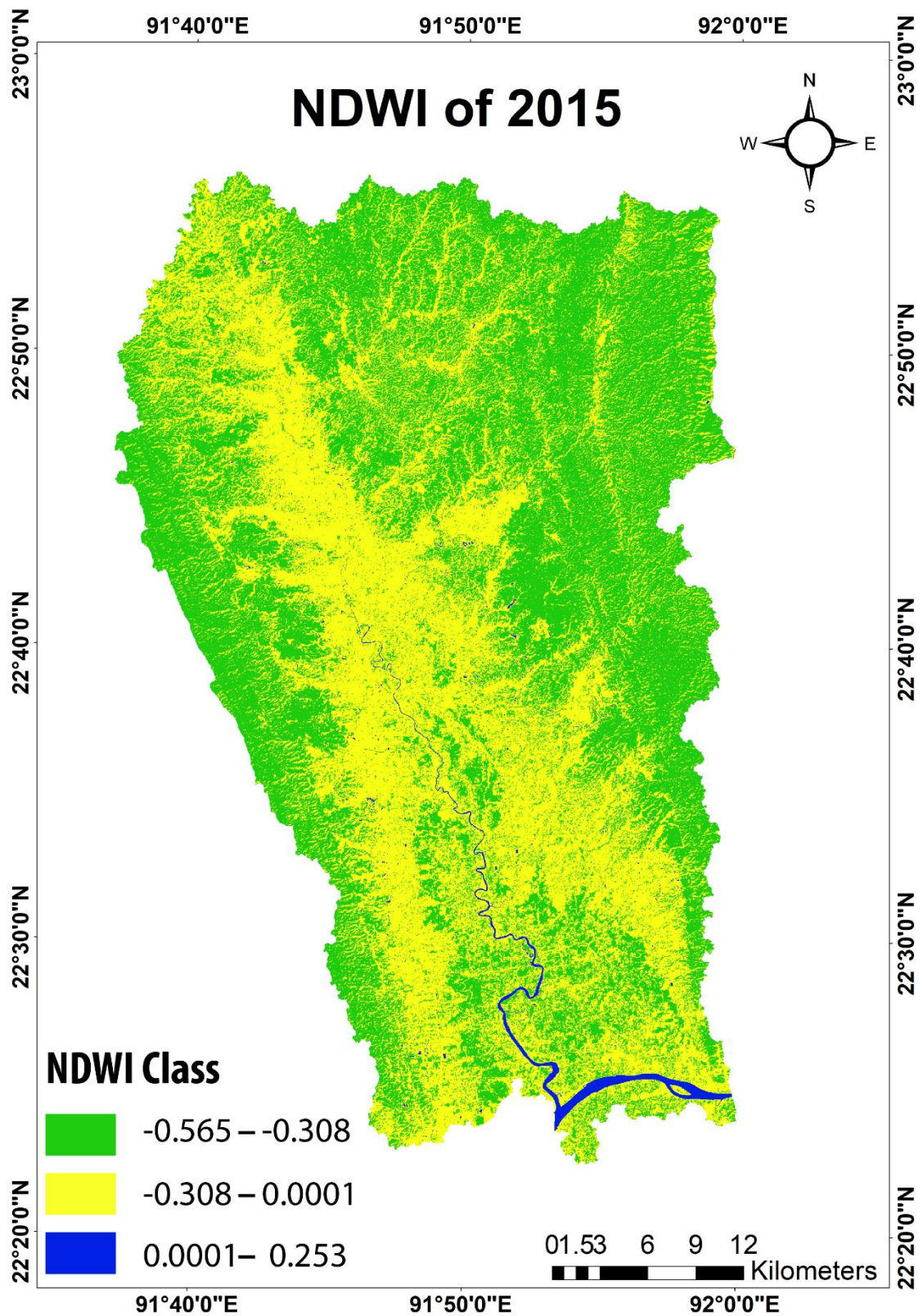


Figure 12: Normalized difference water index in 2015

4.3 Water Transition Over Various Region of Halda

The Water Class Transitions map provides information on the change in seasonality between 1984 to 2015 and captures changes between the three classes of not water, seasonal water and permanent water. Based on these three classes, the following transitions were mapped: unchanging permanent water surfaces; new permanent water surfaces (conversion of land into permanent water); lost permanent water surfaces (conversion of permanent water into land); unchanging seasonal water surfaces; new seasonal water surfaces (conversion of land into seasonal water); lost seasonal water surfaces (conversion of a seasonal water into land); conversion of permanent water into seasonal water; and the conversion of seasonal water into permanent water. The transition class refers changes from the beginning and end of the time series; they do not describe what happened in the intervening years.

In some cases, water is not present at the beginning or the end of the observation record but is present in some of the intervening years. By tracking the inter-annual patterns of such ‘ephemeral’ events and their intra-annual characteristics, each such area was classified as either ephemeral permanent water (land replaced by permanent water that subsequently disappears) or ephemeral seasonal water (land replaced by seasonal water that subsequently disappears), depending on the majority of the observed seasonality during the period of water presence.

Here, based on intensity five region of Halda river is marked as ‘a’, ‘b’, ‘c’, ‘d’, ‘e’ in Figure 13. ‘a’ cover Samitirhat and Guman Mardan, ‘b’ covers Gahira and Garduara, ‘c’ covers Gahira and Mekhal, ‘d’ covers North Madarsha and West Guzara, ‘e’ covers Noapara and 5 no. ward of Chittagong City Corporation. Lost seasonal water body was significantly observed over Gahira, Daulatput, Suabil and Sundarpur union. New seasonal water body was found at Gahira, Garduara, Mekhal, West Guzara and Samitirhat union. Land use and Land cover for ‘a’, ‘b’, ‘c’, ‘d’, ‘e’ is described in Figure 14. Table 7 describes the population density with selected unions. Population data was collected from 2011 census data (Bangladesh Bureau of Statistics, 2019).

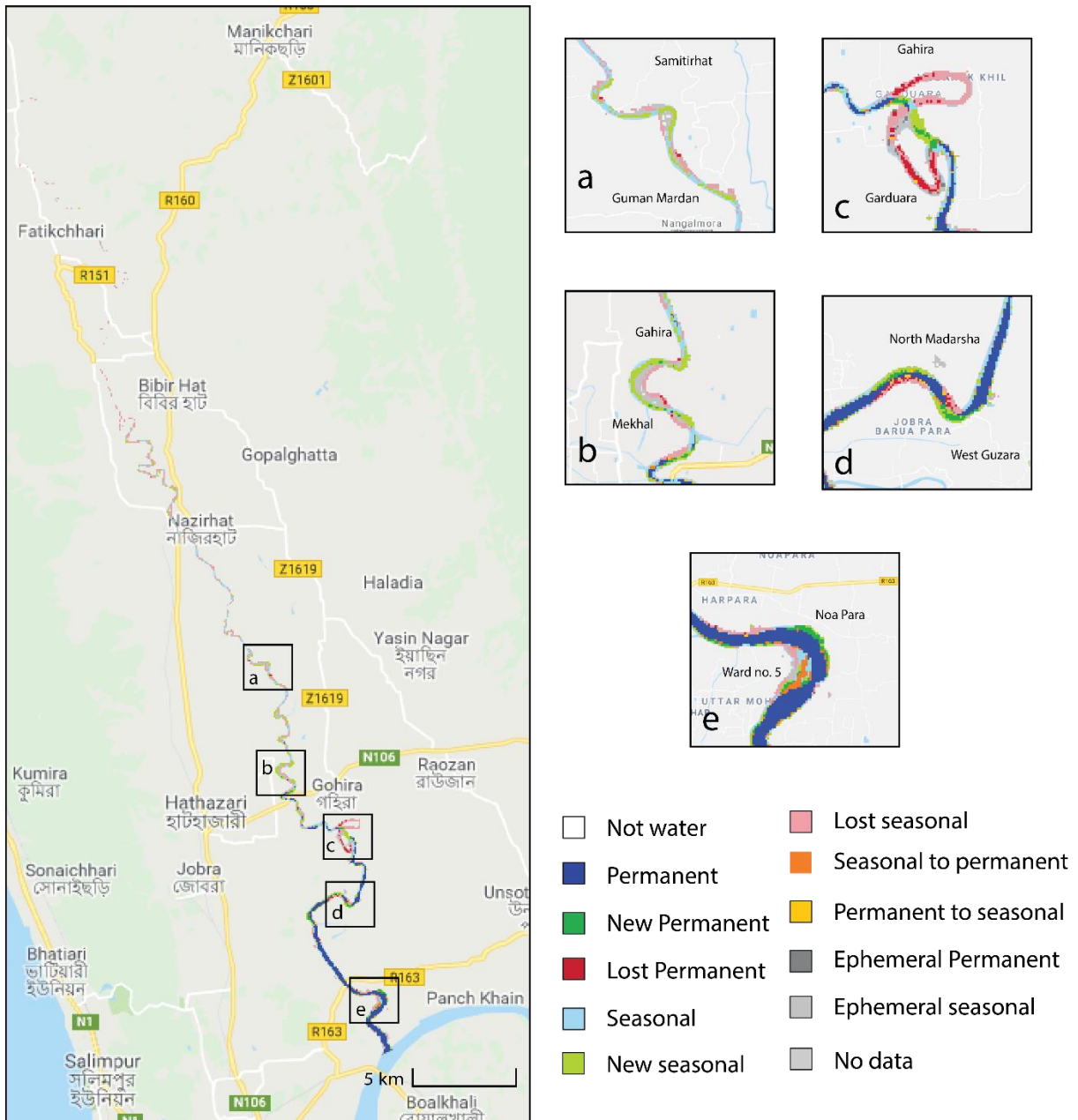


Figure 13: Transition class over various region of Haldia River

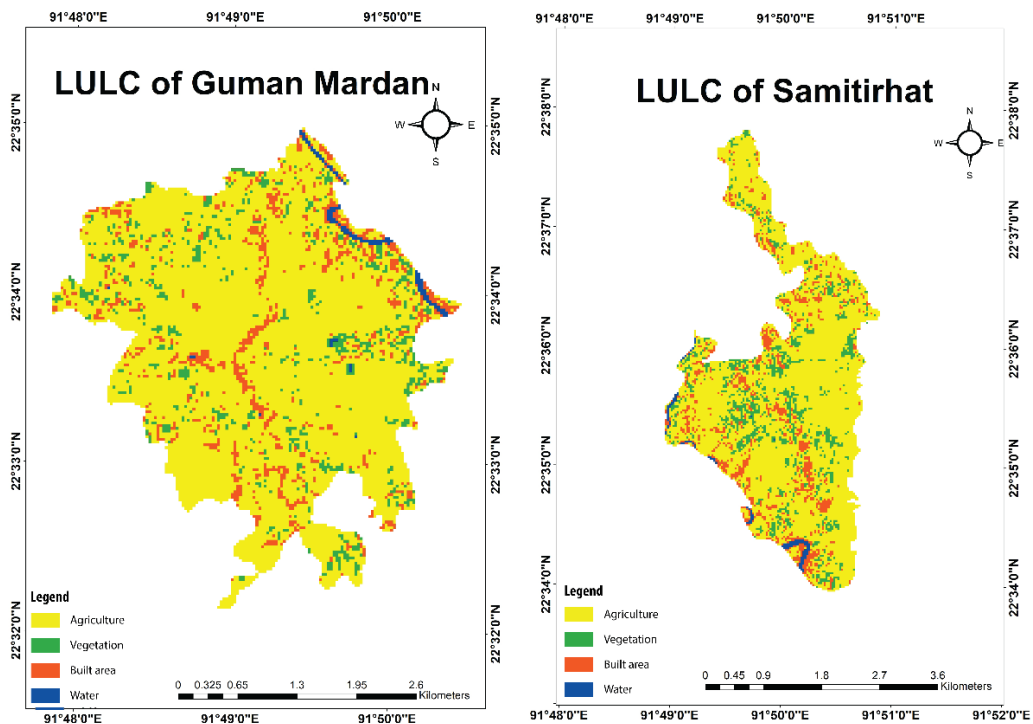


Figure 14 (a): LULC of Guman Mardan and Samitirhat

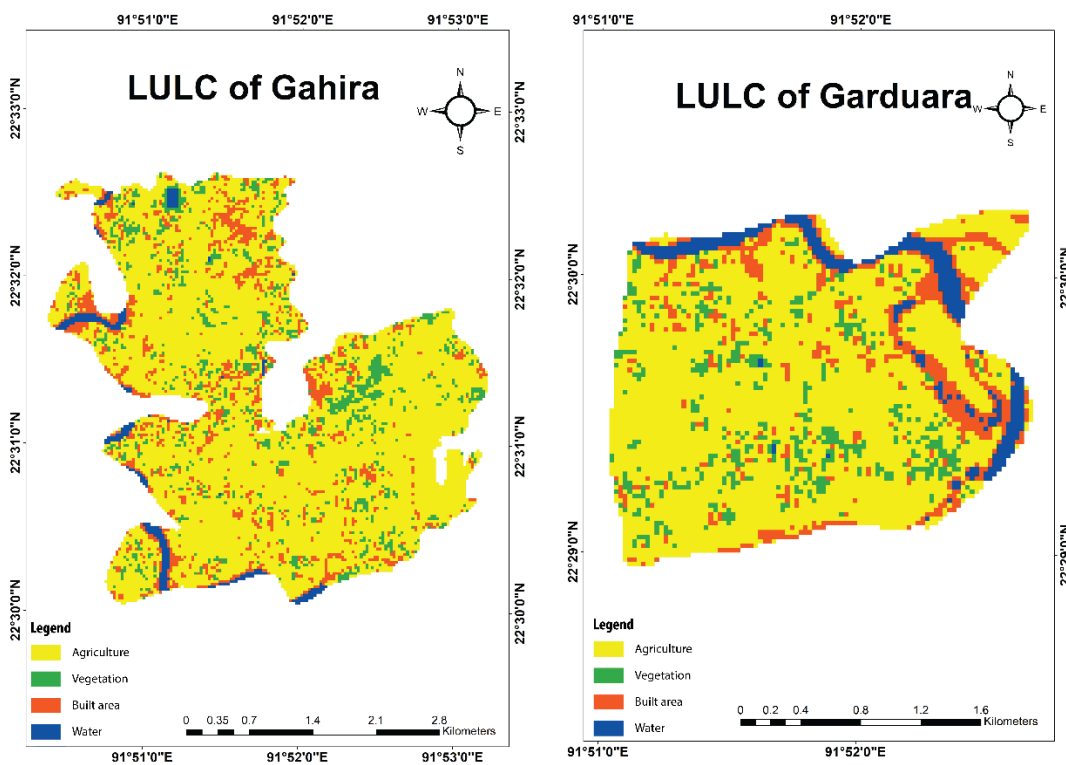


Figure 14 (b): LULC of Gahira and Garduara

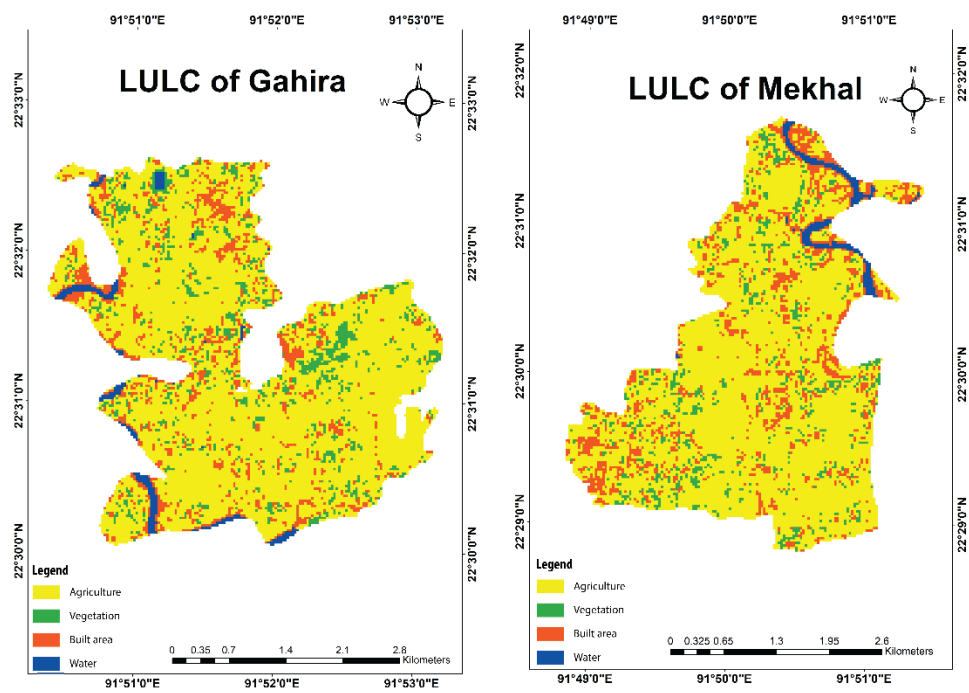


Figure 14 (c): LULC of Gahira and Mekhal

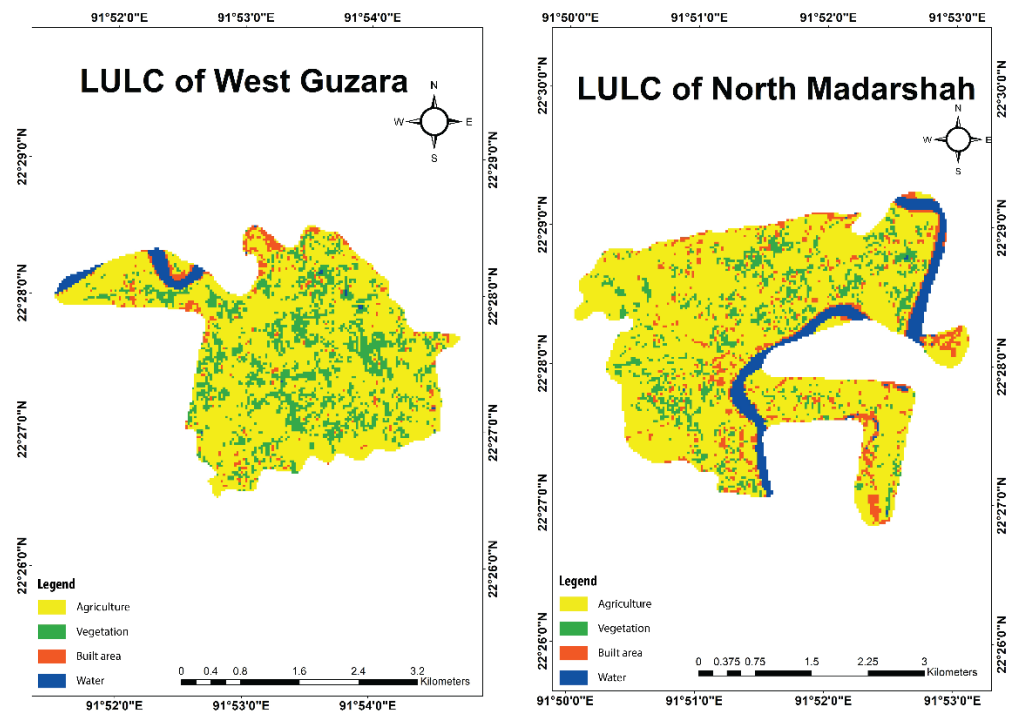


Figure 14 (d): LULC of West Guzara and North Madarshah

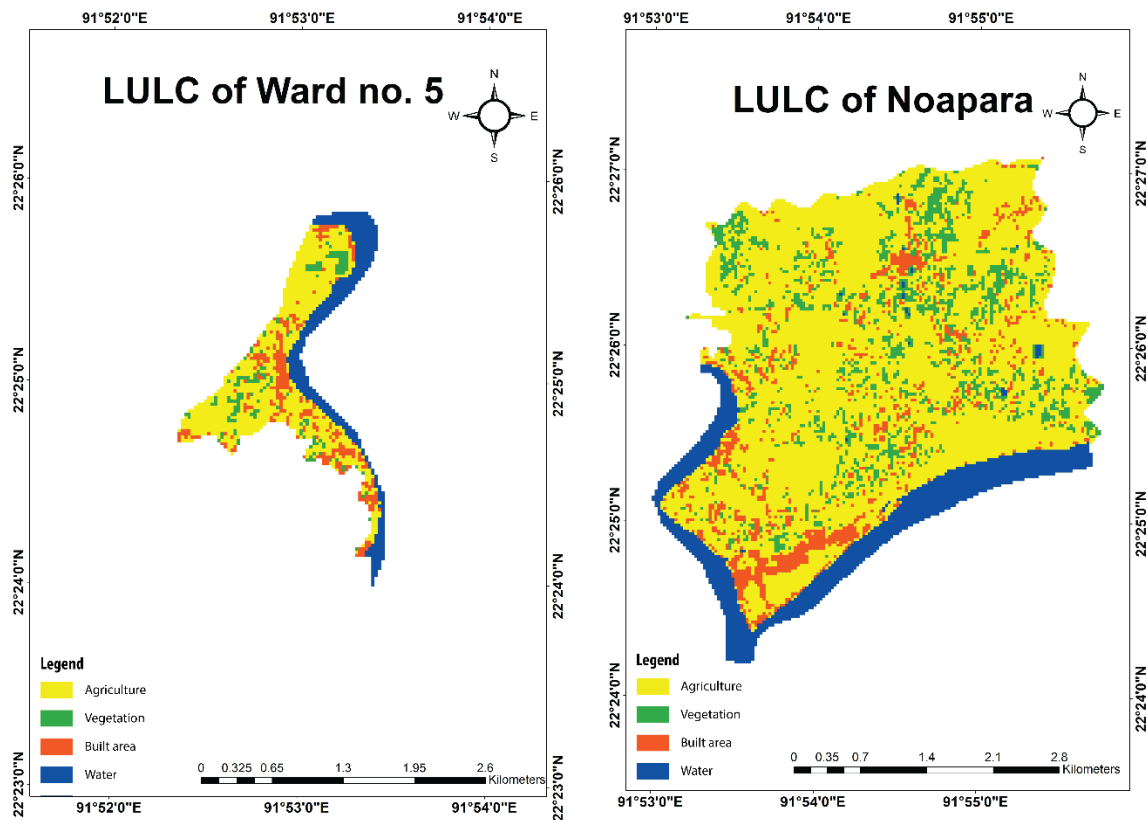


Figure 14 (e): LULC of Ward no. 5 and Noapara

Table 7: LULC of unions and population density

Union	Density (person/acre)	Agriculture	Vegetation	Built area	Water
Samitirhat	7.31	795.24	119.43	117	12.24
Guman Mardan	4.33	994.14	84.51	109.98	12.15
Gahira	7.35	1034.28	118.53	157.23	30.51
Mekhal	10.61	886.95	84.78	174.51	26.19
North Madarsha	7.26	890.37	140.67	108.9	80.46
West guzara	5.32	702.81	216.9	45.9	23.76
Noapara	9.36	1033.38	165.06	135.9	173.88
Ward no. 5	34.01	98.1	14.13	27.99	44.28

Water transition classes were identified and quantified for both Halda river and Halda Basin based on JRC database. Table 8 shows the water transition class with percentage distribution.

A permanent water surface is underwater throughout the year, while a seasonal water surface is underwater for less than 12 months of the year. In Halda basin, 756.91 ha (33.71%) area, waterbody remained permanent over the study period where in 141 ha land (6.28%), unchanged seasonal water surface observed. 333.69 ha (14.86%) of land newly evolved as seasonal water surfaces. 12.06% of seasonally inundated surface has been converted to land area which covers 270.74 ha land.

Table 8: Water transition class with area and percentage

Name of transition class	Area (ha) in Basin	%	Area (ha) in River	%
Permanent	756.91	33.71	228.25	33.69
New permanent	64.6	2.88	22.27	3.29
Lost permanent	16.8	0.75	16.39	2.42
Seasonal	141	6.28	84.79	12.51
New seasonal	333.69	14.86	95.52	14.10
Lost seasonal	270.74	12.06	146.63	21.64
Seasonal to permanent	29.39	1.31	12.58	1.86
Permanent to seasonal	7.28	0.32	4.09	0.60
Ephemeral permanent	2.81	0.13	2.73	0.40
Ephemeral seasonal	622.05	27.70	64.25	9.48

Over the period of 1984 to 2015 at Halda river basin, 16.39 ha (2.42%) of water bodies previously thought of as permanent have converted to land; almost 146.63 ha seasonal water have vanished altogether and over 14.10% have transitioned to a seasonal state covering 95.52 ha. During the same period 84.79 ha of seasonal water body remained unchanged. Land replaced by seasonal water that subsequently disappears termed as ephemeral seasonal was 64.25 ha (9.48%) of river. 12.58 ha of land used to be seasonally flooded but are now underwater all year round. Area occupied by each transition class for both Halda river and Halda Basin are given in Figure 15.

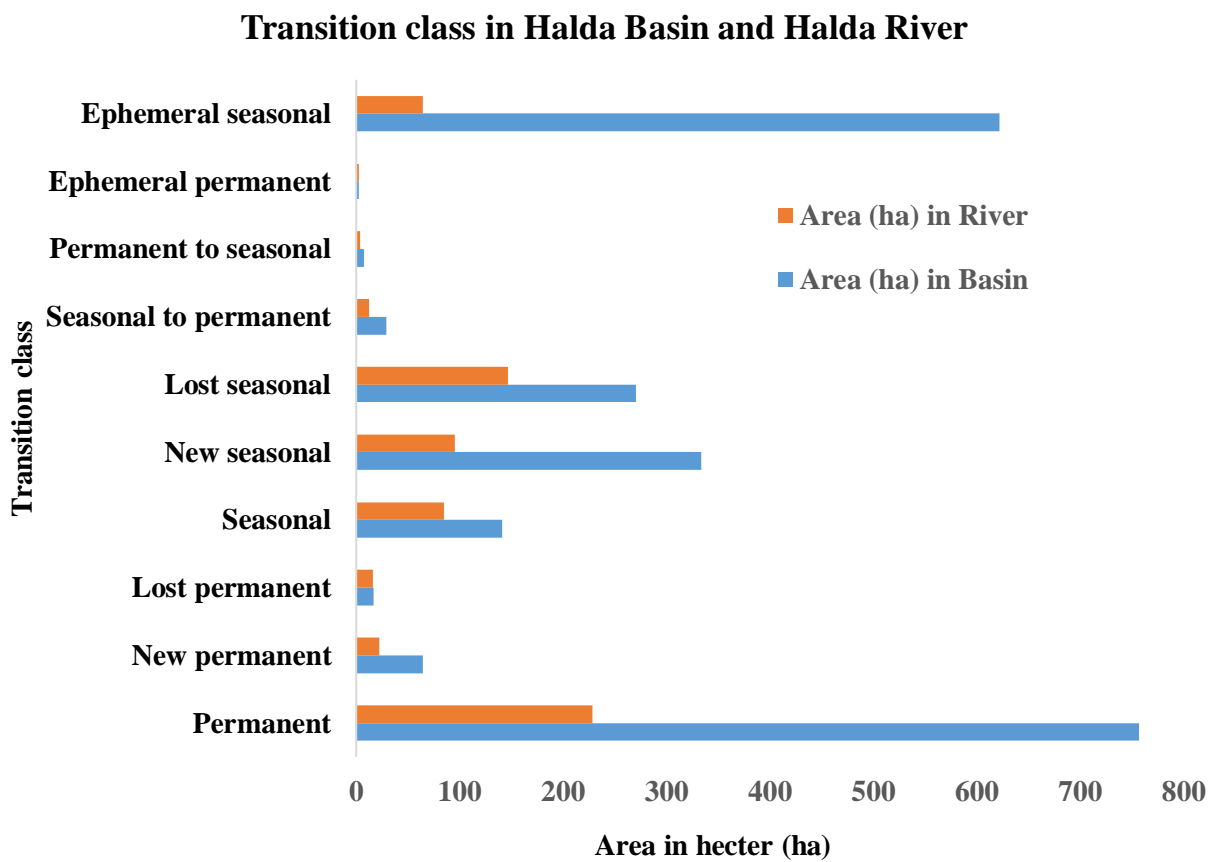


Figure 15: Area occupied by each transition class

4.4 Measuring erosion and accretion

New permanent water body and new seasonal water body refer to that land which was used as land previously. But in the course of time those lands are inundated under water due to river bank erosion. New permanent water body and new seasonal water aggregate covered 117.79 ha of land that has gone under water as eroded land. The river had lost its 16.39 ha of permanent water body and 146.63 ha of seasonal water body. These lands were treated as water in before, but now these water body converted to land due to sedimentation. Total 163.02 ha of land newly accreted from surface water body over 1984 to 2015.

4.5 Occurrence Change Intensity

Occurrence change intensity displayed the area where river changes its water occurrence. Green colored area in Figure 16 indicates the 100% increase the occurrence, where red colored area is 100% decreased in water occurrence. Black colored areas remain unchanged over the period of 1984 to 2015. Unchanged water has occurred mostly where the river meets Karnaphuli. This change intensity refers the water gain and loss in the river bank over a long time. At river bank area, 100% increased and decreased area has been observed. At Noapara, 5 no ward, Gahira, Garduara, Guman Mardan, Samitir hat, the change in occurrence was mostly visible.

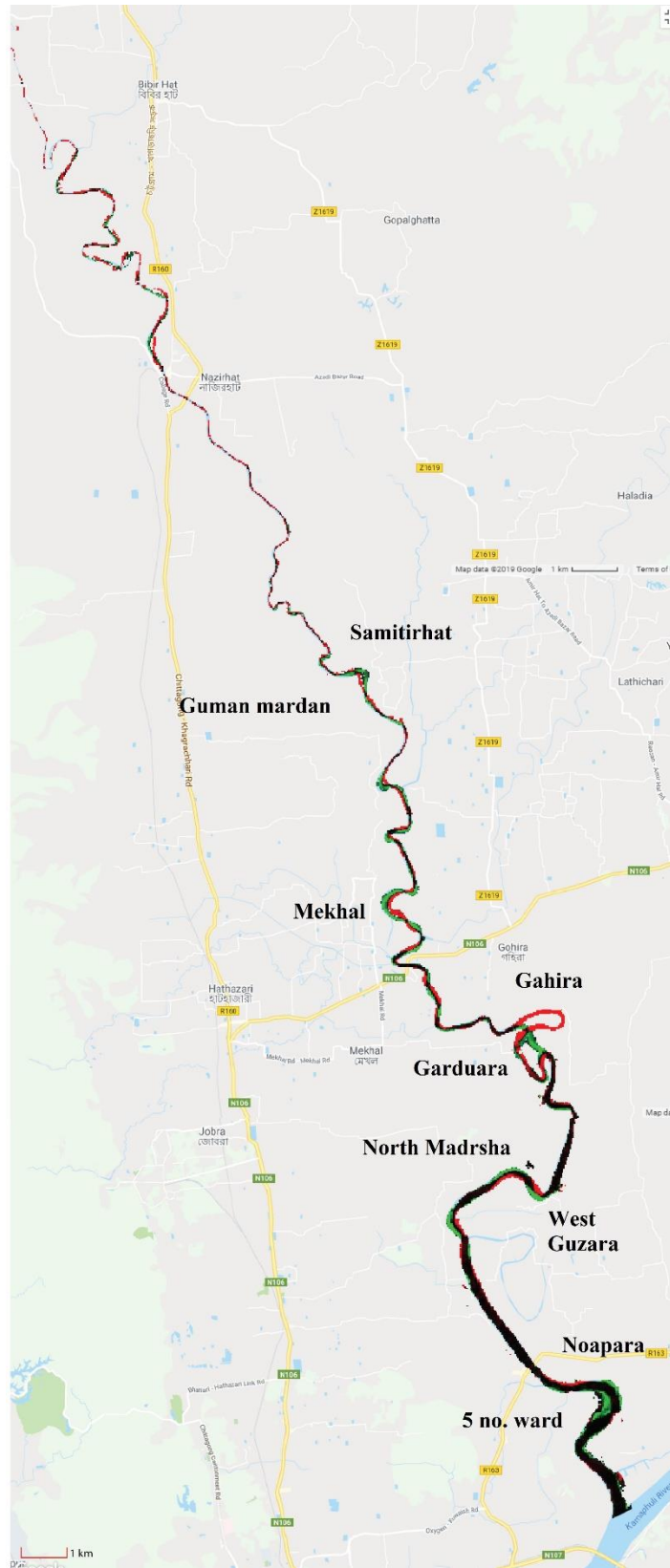


Figure 16: Occurrence change intensity over Halda river

4.6 Mapping Changes in the River Course

Parameters considered for mapping river course change were length, width and number of bends for each year 2001, 2009 and 2018. This parameters for each year exhibits change in river course. Both natural and anthropogenic causes bring change in river flow. Middle line of each year shows dynamic change of river direction. Most changing points are given in Table 9.

Table 9: River course changing points

Point	Location	Union
a	22°48'22.50"N, 91°43'21.54"E	NARAYANHAT
b	22°45'16.99"N, 91°45'38.13"E	BHUJPUR
c	22°39'24.16"N, 91°47'10.67"E	SUABIL
d	22°34'24.97"N, 91°50'15.15"E	SAMITIRHAT
e	22°29'53.18"N, 91°52'28.73"E	GARDUARA

In Garduara, River changes its flow in 2018 due to ox-bow cutting. A notable change occurred at the starting point of Halda river. At Bhujpur union, construction of rubber dam shifts river course in 2018. At Suabil and Samitirhat, Halda river experienced significant course change.

4.6.1 Changes in the Length of the river

Due to change in direction, the river also changes its length. In 2001, total length of Halda river was 81 km. In 2009, river length increased and it was 82 km where, in 2018 river length again decreased to 80.8km. Due to oxbow cutting and erosion-sedimentation, the river course is continuously changing with an increase or decrease in length.

4.6.2 Changes in the Width of the river

As Halda river shifts its direction over space and time, the river width is also changing. Randomly 20 points were taken into consideration for measuring river width changes. Increased and decreased in width was observed over the same location by comparing the widths in 2001, 2009 and 2018 (Table 10). Over the periods, accretion and erosion has occurred due to anthropogenic and natural events resulting in fluctuation of width. Increase and decrease in river width are shown in Figure 19.

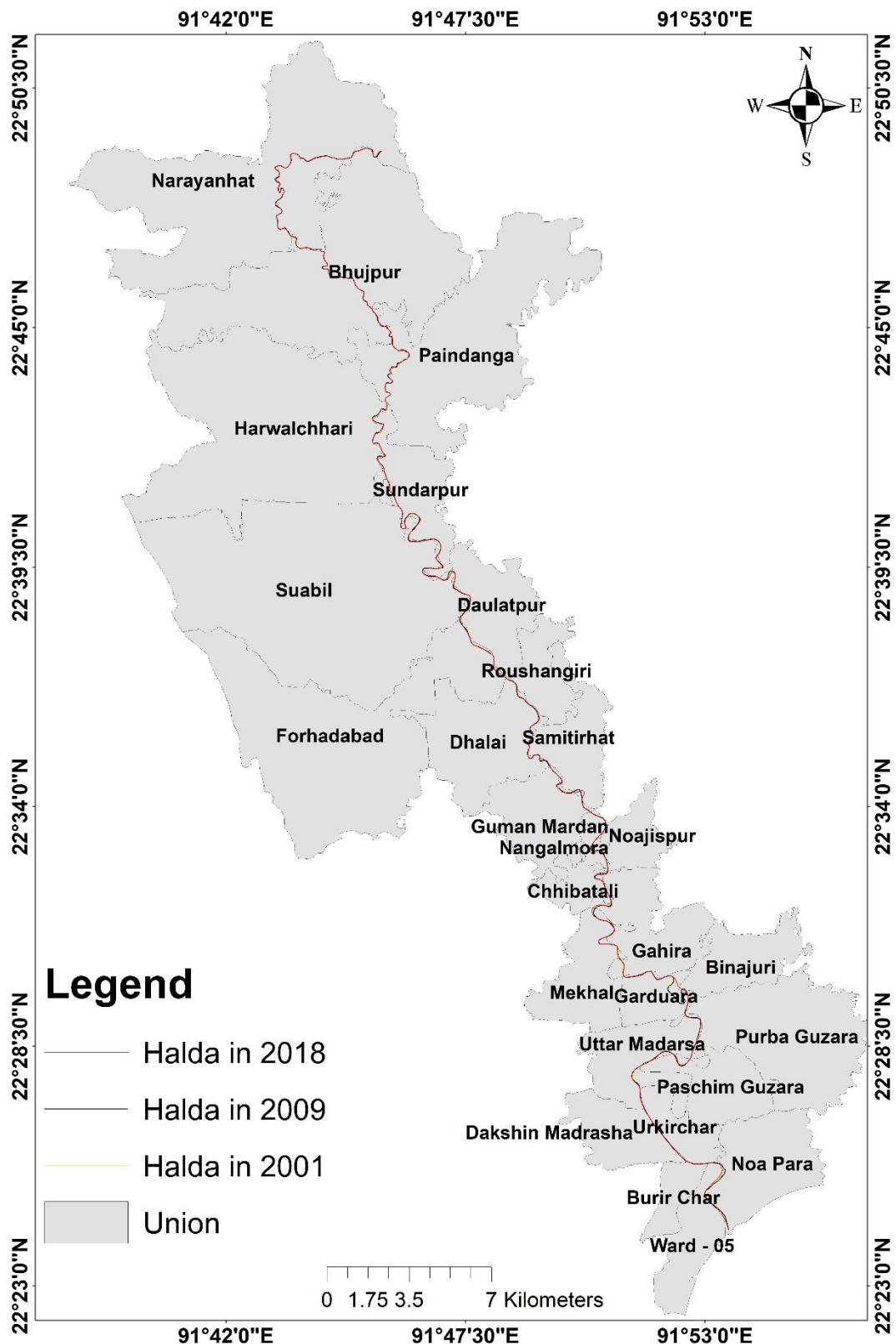


Figure 17: Halda river with adjacent Unions

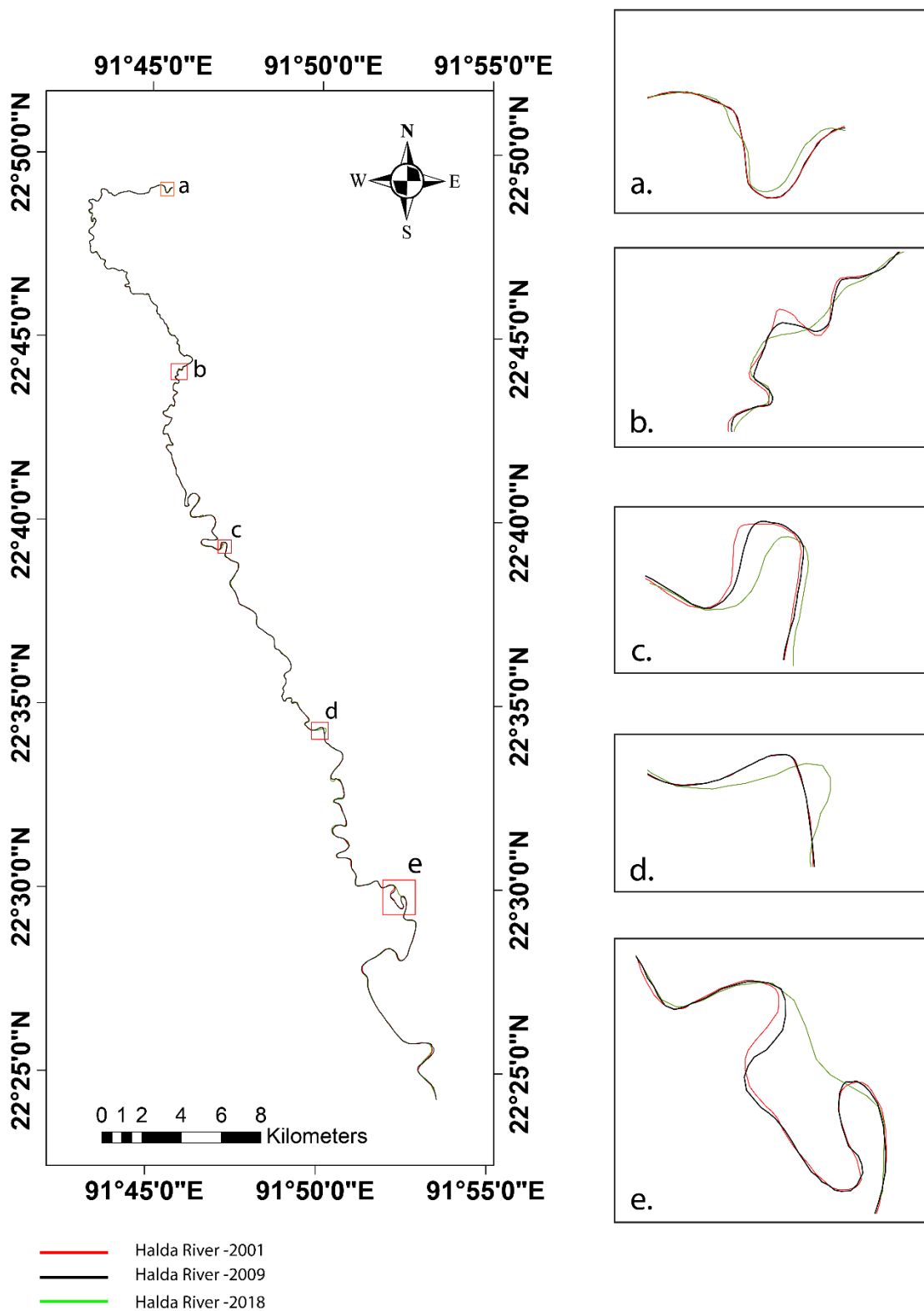


Figure 18: Shifting of Halda River from 2001 to 2018



Figure 19: River Width fluctuation on different points

The highest increase value (89 m) was observed for point K located at Najirhat and the highest decreased value was observed (-27.8) at point O located at Kumarpara, 2.42 km downward of Bhujpur Rubber Dam over the period of 2009 to 2018. It indicates the negative impact of the rubber dam on the river morphology. It will be interesting to do a comprehensive comparison between upstream and downstream of the rubber dam to get a better picture.

Table 10: River Width Change in 2001, 2009 and 2018

Point no.	Width in 2001 (m)	Width in 2009 (m)	Width in 2001 (m)	Change in 2009-2001	Change in 2018-2009	Change in 2018-2001
A	304	303	319	-1	16	15
B	170	172	188	2	16	18
C	149	147	154	-2	7	5
D	121	114	131	-7	17	10
E	101	93	131	-8	38	30
F	88.4	75	111	-13.4	36	22.6
G	52.6	40	110	-12.6	70	57.4
H	52.7	48.8	74.4	-3.9	25.6	21.7
I	56.3	48.3	67	-8	18.7	10.7
J	53.1	45.4	88.1	-7.7	42.7	35
K	32	44.1	121	12.1	76.9	89
L	43	38.2	39.2	-4.8	1	-3.8
M	39.2	34	30.4	-5.2	-3.6	-8.8
N	37.6	35.5	31.7	-2.1	-3.8	-5.9
O	32.2	44.9	17.1	12.7	-27.8	-15.1
P	25	24.9	15.7	-0.1	-9.2	-9.3
Q	35.7	34.7	47.5	-1	12.8	11.8
R	28.7	31.7	31.2	3	-0.5	2.5
S	24.01	28.4	28	4.39	-0.4	3.99
T	23.2	32.8	30	9.6	-2.8	6.8

Note: “-” used for denoting decrease in river width

4.6.3 Changes in the number of bends

Halda river flows through undulating surface area covering hilly and flat areas. The physiographic condition along with continuous erosion and sedimentation, resulting in fluctuation bends number. River direction with union are shown in Figure 17. In 2001, observed major bends number was 29 which remained the same in 2009. But oxbow cutting in Garduara union reduced the number of bends to 26 in 2008. Length of river also reduced to 80.8 km from 82 km because of oxbow cutting.

CHAPTER 5: CONCLUSION AND RECOMMENDATIONS

Surface water is critical in promoting sustainability, as it supports human communities, ecosystem functioning and ensures economic growth. Over the period time, due to anthropogenic and natural causes, surface water of Halda constantly modifying its direction resulting in erosion and accretion. JRC database-based water transition helps to identify surface water changes by which erosion and accretion in river bank was quantified. Water occurrence change intensity generates the idea of river bank shifting due to gaining and losing of surface water for the very important and nationally significant Halda river. Regular monitoring of river surface and adjacent bank is crucial as Halda dynamically changed from historical ages. But this will need personnel and will have to face more complexation and difficulties. This research aimed to measure surface water change over the historic periods and resulting erosion and accretion of river bank from surface water change intensity. Length, width and bends of river was calculated to measure the trend of river course change over space and time. LULC classification and NDWI based surface water marking gives the clear concept of decreasing amount of water over the periods. Increase in built area and agricultural land leading to higher sediment flow which may explain the reduction in NDWI. Hence recommend that plantation in Halda basin is crucial.

Erosion and accretion points were identified and it will be possible to predict for taking better measure. Rubber dam downstream showed accretion for which the river width was decreased. This problem can be reduced by the removal of rubber dam.

This research will contribute to measure erosion and accretion over a large period with less tire and shorten time bound. The annual rate of surface water changing could be identified along with accretion and erosion rate. More vulnerable sites can be marked, which will be supportive for authority to take protective measures. This approach introduced here shows the suitability of Global surface water database in accessing surface water change intensity to calculate eroded and accreted land due to river migration. Thus, this approach can be applied not only for the Halda but also for other large basin science surface water and river course change is a common phenomenon for all other rivers.

5.1 Recommendations

- Use of high-resolution image for yielding from different satellite like USGS, Earth explorer, Sentinel mission etc. can render more accuracy in attaining surface water content.
- Land use classification will be more accurate if it was possible to create more classes and use several bands in many combinations. Due to time bound, it was not possible in this research.
- Global surface water database was not available for recent years. Improvement in this dataset will furnish this study.

5.2 Limitations of the study

The entire archive of the Landsat 5 Thematic Mapper (TM), the Landsat 7 Enhanced Thematic Mapper-plus (ETM+) and the Landsat 8 Operational Land Imager (OLI) orthorectified, top-of-atmosphere reflectance and brightness temperature images (L1T) (Alonso et al., 2016) acquired between 16 March 1984 and 10 October 2015 was used (Gorelick et al., 2017a). The ground area imaged by adjacent orbits overlaps by 7.3% at the Equator, increasing to 68.3% overlap at 70° latitude. Landsat 5, launched 1 March 1984, collected TM imagery until November 2011. Landsat 7 was launched 15 April 1999 and acquired imagery normally until 31 May 2003 when the scan line corrector (SLC) failed, and Landsat 8 began operational imaging in April 2013. The SLC failure causes around 22% of each scene to be lost (Dong et al., 2016). This loss increases from the center, giving SLC-off images a slatted appearance at the edges. Geographic and temporal unevenness are particularly apparent up to 1999; the Americas, Western Europe and Africa were first imaged in 1984, Australia and South East Asia in 1986, but Kolyma was not imaged until 1995 and the northeastern part of the Siberian plateau not until 1999. These gaps are a feature of all global data sets based on the Landsat 30-m archives (Donchyts et al., 2016). However, the efficiency of the database in 2016 using over 40,000 reference points was measured and found that the classifier produces less than 1% of false water detections and misses less than 5% of water over the world (Pekel et al., 2016).

This study attempted to estimate erosion and accretion through surface water occurrence from previously developed JRC database rather than using robust satellite imagery analysis. This database experiences some no data value around the world, for this some region of Halda river produces no occurrence of water. These no data values are masked out by a transparent color in the map layer.

Landsat images are freely available but the problem is its lower spatial resolution. The spatial resolution of Landsat 8 is 30 m, while IKONIS, Quickbird, SPOT are high resolution images. But these are not free. Actual scenario of 1990 images could not be found properly by google earth due to the lack of referenced material. While measuring river width, at some places picture quality was obscure for 2001 imagery due to low resolution and poor image quality. On the other hand, results in NDWI will be more reliable if we could count NDWI for several month and years

It was found that all the areas of Halda river was not enumerated in JRC database. Satellite imagery was not clearly observed at starting years, for that water body at the starting points of Halda river was not captured as water. Bodies of water smaller than 30 m by 30 m, overhanging and standing vegetation or hidden by infrastructure such as bridges were not included. After all, data gaps were created by cloud cover and other atmospheric events.

REFERENCES

- Afify, H.A., 2011. Evaluation of change detection techniques for monitoring land-cover changes: A case study in new Burg El-Arab area. *Alexandria Engineering Journal* 50, 187–195. <https://doi.org/10.1016/j.aej.2011.06.001>
- Akhtaruzzaman, M., Osman, K.T., Sirajul, H., 2015. Properties of Soils under Different Land Uses in Chittagong Region, Bangladesh. *Journal of forest and environmental science* 31, 14–23.
- Akhter, F., 2015. Change of Halda river flow due to different water control structures and its impact on Halda ecosystem. URL:<http://lib.buet.ac.bd:8080/xmlui/handle/123456789/4657>
- Akter, A., Ali, M.H., 2012a. Environmental flow requirements assessment in the Halda River, Bangladesh. *Hydrological sciences journal* 57, 326–343.
- Akter, A., Ali, M.H., 2012b. Environmental flow requirements assessment in the Halda River, Bangladesh. *Hydrological sciences journal* 57, 326–343.
- Alam, M.S., Hossain, M.S., Monwar, M., 2013. Assessment of fish distribution and biodiversity status in Upper Halda River, Chittagong, Bangladesh 9.
- Alam, S., 2001. A critical evaluation of sedimentation management design practice. *International Journal on Hydropower & Dams* 8, 54–59.
- Alonso, A., Muñoz-Carpena, R., Kennedy, R.E., Murcia, C., 2016. Wetland landscape spatio-temporal degradation dynamics using the new Google Earth Engine cloud-based platform: Opportunities for non-specialists in remote sensing. *Transactions of the ASABE* 59, 1331–1342.
- Al-Qadery, S.M., Muhibullah, M., 2008. People's perception on urban traffic congestion; a case study on Chittagong Metropolitan City, Bangladesh. *Chittagong University Journal of Biological Sciences* 149–160.
- Anderson, J.R., 1976. A land use and land cover classification system for use with remote sensor data. US Government Printing Office.
- ARSHAD-UL-ALAM, M., 2013. Fishing intensity of the Halda River, Chittagong, Bangladesh. *Int. J. Sci. Inn. Tech. Sec. A* 2, 10–16.
- Arshad-Ul-Alam, M., Azadi, M.A., 2015. Efficiency of fishing gears in the river Halda, Chittagong, Bangladesh. *Journal of Fisheries* 3, 275–284.

- Azadi, M.A., 2004. Management of spawn fishery of major carps (*Labeo rohita*, *Catla catla* and *Cirrhinus circhosus*) in the Halda River, Chittagong, Bangladesh. *Bangladesh Journal of Fisheries (Special Issue)* 27, 50–51.
- Azadi, M.A., 1979. Studies on the Limnology of the River Halda with special reference to the spawning of major carps. Department of Zoology. University of Chittagong, Chittagong 232.
- Azadi, M.A., Alam, M.A.U., 2013. Ichthyofauna of the River Halda, Chittagong, Bangladesh. *Bangladesh Journal of Zoology* 41, 113–133.
- Azadi, M.A., Arshad-ul-Alam, M., 2011. Diversity of Finfish and Shellfish of the river Halda with notes on their conservation, in: Proceedings of the International Conference on Biodiversity-Present State, Problems and Prospect of Its Conservation. pp. 91–101.
- Badiuzzaman, M., 1978. Development of unit hydrograph for the Halda river basin.
- Bangladesh Bureau of Statistics , 2019. URL <http://203.112.218.65:8008/> (accessed 3.8.19).
- Banglapedia , 2015. URL <https://www.banglapedia.org/> (accessed 3.7.19).
- BBS, 2013. District Statistics 2011, Chittagong. Statistics and Information Division (SID),MoP.
- Bhuyan, Bakar, 2017. Seasonal variation of heavy metals in water and sediments in the Halda River, Chittagong, Bangladesh. *Environ Sci Pollut Res* 24, 27587–27600.
<https://doi.org/10.1007/s11356-017-0204-y>
- Bhuyan, M., Bakar, M., 2017. Assessment of water quality in Halda River (the Major carp breeding ground) of Bangladesh. *Pollution* 3, 429–441.
- Bhuyan, M.S., Bakar, M.A., 2017. Seasonal variation of heavy metals in water and sediments in the Halda River, Chittagong, Bangladesh. *Environmental Science and Pollution Research* 24, 27587–27600.
- Burrough, P.A., 1986. Principles of Geographical Information Systems for Land Resources Assessment. Clarendon Press.
- BWDB, 2017. Study for Upgrading and Rehabilitation of (a) Karnafuly Irrigation Project (Halda & Ichamoti Unit), (b) Fatikchari FCDI Project, (c) Halda Extension Irrigation Project and (d) Nishchintapur FCDI Project with ESIA in Hathazari, Rauzan, Rangunia and Fatilchari Upazilas in Chittagong District, Draft Final Report (Volume II).

- Carroll, M., Wooten, M., DiMiceli, C., Sohlberg, R., Kelly, M., 2016. Quantifying surface water dynamics at 30 meter spatial resolution in the North American high northern latitudes 1991–2011. *Remote Sensing* 8, 622.
- Chatterjee, M., Prasad, N., 2011. Riverine morphology and socio-economic environment—a review.
- Chittagong Region River System - Banglapedia , 2014. URL
http://en.banglapedia.org/index.php?title=Chittagong_Region_River_System (accessed 3.7.19).
- Chowdary, V.M., Chandran, R.V., Neeti, N., Bothale, R.V., Srivastava, Y.K., Ingle, P., Ramakrishnan, D., Dutta, D., Jeyaram, A., Sharma, J.R., Singh, R., 2008. Assessment of surface and sub-surface waterlogged areas in irrigation command areas of Bihar state using remote sensing and GIS. *Agricultural Water Management* 95, 754–766.
<https://doi.org/10.1016/j.agwat.2008.02.009>
- Chowdhury, M., Hasan, M.E., Abdullah-Al-Mamun, M.M., 2018. Land use/land cover change assessment of Halda watershed using remote sensing and GIS. *The Egyptian Journal of Remote Sensing and Space Science*. <https://doi.org/10.1016/j.ejrs.2018.11.003>
- Connor, R., 2015. The United Nations world water development report 2015: water for a sustainable world. UNESCO Publishing.
- Das, K., 2017. NDVI and NDWI based Change Detection Analysis of Bordoibam Beelmukh Wetlandscape, Assam using IRS LISS III data. *ADBU Journal of Engineering Technology* 6.
- Dhar, B.C., Kafi, M.A., Hoque, M., 2015. Construction of deep water pile and pile cap by using prefabricated steel coffer dam technique.
- Donchyts, G., Baart, F., Winsemius, H., Gorelick, N., Kwadijk, J., Van De Giesen, N., 2016. Earth's surface water change over the past 30 years. *Nature Climate Change* 6, 810.
- Dong, J., Xiao, X., Menarguez, M.A., Zhang, G., Qin, Y., Thau, D., Biradar, C., Moore III, B., 2016. Mapping paddy rice planting area in northeastern Asia with Landsat 8 images, phenology-based algorithm and Google Earth Engine. *Remote sensing of environment* 185, 142–154.
- Earth Engine Code Editor , 2019. URL <https://code.earthengine.google.com/> (accessed 3.8.19).

- Earth Engine Data Catalog , 2019. . Google Developers. URL
<https://developers.google.com/earth-engine/datasets/> (accessed 3.7.19).
- Eastman, J.R., 1999. IDRISI 32: Guide to GIS and image processing. Clark University.
- Foley, J.A., DeFries, R., Asner, G.P., Barford, C., Bonan, G., Carpenter, S.R., Chapin, F.S., Coe, M.T., Daily, G.C., Gibbs, H.K., 2005. Global consequences of land use. *science* 309, 570–574.
- Fubara-Manuel, I., Jumbo, R.B., 2014. Investigation of ground water quality during the dry season in rivers state, Nigeria: a case study of port Harcourt metropolis. *Journal of Agricultural Engineering and Technology* 22, 105–111.
- Ghose, B., 2014. Fisheries and aquaculture in Bangladesh: Challenges and opportunities. *Annals of Aquaculture and Research* 1, 1–5.
- Global Forest Watch , 2019. URL <https://www.globalforestwatch.org/> (accessed 3.7.19).
- Global Surface Water Explorer , 2019. URL <https://global-surface-water.appspot.com/> (accessed 3.7.19).
- Goldblatt, R., You, W., Hanson, G., Khandelwal, A., 2016. Detecting the boundaries of urban areas in india: A dataset for pixel-based image classification in google earth engine. *Remote Sensing* 8, 634.
- Google Earth Engine API , 2019. . Google Developers. URL <https://developers.google.com/earth-engine/> (accessed 3.7.19).
- Gorelick, N., Hancher, M., Dixon, M., Ilyushchenko, S., Thau, D., Moore, R., 2017a. Google Earth Engine: Planetary-scale geospatial analysis for everyone. *Remote Sensing of Environment* 202, 18–27.
- Gorelick, N., Hancher, M., Dixon, M., Ilyushchenko, S., Thau, D., Moore, R., 2017b. Google Earth Engine: Planetary-scale geospatial analysis for everyone. *Remote Sensing of Environment, Big Remotely Sensed Data: tools, applications and experiences* 202, 18–27.
<https://doi.org/10.1016/j.rse.2017.06.031>
- Halda River - Banglapedia , 2015. URL http://en.banglapedia.org/index.php?title=Halda_River (accessed 2.23.19).
- Halda River , 2012. URL <http://www.haldariver.org/> (accessed 3.7.19).
- Hansen, M.C., Potapov, P.V., Moore, R., Hancher, M., Turubanova, S.A., Tyukavina, A., Thau, D., Stehman, S.V., Goetz, S.J., Loveland, T.R., Kommareddy, A., Egorov, A., Chini, L.,

- Justice, C.O., Townshend, J.R.G., 2013. High-Resolution Global Maps of 21st-Century Forest Cover Change. *Science* 342, 850–853. <https://doi.org/10.1126/science.1244693>
- Hassan, S.T., Syed, M.A., Mamnun, N., 2017. Estimating erosion and accretion in the coast of Ganges-Brahmaputra-Meghna Delta in Bangladesh.
- Herring, J.W. and D., 2000. Measuring Vegetation (NDVI & EVI): Feature Articles . URL https://earthobservatory.nasa.gov/Features/MeasuringVegetation/measuring_vegetation_2.php (accessed 8.12.17).
- Hoekstra, A.Y., Chapagain, A.K., Van Oel, P.R., 2017. Advancing Water Footprint Assessment Research: Challenges in Monitoring Progress towards Sustainable Development Goal 6. *Water* 9, 438. <https://doi.org/10.3390/w9060438>
- Islam, Akbar, A., Akhtar, A., Kibria, M.M., Bhuyan, M.S., 2017. Water Quality Assessment Along With Pollution Sources of the Halda River. *Asia. Soci. J* 43, 61–70.
- Islam, K., Jashimuddin, M., Nath, B., Nath, T.K., 2018. Land use classification and change detection by using multi-temporal remotely sensed imagery: The case of Chunati wildlife sanctuary, Bangladesh. *The Egyptian Journal of Remote Sensing and Space Science* 21, 37–47.
- Islam, K., Jashimuddin, M., Nath, B., Nath, T.K., 2017. Land use classification and change detection by using multi-temporal remotely sensed imagery: The case of Chunati wildlife sanctuary, Bangladesh. *The Egyptian Journal of Remote Sensing and Space Science*. <https://doi.org/10.1016/j.ejrs.2016.12.005>
- Islam, M.R., Begum, S.F., Yamaguchi, Y., Ogawa, K., 1999. The Ganges and Brahmaputra rivers in Bangladesh: basin denudation and sedimentation. *Hydrological Processes* 13, 2907–2923.[https://doi.org/10.1002/\(SICI\)1099-1085\(19991215\)13:17<2907::AID-HYP906>3.0.CO;2-E](https://doi.org/10.1002/(SICI)1099-1085(19991215)13:17<2907::AID-HYP906>3.0.CO;2-E)
- Joseph, B., Kelvin, 2013. Technology Development and Platform Enhancements for Successful Global E-Government Design. IGI Global.
- Joshi, A.R., Dinerstein, E., Wikramanayake, E., Anderson, M.L., Olson, D., Jones, B.S., Seidensticker, J., Lumpkin, S., Hansen, M.C., Sizer, N.C., Davis, C.L., Palminteri, S., Hahn, N.R., 2016. Tracking changes and preventing loss in critical tiger habitat. *Science Advances* 2, e1501675. <https://doi.org/10.1126/sciadv.1501675>

- Kabir, H., Kibria, M., Jashimuddin, M., Hossain, M.M., 2015a. Conservation of a river for biodiversity and ecosystem services: the case of the Halda – the unique river of Chittagong, Bangladesh. International Journal of River Basin Management 13, 333–342. <https://doi.org/10.1080/15715124.2015.1012514>
- Kabir, H., Kibria, M., Jashimuddin, M., Hossain, M.M., 2015b. Conservation of a river for biodiversity and ecosystem services: the case of the Halda—the unique river of Chittagong, Bangladesh. International Journal of River Basin Management 13, 333–342.
- Kabir, H., Kibria, M., Jashimuddin, M., Hossain, M.M., 2011. Original Article Economic Valuation of Tangible Resources From Halda— The Carp Spawning Unique River Located at Southern Part of Bangladesh 8.
- Kabir, M., Kibria, M., Jashimuddin, M., Hossain, M.M., 2016. Community Involvement in River Management for Ecosystem Services and Livelihood: A Case Study Of Halda River In Bangladesh. Environmental Research Journal 10.
- Kabir, M.H., Kibria, M.M., Jashimuddin, M., Hossain, M.M., 2013. Economic valuation of tangible resources from Halda—the carp spawning unique river located at southern part of Bangladesh. Int. J. Water Res 1, 30–36.
- Kamal, R., Alam, S., Matin, M.A., 2013. Modelling Monsoon Flood Flows of Lower Meghna River Due to Climate Change and Sea Level Rise.
- Kibria, M., Farid, I., Ali, M., 2009. Halda River natural breeding ground restoration project: People's expectation and reality. Chittogram Nagorik Uddogh, Chowdhury Mansion, Polytecnic Road, Nasirabad
- Kibria, M., Jashimuddin, M., Hossain, M.M., 2015. Conservation of a river for biodiversity and ecosystem services: the case of the Halda – the unique river of Chittagong, Bangladesh AU - Kabir, Humayain. International Journal of River Basin Management 13, 333–342. <https://doi.org/10.1080/15715124.2015.1012514>
- Kibria, M.M., Begum, M.A., Bhuyan, M.S., Hossain, M.E., 2018. Livelihood status of egg collector and traditional knowledge of Carps Egg collection in the Halda River: A natural fish spawning heritage in Bangladesh.
- Koning, C.O., 2005. Vegetation patterns resulting from spatial and temporal variability in hydrology, soils, and trampling in an isolated basin marsh, New Hampshire, USA. Wetlands 25, 239–251.

- Kumar, L., Mutanga, O., 2018. Google Earth Engine Applications Since Inception: Usage, Trends, and Potential . ResearchGate. <http://dx.doi.org/10.3390/rs10101509>
- Landis, J.R., Koch, G.G., 1977. An Application of Hierarchical Kappa-type Statistics in the Assessment of Majority Agreement among Multiple Observers. *Biometrics* 33, 363. <https://doi.org/10.2307/2529786>
- Landsat Missions, 2019. URL <https://landsat.usgs.gov/landsat-missions-timeline> (accessed 3.7.19).
- Lee, J.S.H., Wich, S., Widayati, A., Koh, L.P., 2016. Detecting industrial oil palm plantations on Landsat images with Google Earth Engine. *Remote Sensing Applications: Society and Environment* 4, 219–224. <https://doi.org/10.1016/j.rsase.2016.11.003>
- Li, L., Vrieling, A., Skidmore, A., Wang, T., Turak, E., 2018. Monitoring the dynamics of surface water fraction from MODIS time series in a Mediterranean environment. *International journal of applied earth observation and geoinformation* 66, 135–145.
- Liu, X., Hu, G., Chen, Y., Li, X., Xu, X., Li, S., Pei, F., Wang, S., 2018. High-resolution multi-temporal mapping of global urban land using Landsat images based on the Google Earth Engine Platform. *Remote Sensing of Environment* 209, 227–239. <https://doi.org/10.1016/j.rse.2018.02.055>
- Longley, P.A., Goodchild, M., Maguire, D.J., Rhind, D.W., 2010. *Geographic Information Systems and Science*, 3 edition. ed. Wiley, Hoboken, NJ.
- Mahmud, I.M., Mia, J.A., Uddin, R., 2017. Assessment on seasonal variations in waterlogging using remote sensing and GIS techniques in Satkhira district in Bangladesh . ResearchGate. URL (accessed 3.1.19).
- McFeeters, S.K., 1996. The Use of Normalized Difference Water Index (NDWI) in the Delineation of Open Water Features | Request PDF . ResearchGate. <http://dx.doi.org/10.1080/01431169608948714>
- McVicar, T.R., Briggs, P.R., King, E.A., Raupach, M.R., 2003. A review of predictive modelling from a natural resource management perspective: The role of remote sensing of the terrestrial environment. published by CSIRO Land and Water and the CSIRO Earth Observation Centre, Canberra, Australia. URL: http://www.clw.csiro.au/publications/consultancy/2003/Review_Of_Remote_Sensing.pdf.
- Meyer, W.B., 1995. Past and present land use and land cover in the USA. *Consequences* 1, 25–33.

- Meyer, W.B., Turner, B.L., 1992. Human population growth and global land-use/cover change. Annual review of ecology and systematics 23, 39–61.
- Mondal, M.A.M., Water, B.I., 2001. Sea level rise along the coast of Bangladesh. Report, Ministry of Shipping, Dhaka.
- Olorunfemi, J.F., 1983. Monitoring urban land use in developing countries—an aerial photographic approach. Environment International 9, 27–32. [https://doi.org/10.1016/0160-4120\(83\)90111-3](https://doi.org/10.1016/0160-4120(83)90111-3)
- Patel, N.N., Angiuli, E., Gamba, P., Gaughan, A., Lisini, G., Stevens, F.R., Tatem, A.J., Trianni, G., 2015. Multitemporal settlement and population mapping from Landsat using Google Earth Engine. International Journal of Applied Earth Observation and Geoinformation 35, 199–208. <https://doi.org/10.1016/j.jag.2014.09.005>
- Patra, Ronald WR, Azadi, M.A., 1985a. Limnology of the Halda river. The Journal of.
- Patra, RONALD WR, Azadi, M.A., 1985. Hydrological conditions influencing the spawning of major carps in the Halda River, Chittagong, Bangladesh. Bangladesh Journal of Zoology 13, 63–72.
- Patra, Ronald WR, Azadi, M.A., 1985b. Limnology of the Halda river. The Journal of.
- Patra, R.W.R., Azadi, M.A., 1987. Ecological studies on the planktonic organisms of the Halda River. Bangladesh J. Zool 15, 109–123.
- Pekel, J.-F., Cottam, A., Gorelick, N., Belward, A.S., 2016. High-resolution mapping of global surface water and its long-term changes. Nature 540, 418.
- Podder, M., Islam, M.S., Kibria, M.M., Bhuyan, M.S., 2017. Inventory of Watershed Area of the Halda River Basin for Ecosystem Health Management. Environmental Sciences 11, 170–176.
- Richards, J.A., 2013. Supervised Classification Techniques, in: Remote Sensing Digital Image Analysis. Springer Berlin Heidelberg, pp. 247–318. https://doi.org/10.1007/978-3-642-30062-2_8
- Riebsame, W.E., Meyer, W.B., Turner, B.L., 1994. Modeling land use and cover as part of global environmental change. Climatic Change 28, 45–64. <https://doi.org/10.1007/BF01094100>
- River - Banglapedia , 2015. URL <http://en.banglapedia.org/index.php?title=River>
- River and Drainage System - Banglapedia , 2014. URL http://en.banglapedia.org/index.php?title=River_and_Drainage_System (accessed 3.7.19).

- Rony, Z.I., Khan, M.S.I., Asgar, M.A., Begum, M.R., Kibria, A.G., 2016. Effects of saline water on health status of pregnant women in coastal regions of Bangladesh. *Asian Journal of Medical and Biological Research* 2, 55–61.
- Saimon, M.K., Mustafa, M.G., Sarker, B.S., Hossain, M.B., Rahman, M.M., 2016. Marketing channels of Indian carp fry collected from Halda River and livelihood of the fry traders. *Asian J. Agric. Res* 10, 28–37.
- Sarwar, M.G.M., Woodroffe, C.D., 2013. Rates of shoreline change along the coast of Bangladesh. *Journal of Coastal Conservation* 17, 515–526. <https://doi.org/10.1007/s11852-013-0251-6>
- Shibly, A.M., Takewaka, S., 2012. Morphological changes along Bangladesh coast derived from satellite images. *Proceedings of Coastal Engineering* 3, 41–45.
- Sims, D.A., Gamon, J.A., 2003. Estimation of vegetation water content and photosynthetic tissue area from spectral reflectance: a comparison of indices based on liquid water and chlorophyll absorption features. *Remote Sensing of Environment* 84, 526–537. [https://doi.org/10.1016/S0034-4257\(02\)00151-7](https://doi.org/10.1016/S0034-4257(02)00151-7)
- Takagi, T., Oguchi, T., Matsumoto, J., Grossman, M.J., Sarker, M.H., Matin, M.A., 2007. Channel braiding and stability of the Brahmaputra River, Bangladesh, since 1967: GIS and remote sensing analyses. *Geomorphology* 85, 294–305.
- Tsai, C., Islam, M.N., Karim, R., Rahman, K.S., 1981. Spawning of major carps in the lower Halda River, Bangladesh. *Estuaries* 4, 127–138.
- Turner, B.L., Meyer, W.B., Skole, D.L., 1994. Global Land-Use/Land-Cover Change: Towards an Integrated Study. Allen Press, Royal Swedish Academy of Sciences 23.
- UCSF, 2014. . UC San Francisco. URL <https://www.ucsf.edu/news/2014/09/116906/ucsf-google-earth-engine-making-maps-predict-malaria> (accessed 3.7.19).
- van Vliet, J., Bregt, A.K., Hagen-Zanker, A., 2011. Revisiting Kappa to account for change in the accuracy assessment of land-use change models. *Ecological Modelling* 222, 1367–1375. <https://doi.org/10.1016/j.ecolmodel.2011.01.017>
- Verheyen, W.H., 1997. Land use planning and national soils policies. *Agricultural Systems* 53, 161–174. [https://doi.org/10.1016/S0308-521X\(96\)00064-9](https://doi.org/10.1016/S0308-521X(96)00064-9)
- Wang, X., Xiao, X., Zou, Z., Chen, B., Ma, J., Dong, J., Doughty, R.B., Zhong, Q., Qin, Y., Dai, S., Li, X., Zhao, B., Li, B., 2018. Tracking annual changes of coastal tidal flats in China

- during 1986–2016 through analyses of Landsat images with Google Earth Engine. *Remote Sensing of Environment*. <https://doi.org/10.1016/j.rse.2018.11.030>
- Xiong, J., Thenkabail, P.S., Gumma, M.K., Teluguntla, P., Poehnelt, J., Congalton, R.G., Yadav, K., Thau, D., 2017. Automated cropland mapping of continental Africa using Google Earth Engine cloud computing. *ISPRS Journal of Photogrammetry and Remote Sensing* 126, 225–244. <https://doi.org/10.1016/j.isprsjprs.2017.01.019>
- Yang, X., Lo, C.P., 2002. Using a time series of satellite imagery to detect land use and land cover changes in the Atlanta, Georgia metropolitan area. *International Journal of Remote Sensing* 23, 1775–1798. <https://doi.org/10.1080/01431160110075802>
- Zaman, F., 2014. River halda awakening: a research training and awareness centre at Burischar, Chittagong (PhD Thesis). BRAC University.

APPENDICES

APPENDIX 1: Error Matrix showing accuracy of 1990 supervised classification of land uses of Halda Basin

Class Name	Reference Totals	Classified Totals	Number Correct	Producers Accuracy	Users Accuracy
Agriculture	12	15	11	100.00%	80.00%
Water_body	13	12	12	92.00%	100.00%
Vegetation	17	14	14	82.00%	91.67%
Built area	5	6	3	60.00%	83.33%
Total	47	47	40		

Overall Classification Accuracy = 88.75%

APPENDIX 2: ERROR MATRIX SHOWING ACCURACY OF 2015 SUPERVISED CLASSIFICATION OF LAND USES OF HALDA BASIN

Class Name	Reference Totals	Classified Totals	Number Correct	Producers Accuracy	Users Accuracy
Agriculture	12	15	12	100.00%	80.00%
Water_body	27	24	24	88.89%	100.00%
Vegetation	13	12	11	84.62%	91.67%
Built area	5	6	5	100.00%	83.33%
Total	57	57	52		

Overall Classification Accuracy = 91.23%

APPENDIX 3: Screenshot of Transition classes in Halda Basin

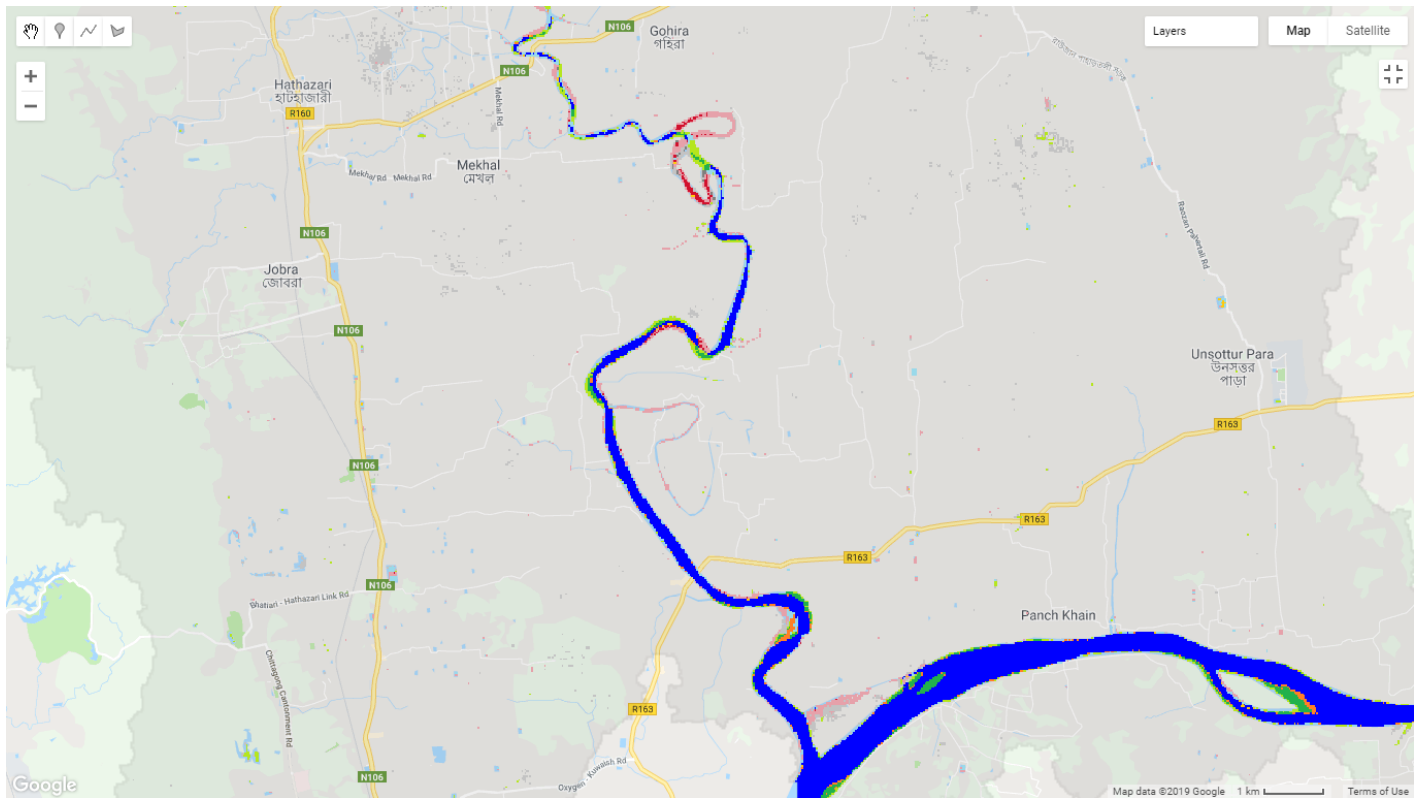


Figure 20: Part 1 (Halda Basin)

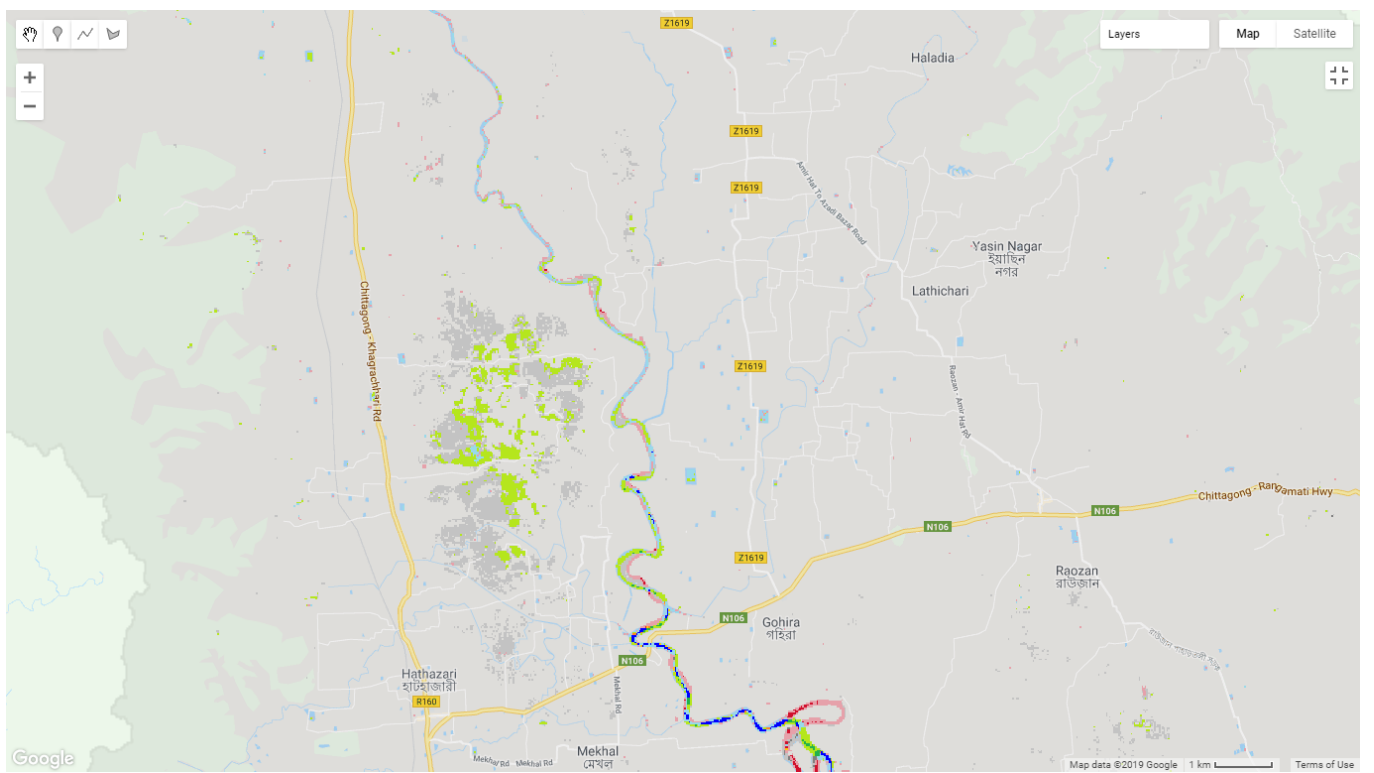


Figure 21: Halda basin (Part 2)

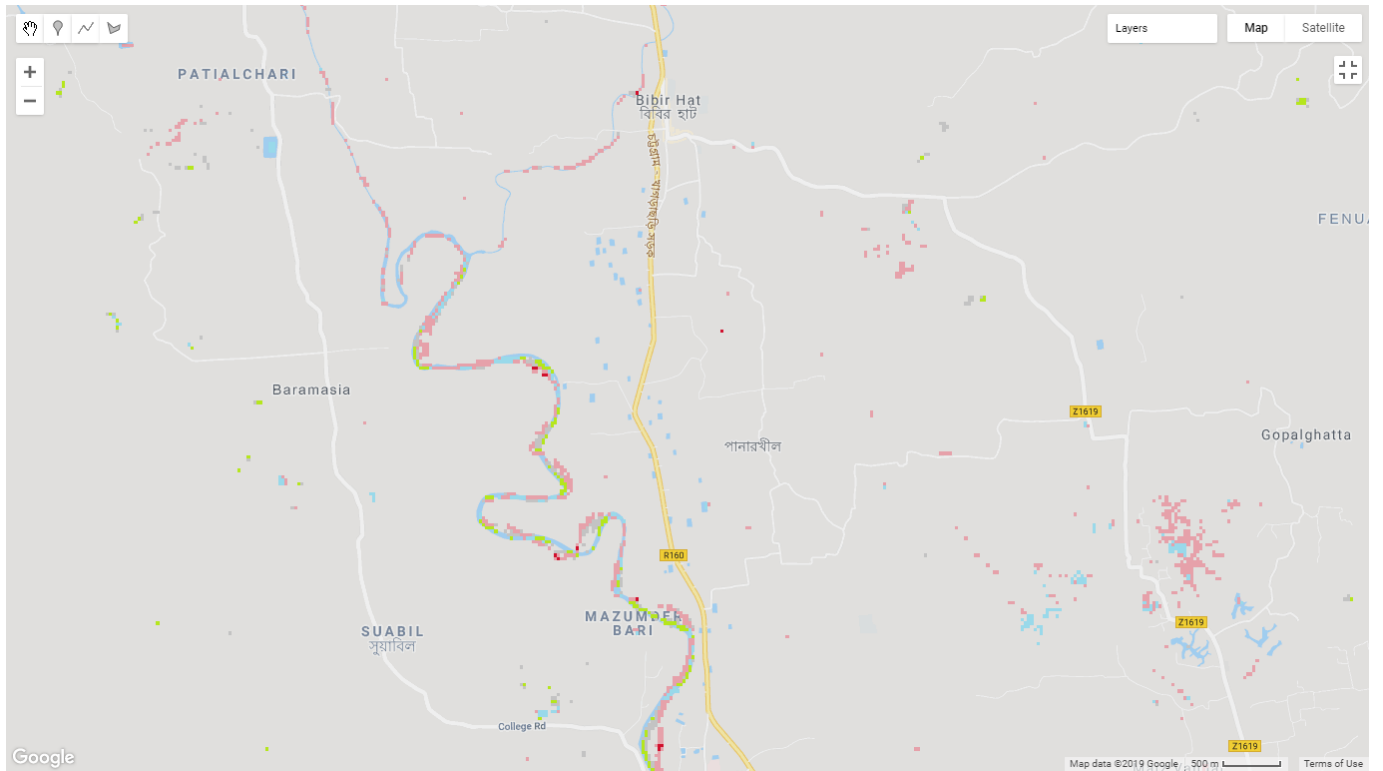


Figure 22: Halda Basin (Part 3)